A STAND-ALONE INDUCTION POWERED CURRENT AND CURRENT HARMONICS MEASUREMENT SYSTEM FOR DISTRIBUTION LINES

A THESIS SUBMITTED TO
THE GRADUATE SCHOOL OF NATURAL AND APPLIED SCIENCES
OF
MIDDLE EAST TECHNICAL UNIVERSITY

BY

SİNAN GÖKGÖZ

IN PARTIAL FULFILLMENT OF THE REQUIREMENTS
FOR
THE DEGREE OF MASTER OF SCIENCE
IN
ELECTRICS ELECTRONICS ENGINEERING

SEPTEMBER 2012

Approval of the thesis:

A STAND-ALONE INDUCTION POWERED CURRENT AND CURRENT HARMONICS MEASUREMENT SYSTEM FOR DISTRIBUTION LINES

submitted by **SİNAN GÖKGÖZ** in partial fulfillment of the requirements for the degree of **Master of Science in Electrics Electronics Engineering Department, Middle East Technical University** by,

Prof. Dr. Canan ÖZGEN _____
Dean, Graduate School of **Natural and Applied Sciences**

Prof. Dr.İsmet ERKMEN _____
Head of Department, **Electrics Electronics Engineering**

Prof. Dr. Mirzahan Hızal _____
Supervisor, **Electrics Electronics Engineering Department**

Examining Committee Members:

Prof. Dr. Ahmet RUMELİ
Electrical and Electronics Engineering Dept., METU _____

Prof. Dr. Mirzahan HIZAL
Electrical and Electronics Engineering Dept., METU _____

Prof. Dr. Arif ERTAŞ
Electrical and Electronics Engineering Dept., METU _____

Assist. Prof. Dr. Hakan ÖKTEM
Institute of Applied Mathematics., METU _____

M.Sc. Mustafa DENİZ
TUBITAK-UZAY _____

Date: _____

I hereby declare that all information in this document has been obtained and presented in accordance with academic rules and ethical conduct. I also declare that, as required by these rules and conduct, I have fully cited and referenced all material and results that are not original to this work.

Name, Last Name: SİNAN GÖKGÖZ

Signature :

ABSTRACT

A STAND-ALONE INDUCTION POWERED CURRENT AND CURRENT HARMONICS MEASUREMENT SYSTEM FOR DISTRIBUTION LINES

Gökgöz, Sinan

M.S., Department of Electrics Electronics Engineering

Supervisor : Prof. Dr. Mirzahan Hızal

September 2012, 114 pages

The presence of information and communication technologies in the field of energy is increasing every day. Smart grid subject which aims to increase the percentage of energy generation through renewable resources and to make consumers to be involved in grid actively, is gaining importance day by day. In order to provide an efficient and reliable operation of smart grid network, it is necessary to collect relevant parameters from network components via communication infrastructure and to evaluate collected information. Also, with the inclusion of distributed energy sources in the power lines, collection of relevant data becomes important in order to ensure the quality of power. In the scope of this study, to measure current parameters, two DSP based electronic circuits and necessary embedded software have been developed. Data acquisition card is a fixed device which is to be installed to a point on the power line to gather current value samples. By means of being fed through magnetic induction from the line, this part of the system could stay on-line permanently and this allows taking measurements on demand. Sampling of line current is performed through principle of magnetic induction from the line on current sensing instrument which is connected to data-acquisition part. Also by utilization of clamp-on instruments, cutting of energy lines is not needed. Samples received by control card over radio frequency or infrared communication, are evaluated

with the help of Discrete Fourier Transform (DFT). Control card can show information about Root mean square (RMS) value and harmonic components of line current and total harmonics distortion (THD) on graphic LCD.

Present state of the system was tested in LV and MV environments and shown to be used on distribution lines. The system presented in this study is open to improvements and suggestions to make the system to be able to work on high voltage lines are made.

Keywords: Distribution Lines, High Voltage Lines, Current Value, Harmonic Analysis, Total Harmonic Distortion

ÖZ

DAĞ ITIM HATLARI İÇİN İNDÜKLENME İLE BESLENEN AKIM VE AKIM HARMONİKLERİ ÖLÇÜM SİSTEMİ

Gökgöz, Sinan
Yüksek Lisans, Elektrik Elektronik Bölümü
Tez Yöneticisi : Prof. Dr. Mirzahan Hızal

Eylül 2012, 114 sayfa

Bilgi ve haberleşme teknolojilerinin enerji alanındaki varlığıher geçen gün artmaktadır. Yenilenebilir kaynaklıelektrik enerjisinin şebekedeki payının artırılmasıve tüketicilerin aktif bir şekilde şebekeye dahil olmalarınıhedefleyen akıllışebeke konusu gün geçtikçe önem kazanmaktadır. Verimli ve güvenli bir akıllışebeke ağıişletimi için şebeke elemanlarına haberleşme altyapısıüzerinden ulaşılarak ilgili parametrelerin toplanmasıve toplanan bilgilerin değerlendirilmesi gereklidir. Dağıtılmış üretim kaynaklarının da enerji hatlarına dahil olmasıile enerji hatlarının kalitesinin sağlanmasıamacıyla ilgili veri toplamanın önemi de artmaktadır. Bu tez çalışmasında, akım parametrelerini ölçmek için, iki dijital sinyal işlemci bazlıelektronik devre ve gerekli gömülü yazılımlar geliştirilmiştir. Veri toplama kartı, akım değeri örneklemeleri toplamak için güç hattıüzerinde bir noktaya takılacak sabit bir ölçüm cihazıdır. Hattan manyetik indüklenme ile beslenebilmesi sayesinde, sistemin bu kısmıhat üzerinde sürekli bulunabilmekte ve istenildiği zaman ölçüm alınabilmesine olanak sağlamaktadır. Hat akımıörneklemesi, sistemin data toplama kısmına bağlıolan bir akım ölçme entrumanının hattan akım indüklemesi prensibiyle yapılmaktadır. Kelepçeli enstrumanların kullanımıile enerji hattının kesilmesine de gerek kalmamaktadır. Radio frekansıveya kızılötesi iletişimi vasıtasıyla kontrol kartıtarafından alınan örneklemeler ayrık Fourier dönüşümü yardımıyla yorumlamaktadır. Kontrol kartı,

hattın akımının etken değeri, harmonik bileşenleri ve toplam harmonik bozulma (THB) hakkında bilgileri grafik LCD üzerinde gösterebilmektedir.

Sistemin sunulan hali, alçak gerilim ve orta gerilim ortamlarında test edilip şu anki hali ile dağıtım hatlarında kullanılabileceği gösterilmiştir. Bu tez çalışmasıkapsamında sunulan sistem geliştirmelere açıktır ve sistemin yüksek gerilim hatlarında çalışabilmesi için çeşitli öneriler sunulmuştur.

Anahtar Kelimeler: Dağıtım Hatları, Yüksek Gerilim Hatları, Akım Değeri, Harmonik Analizi, Toplam Harmonik Bozulma

To My Family
To All Fathers

ACKNOWLEDGMENTS

First of all, I would like to thank to my supervisor, Prof. Dr. Mirzahan Hızal for his guidance and recommendations.

I would like to thank Mustafa Deniz and Dr. Erdal Bizkevelci for their ideas and advices.

I would like to express my thanks to my friends Doğan Gezer, Tunahan Kırılmaz, Muhsin Bölücek, and Hakan Özyürek for their brotherhood and encouragements.

I owe a debt of gratitude to Selçuk Çelik and Ayşe Vildan Ekşi for their fun and cheerfulness.

I am deeply grateful with my family. Their support has always been with me not only for this study but also for my whole life.

TABLE OF CONTENTS

LIST OF TABLES

TABLES

LIST OF FIGURES

FIGURES

CHAPTER 1

INTRODUCTION

Power quality can be briefly described as the total quality of current and voltage values and waveforms. In order to measure quality of a power system, waveforms of current and voltage as well as their effective values are examined. Quality is a two way path between suppliers and consumers. Voltage quality is assured by supplier; current is drawn by load at the consumer side. Characteristic of load at the consumer side affects current waveform which in adverse affects voltage quality, both of which specifying the total power quality.

Keeping the quality of a power system at a high level, starts with monitoring the parameters and events in the system. For a stable system, power parameters should be observed and events should be seized. Power engineers, monitor system to find out problems and make improvements with the help of power monitoring devices.

Smart grid phenomena also increased the need for power quality monitoring systems. Smart grid aims to increase the percentage of electricity generation through renewable resources and participation of consumers to generation through medium voltage (MV) and low voltage (LV) distribution systems. Benefits of smart grid also bring about some power quality issues. Renewable sources like wind turbine and solar panels have non-uniform generation characteristics which badly affect power quality. Interventions on power system in smart grids are important to keep the system running. In order to provide an efficient and reliable operation of the network, it is necessary to collect relevant parameters from network components by the use of power monitoring devices.

There are many power monitoring techniques and devices which were developed by engineers and researchers all over the world. After literature survey it can be seen that power monitoring is not a unique way. Engineers developed many systems which can have many

data-acquisition units and communicate over LAN [1], there are systems which can be connected to energy lines up to 69kV directly by clamp-on structure [2]. Some systems use internet connection to transfer samples data to analysis center[3]. Taking into account the constraints, a suitable power monitoring system can be chosen for the system which is to be monitored. Every system has advantages and disadvantages over each other. One of the advantages of the presented system in this thesis is its price. Cost of this presented system which is consisted of two electronic cards, is not higher than 150. Another advantage of this system is that, with the use of clamp-on current measurement instruments, there is no need to cut energy lines. Battery charging property is another advantage which eliminates the need for changing battery when it is discharged.

The starting point of this thesis comes from examining the transient events and harmonic measurement system which was built in Tubitak Space Technologies Research Institute by power electronics group. This system uses optical voltage and current transducers can measure current from 0Hz to 20kHz frequency and can measure voltage from 0.5Hz to 6kHz. With deploying NXVCT-229, system can also measure 420kV and 2000A[4]. System can be seen from Figure 1.1. This is a very high precision system, however expensive and not suitable to be mobile. Because of its expense, system is not suitable for deploying to the line permanently. In order to deploy the system, energy lines should be cut, wire should be passed through the ring of current sensor and should be reconnected for current measurement. For voltage measurements, line should be cut and connected to voltage sensor. This procedure can be seen in Figure 1.2.

Examining the transient events and harmonic measurement system,gave the idea of designing a mobile and stand-alone system where permanent standing, price and mobility is more important other than great precision. Cutting of energy lines brings in a lot of burden while deploying the system. Hence eliminating the need of cutting energy lines was set as a goal of the study.

With the motivation of mentioned goals, two dsPIC based electronic cards are designed and implemented, in this study. First card is designed to collect current data from a current measuring instrument. Second card is designed to control the first card and receive data from it. Graphical display is employed on control card in order to display signal waveform and necessary parameters about the flowing current through the energy line. In order to measure

Figure 1.1: Transient events and harmonic measurement system

accuracy of the cards, software tests, tests with signal generators and tests with different current measurement instruments are conducted. Implementation details of the electronic cards by hardware and software aspects are defined throughout the thesis. Test procedures are explained and obtained results are presented for this system.

In transmission systems current measurements are also performed by conventional current transformers which are high in cost, large in size and dangerously explosive when secondary side opened. Every benefits of the proposed design which have advantages over traditional methods, are summarized in this paragraph. It is easy to be mobile and easy to be installed because of clamp-on structure and light weight which makes the system also to be replaced easily. Cost of the system is very low which makes the system to be employed in many places with low expense. System is able to monitor current harmonics which makes it to be used in power quality studies. Data acquisition part is self-powered, needs no external power source and connected wireless to control units. In literature, approaches similar to the mentioned design can be found[66-71]. Energy harvesting is performed through small current transformers alongside with the main measurement instrument or from the main current instrument[67][68][70]. Lightweight, mobility and low cost is achieved by different structures

Figure 1.2: Cutting of high voltage lines

and designs [68] [66]. There are also designs which can perform harmonic measurements and transfer data through LED light and fiber optical cables [68][69]. The design in this thesis works up for all of the features mentioned.

Thesis is organized as five chapters. Firstly, in Chapter 2, as the system is suggested to be used in smart grids and distributed generation systems, background information about these topics are given. Following these topics, power quality and power quality monitoring systems are discussed. Current measurement instruments are also presented and compared from different aspects in this section. Total harmonic distortion, Fast Fourier transform, discrete Fourier transform, Cooley-Tukey algorithm and Root mean square are explained as they are used in mathematical calculations in this study.

Chapter 3 is devoted to explain the designed electronic cards. Firstly, designed system is explained on system basis with functional block diagrams. Following that, data-acquisition card is explained from hardware and software aspects. Control card is examined in a similar way.

In Chapter 4, tests conducted with the electronic cards are described. Test procedures for software based tests, tests with signal generator and tests with different sensors are explained. Results for those tests are analyzed and observations are reported at the end of the section.

Chapter 5 concludes this study with remarks on important points and suggestions for future work. A proposed architecture is presented at the end of this chapter.

CHAPTER 2

GENERAL BACKGROUND

In Electrical and Electronics Engineering obtaining information about the behavior of a circuit is essential. Measurements about current and voltage values are necessary to obtain knowledge about that behavior. In some applications, besides current and voltage values, waveforms of these parameters are required to be monitored and studied. In Electrical Engineering, voltage - current value, their waveforms and frequency of the system are important in terms of monitoring the system stability. Those measurements are mandatory in power quality improvement studies.

General background chapter gives information about power quality and power quality monitoring. Smart grids and distributed generation systems are the other topics which are also discussed in this chapter. Total harmonic distortion, Fast Fourier transform, discrete Fourier transform, Cooley-Tukey algorithm and Root mean square are explained as they are used in mathematical calculations in this study.

2.1 Distributed Generation

In the traditional view electricity is produced by large energy sources like nuclear, hydroelectric or coal-fired plants and transmitted via transmission lines. A new kind of electricity generation has been popular after 1990's. In this kind of generation many small generation sources are connected directly to distribution lines. This method is called distributed generation (DG). Figure 2.1 illustrates an example of DG.

Reciprocating engines, combustion turbines, micro turbines, fuel cells, photovoltaic systems, wind turbines, small scale hydro turbines, solar thermal, wave turbines and geothermal source

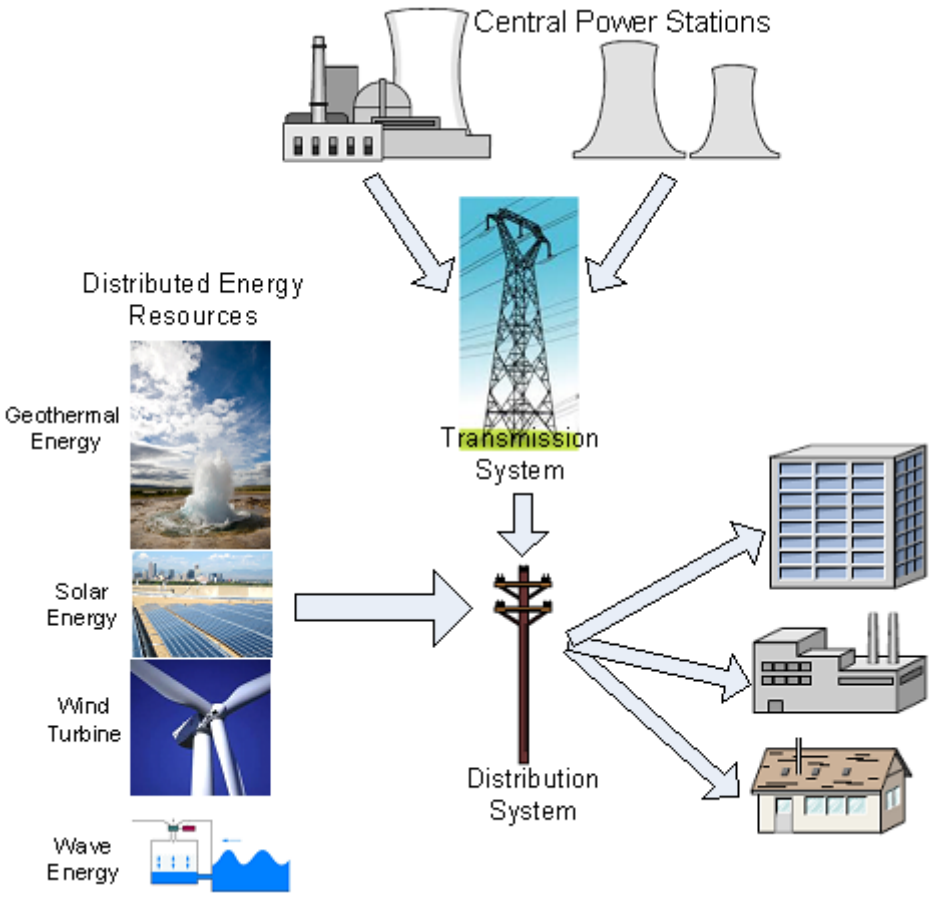

Figure 2.1: An illustration of distributed generation system

are some examples to sources of DG.[5]

DG has many benefits for suppliers, customers and society. Primary benefit of DG is that energy is consumed where it is generated. This leads to reduction of line losses. Small generating sources which have capacity under 50MW are interconnected at the distribution level. In the current literature, there is not only one consistent definition to be accepted for defining DG. International Council on Large Electric Systems (CIGRE) Work Group 37-23 defines DG as [6]:

- Not centrally planned
- Today not centrally dispatched
- Usually connected to the distribution network
- Smaller than 50-100 MW.

Investment made for DG energy sources are small compared to central power plants. DG allows customers to install their own small sized plants, supply own needs even sell electricity to power grid. Attractive benefits of DG draw attention of many customers. DG is expected to be more extensive and popular in near future. Such a matter gaining great importance and closely related to power quality should be examined in details.

DG has many benefits in addition to reduction of line losses. In case a central power plant breaks down in traditional systems, many customers face deficiency of electricity. DG reduces the dependency on central plants by deploying many small sized plants. This condition improves the reliability about continuity of the system [7]. As mentioned before, DG allows customers to produce their own electricity and even sell to grid, allows reducing their bills. Locating sources near to customer reduces the investments to be made on transmission systems. DG can be considered as environmental friendly. Many of the sources are renewable energy sources. As the share of DG sources increase, fossil fuel based systems lose their share.

Insertion of DG sources would definitely cause PQ events in the system. Analyses and researchers are being conducted about the effects of DG sources on PQ events. One of the PQ events those sources are undesired voltage variations in distribution systems. IEEE 1547 Standard for Interconnecting Distributed Resources with Electric Power System, states that

maximum allowable variation in a distribution system would be ±10, ±5 in the low voltage part and ±5 for the medium voltage part of the distribution system [8]. Analyses are performed persistently about the impact of DG sources on voltage variations [5][9][10].

Islanding occurs when the electric utility powers down but DG generator continues its powering operation the grid close to itself [11][12]. Islanding of DG sources have negative effect on voltage, frequency and power quality as they cannot provide voltage, frequency and harmonics levels as the utility system does [13][14]. Even, ferroresonance with overvoltages up to 3 p.u. may occur with existence of some conditions related with DG sources.[14].

Studies have shown that small number of DG sources may cause harmonics distortion limits to be exceeded [15][16]. Wind energy systems may inject voltage distortion because of rotating machine characteristics and power electronic interface[17][18].

All of the PQ problems originating from DG sources are depicted in Figure 2.2.

Effects of DG sources on distribution network shows a variance according to some conditions like type of source, number of DG sources in the system, distance of the sources with each other and with end-user, environmental conditions (especially for wind plants, solar plants) etc. Significant result of DG sources' impacts on distribution networks is that monitoring systems gain importance as DG gain popularity. In order to observe power quality events in a power system with number of generation sources, engineers need power quality monitoring devices and systems in large numbers more than ever.

2.2 Smart Grid

Smart grid is a new concept that is defined as an enhanced type of electrical grid which is highly equipped with technological devices in order to control and manage the system easily. Gaining more control over the system, improvement of reliability, improvement of efficiency, integration of distributed energy sources and electricity market operations are main purposes of smart grids[20]. Smart grid makes low and medium voltage grids intelligent and technological.

In traditional systems, electricity flow is one directional and hierarchical. Electricity is produced in central power stations and transferred through transmission lines and distribution

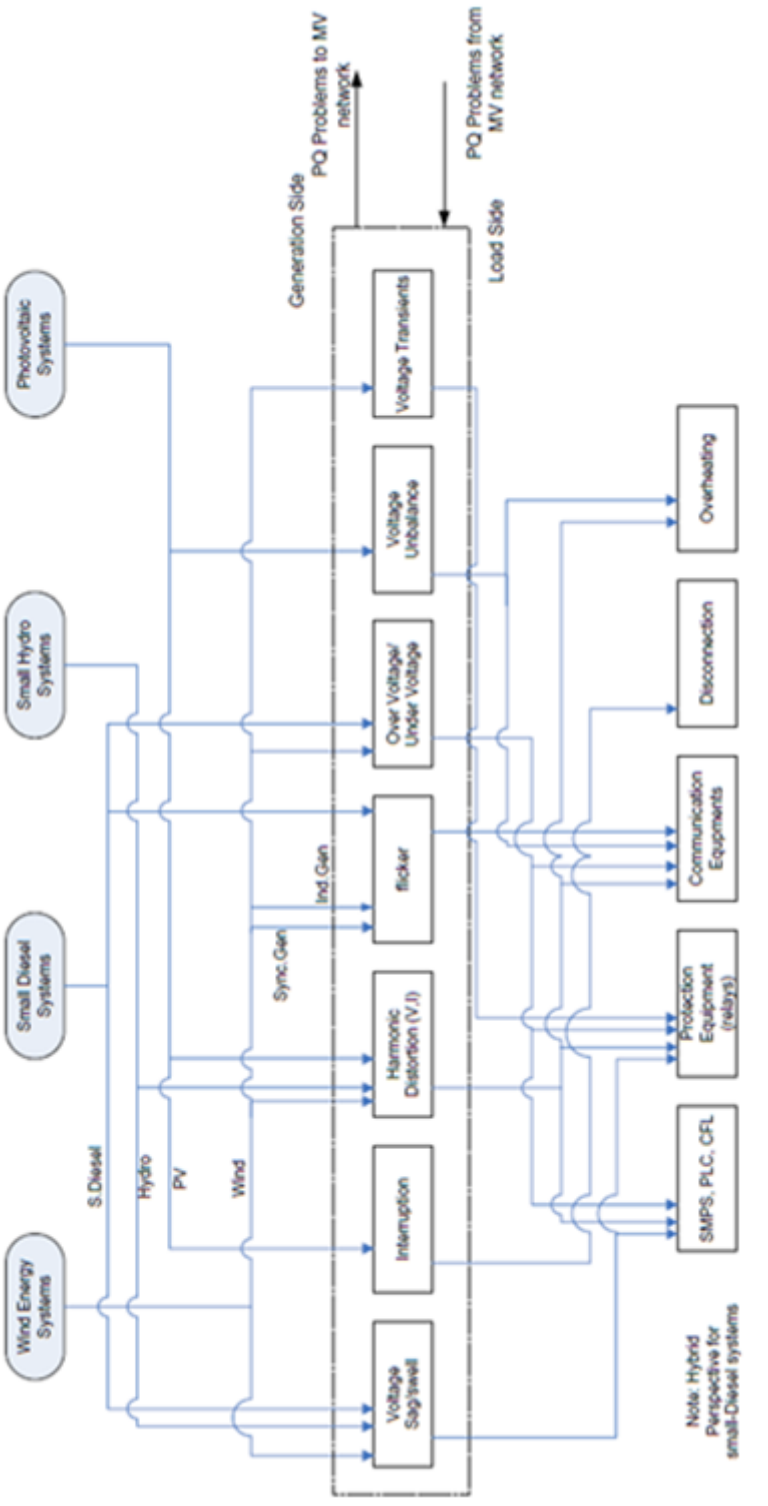

Figure 2.2: PQ problems originating from DG sources [19]

lines. Distributed generation sources are not very common and power generation is concentrated on central systems. Usage of sensors is not very frequent and in cases where they are used, communication is one way only. Checking and test are done manually and operators have limited control over system. Customers are billed at fixed rates with having lack of options for tariffs. Smart grid introduces network type power flow, power flows on the grid to areas which demand more. Power generation dependency decrease with participation of distributed generation sources to the system. Great number of sensors and sensing devices enable the system to be checked and to be under observation permanently. Two way communications with devices and control center allows intervention from a distance in fault conditions even before fault conditions. Necessary algorithms in control center and device installation even enable self-healing of the grid. Smart power meters allow customers to reduce their bills and allow suppliers to decrease the peak power demand from the system. An example of illustration for smart grid is given in Figure 2.3.

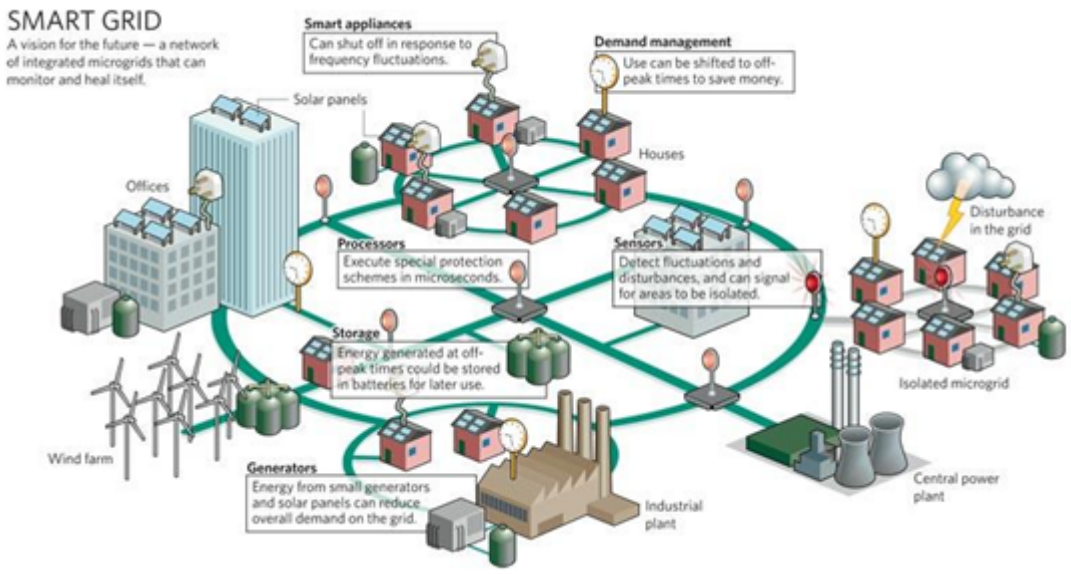

Figure 2.3: An illustration of smart grid [21]

Technologies take place in smart grids can be examined in the following five areas [22]:

Integrated Communications-In the traditional structure one way communication was used, information used to flow from customer to supplier only. Smart grid relies on two way communication which enables to exchange information dynamically from supplier to customer and vice versa. In this open communication architecture grid components keeps listening,

talking and interacting constantly with the system.

Sensing and Measurement - With the help of sensing and measurement devices, parameters about the power system are under observation permanently. Those monitoring devices are distributed on the network intensively to evaluate the health of the system and support advanced protective relaying.

Advanced Components - Usage of advanced technology in smart grids is one of the key points of this concept. New technologies in material science, superconductivity, energy storage, microelectronics etc. also play role in smart grid to increase the system reliability, efficiency and controllability.

Improved Interfaces and Decision Support- Smart grid helps decision-making people with advanced interfaces, applications and tools to protect the health of the system. In many fault conditions, the time available for operators is short and critical. Decision support systems assist operators for making decisions quickly.

Advanced Control Methods - Those algorithms predict events in the grid and take necessary corrective actions. Control method devices acquire data from sensing devices through communication interface and make the diagnosis with the help of decision support devices.

Smart grids rely on the mentioned devices heavily. Sensing and monitoring devices are one of the key points for these new technological grids. As smart grid concept gains importance, the need for variety of sensing and monitoring devices increase. This increase of need actuates researchers around the world to design and implement various kinds of monitoring devices and sensors [23][24][25][26].

2.3 Power Quality and Power Quality Monitoring

A Power System has properties like frequency, RMS current value, voltage fluctuations etc. Those properties are initially designed to be between some limits which aim that the system functions with desired performance. Power Quality is the measure that how much electrical system obeys the limits i.e. how close to the ideal conditions in which system can be favorable or poor by means of Power Quality. IEEE standard 1159 defines those conditions and Power Quality events in details.

Power which can be considered as energy is carried by voltage and current. Quality of this energy is described by parameters of voltage and current such as;

- Harmonic components in voltage and current waveforms
- Transients in voltage and current waveforms
- Voltage and current magnitude variations
- Variations in the system frequency

Those defined situations lead to or may be caused by voltage swells, sags, flickers, spikes etc. Voltage ”swell” is used to describe the increase in voltage values for short periods. Voltage ”sag” and ”dip” terms are used for short period reductions from 0.1 to 0.9 p.u.in voltage level and which can last for 0.5 to 30 periods [27][28]. Voltage sags are mainly caused by sudden increases of loads which may lead to dimming of lights and unreliable operation of test equipments. Voltage ”swells” are short increases of voltage value of the system and caused by sudden reduction of system loads and damaged neutral connection. Swells may lead to defects in system equipments and end-user devices. Variation of voltage between over and under values is defined as ”flicker”. ”Spikes” and ”surges” are high increases in voltage value for a very short time period.

Poor Power Quality causes aging of insulation equipment and electrical devices easily and may cause malfunction and irreversible defects in electrical devices.[3]

Voltage quality is supplied by the power system and supplier. Subsequent to supplying voltage and current to customer, current waveform may get distorted. Distortion of current waveform distorts voltage waveform which together decreases the power quality. This basic phenomenon is illustrated in Figure 2.4.

There have been changes in the perception of Power Quality in the last years. Providing the standards have become harder because system loads have become complex and end-user equipments have become more sensitive to Power Quality. Insertion of complex characterized loads made the system easy to be distorted. Non- linear loads increased the amount of harmonic currents. End user devices like computers, telecom devices and control equipments which are sensitive to voltage fluctuations have been used more and more with the need of

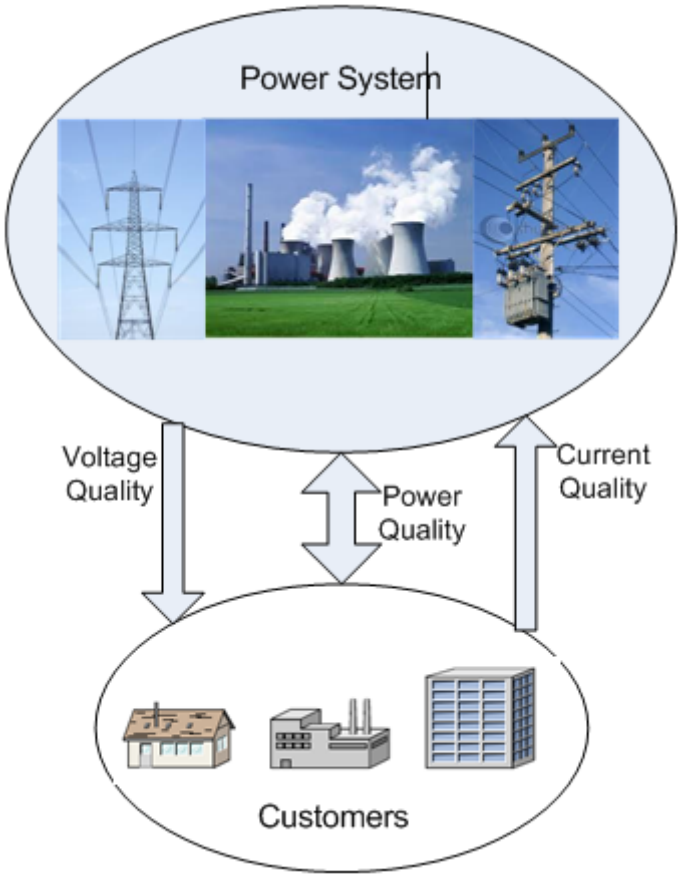

Figure 2.4: Voltage, current and power quality

work productivity. [29][30] Also the trend in the world tends to distributed generation. The main idea of distributed generation is to consume energy where it is generated by connecting sources to distribution system, in order to reduce transportation costs. Disadvantage of this idea by means of power quality is that distributed generation sources have non-uniform generation characteristics which inject disruption and harmonics into the system. All of those reasons caused that the maintaining the standard of power quality become harder.

Electricity market is a competitive market and power is merchandise which is sold to customers. In this market, it is essential for a supplier to sell better quality goods. To maintain the quality, it is essential to monitor power quality and find out the sources of degradation. To monitor quality, power monitoring units are used which are installed in many places in a power network.

There is a demand for the power quality monitoring systems to deal with the electric network pollution. Monitoring gives more ability to engineers to diagnose the corruptions and develop new solutions which give rise to insertion of new environment- friendly power sources into the system. Maintaining the power quality starts with regular monitoring. Every aspect of quality has its own defining and standards. To diagnose the degradation and make improvements, first of all every parameter of power quality should be monitored.

Demand for monitoring systems actuated people to develop various kinds of systems. Improvement in technology also reflected itself in this area. In market there can be found many systems based on Web, GPRS, Wi-Fi, Bluetooth, Ir etc.

Monitoring systems are generally composed of three main parts: 1) data acquisition part collects data and sends to desired locations; 2) an interconnection system to provide communication between data-acquisition and analysis center; 3) Analysis center which gathers data from end terminals and performs quality analysis[31]. Functions of storage, event logging and alarm generation to authorized personnel can also be added to those systems.

Data acquisition is basically gathering samples of voltage and current waveforms. Those samples are analyzed after being gathering and parameters of quality like harmonic events, frequency RMS values are obtained. In the case of capacitive loads current leads voltage. Current lags voltage in the case of inductive loads. Simultaneous monitoring of current and voltage waveforms also gives information of load type and power consumption.

This thesis mainly focused on current and current harmonics measurements. Current measurement devices and techniques will be discussed instead of voltage measurements. There are different tools and methods used in current measurement. Current shunts and transducers are the most common practices[32]. Next section focuses on those instruments.

Current Shunts Current shunts are easy and cost effective way of sensing system current. Idea is to connect a series resistor along current path. As depicted in Figure 2.5 , current value is calculated across the voltage built on shunt resistor. Voltage of shunt resistor is directly proportional to current crossing across shunt resistor according to euation (2.1). Sampling and monitoring the built voltage on resistor gives the information about system current waveform. While being easy to set up and cost-effective, shunts are not suitable for large current carrying systems. Even using low valued resistor as low as 0.001Ω can waste large amount of power by dissipating heat. Dissipated heat would be proportional to quadratic value of system current (equation(2.2)). Shunts are effective by means of sensing frequency variations but risky because they do not isolate sensing device from main current carrying wire.

$$V_{SHNT} = R_{SHNT}.I_{SYS} \tag{2.1}$$

$$P_{DISS} = I_{SYS}^2.R_{SHNT} \tag{2.2}$$

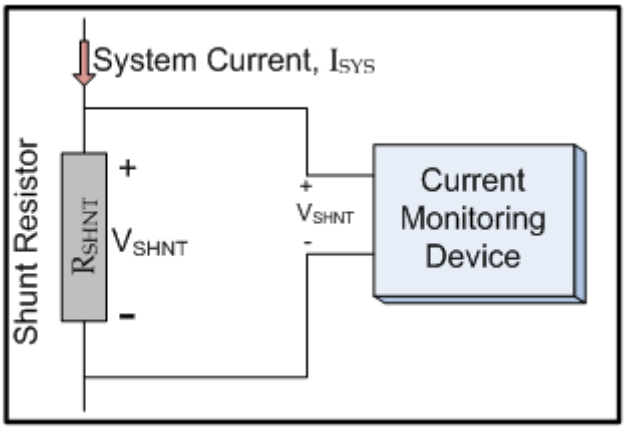

Figure 2.5: Current sensing with a shunt resistor

Transducers Current transformers, Hall effect transducers, Rogowski coils and optical transducers are the most widely used transducers. Current Transformer is a device which converts an AC current into a current which is same in frequency but different by magnitude. Current Transformers are consisted of primary - secondary windings and a magnetic core as illustrated in Figure 2.6. [33]

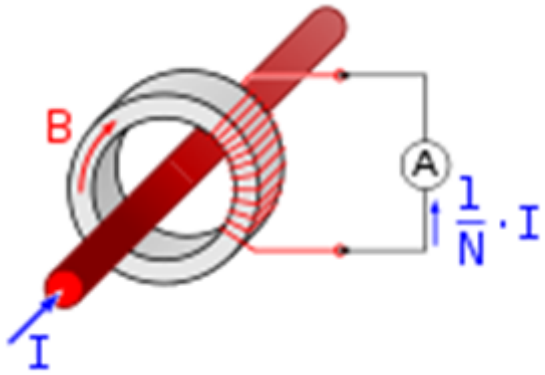

Figure 2.6: Structure of a current transformer

Primary winding is the main current carrying wire and second winding is the small current to be measured. These two windings are magnetically coupled with the help of magnetic core. The advantage of coupling is that secondary winding which is connected to current measuring device is galvanically isolated from current carrying winding. Secondary current is directly proportional in magnitude to the primary current according to equation(2.3). Primary turn ratio is always 1 and equation(2.3) becomes equation(2.4).

$$N_1/N_2 = I_2/I_1 \tag{2.3}$$

$$1/N_2 = I_2/I_1 \tag{2.4}$$

Where N_1 and N_2 are primary and secondary turn ratios and I_1 and I_2 are primary and secondary currents, respectively. Formulas (2.3) and (2.4) are ideal cases which slightly differs from actual practices. A further study can be carried on with a load $ZB = RB + jwLB$ connected to the secondary side of the transformer and including all resistances and inductances. Detailed diagram of a current transformer can be seen in Figure 2.7.

Where;

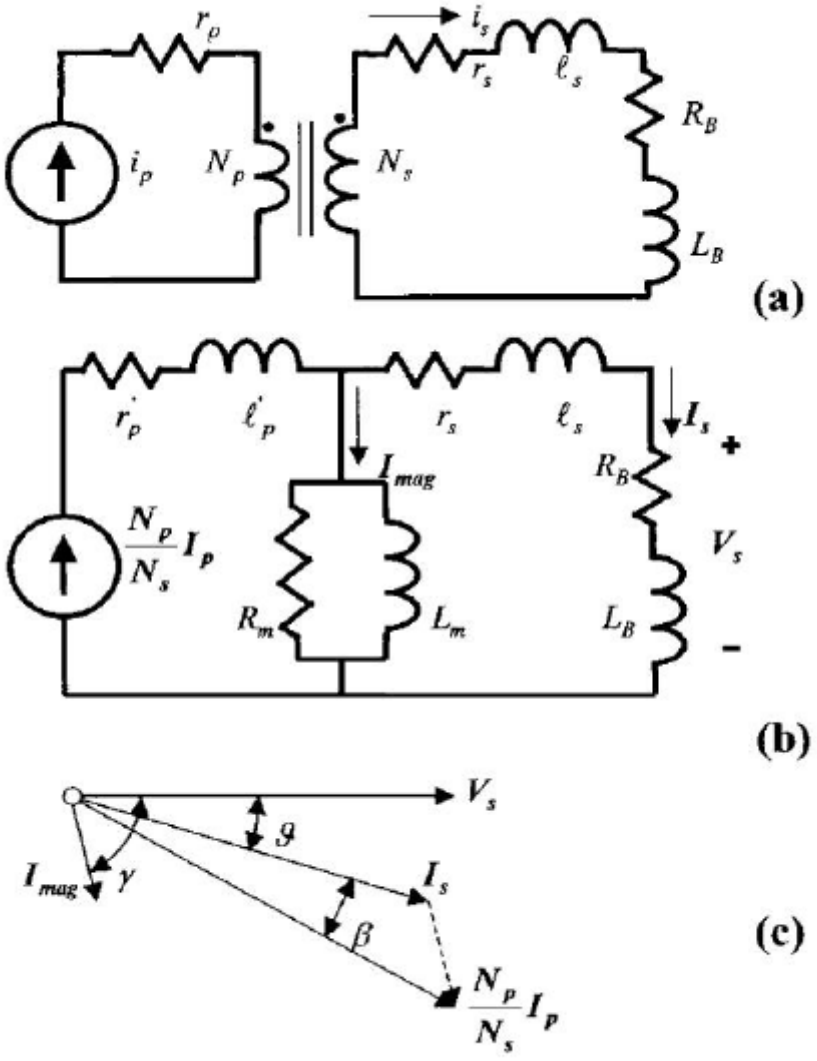

Figure 2.7: Current Transformer.(a) Connection Diagram. (b) Equivalent Circuit

- $(N_p = N_s)I_p$ is the transferred form of primary current phasor I_p to the secondary side,
- r'_p is the primary winding resistance referred to secondary side,
- l'_p is the primary leakage inductance referred to secondary side,
- r_s is the secondary winding resistance,
- l_s is the secondary leakage inductance,
- L_m is the magnetizing inductance,
- R_m is the magnetic core resistance and equal to $Vs2/\Delta PFe$,
- ΔPFe models the magnetic core hysteresis and eddy current losses.

Figure 2.7(b) shows that secondary current measured from secondary windings is I_s, which is slightly different from $(N_1/N_2).I_1$ current given in (3) and (4). From Figure 2.7(b), I_s and V_s are found to be;

$$I_s = (N_p/N_s)I_p - I_{mag} \tag{2.5}$$

$$V_s = (R_B + jwL_B)I_s \tag{2.6}$$

Formulations (2.5) and (2.6) show that Vs is a function of I_s which is a function of I_mag. Flux in the core of transformer is a nonlinear function of magnetizing current. Current division between I_s and I_mag depends on the impedances of secondary and magnetizing loads which are variant with system frequency. Nonlinear behavior of magnetic core and system frequency affects I_s and V_s which are to be used for current measurements. This behavior causes two errors; phase angle error and magnitude error which are given in equations (2.7) and (2.8).
1.Phase Angle Error

$$\beta \approx tan^{-1}\left[\frac{I_{mag}sin(\gamma-\varphi)}{\frac{N_p}{N_s}I_p - I_{mag}cos(\gamma-\varphi)}\right] \tag{2.7}$$

2. Magnitude error characterized by the ratio correction factor (RCF)

$$RCF = \frac{N_p}{N_s}\frac{|I_p|}{|I_s|} \approx \sqrt{1 + \frac{N_s I_{mag}}{N_p I_p}^2 - 2\frac{N_s I_{mag}}{N_p I_p}cos(\gamma-\varphi)} \tag{2.8}$$

Errors mentioned in (2.7) and (2.8) affect accuracy of power quality measurements. Frequency of primary and secondary currents is exactly same but they have a phase shift of

β given by equation (2.7). In low frequencies phase shift is nearly zero, in high frequencies phase shift starts to become significant. Frequency response is related to the internal impedance and secondary side impedance of the transformer.

In harmonics measurement selecting a suitable current transformer is important. Large magnetic core, small residual flux, good frequency response, small secondary resistance and high magnetic permeability are desired features of a current transformer. If rapid changes and inrush currents are important then a large transformer by means of nominal current should be chosen.

Optical Transducers are new in the market and produced to overcome deficiencies of traditional current and voltage measurement instruments. An optical transducer is combination of high technology which involves optics, optical communication, electromagnetism, electronics and computer technology.

Those transducers can contain a voltage transducer, a current transducer or both. In the scope of this thesis, only optical current transducers will be examined. An example of optical current transducer is given in Figure 2.8 Optical current transducers have advantages over con-

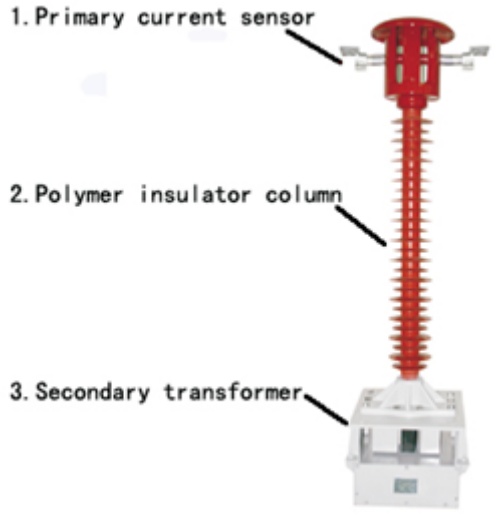

Figure 2.8: An optical current transducer

ventional current measurement instruments by means of phase shift and amplitude accuracy. Usage of optical devices allows the device to galvanically isolate primary side from secondary side. Measurement bandwidth is high and can reach from DC up to 20 kHz. Lacking

of magnetic core disposes many deficiencies like saturation, trapped charges and secondary open-short circuit problems. They can measure high fault currents up to 400kA because of having no magnetic core. [4] Internal block diagram of the optical part is illustrated in Figure

optical current sensor.png

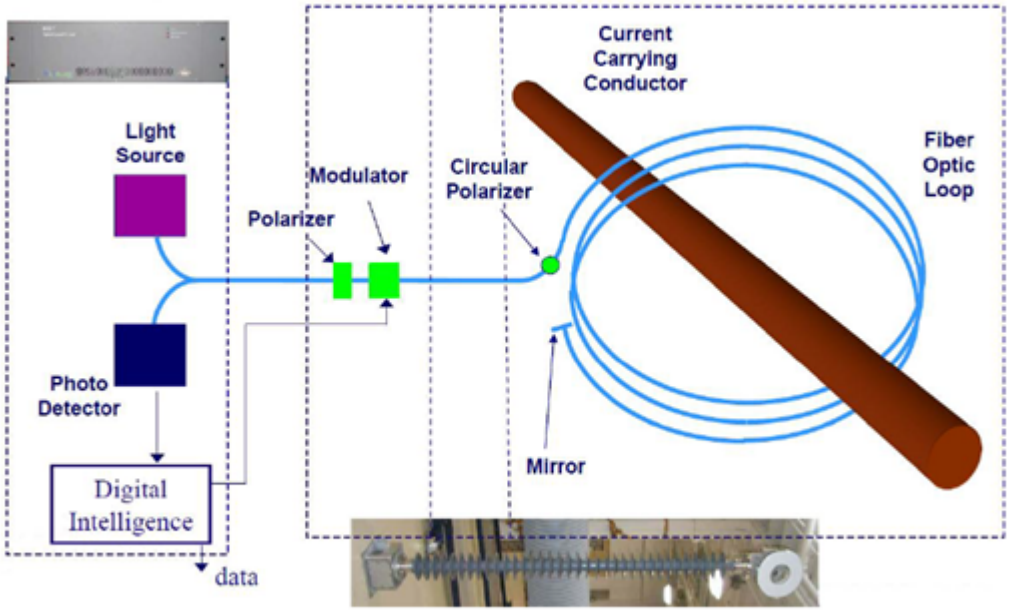

Figure 2.9: Fiber optical current sensor - optical block diagram [34]

2.9 to explain operation of the device in details. Light produced from the light source is sent to polarizer module. Linearly polarized light is then transferred to polarization splitter to be split into two polarized waves. After being modulated by modulator those two modulated linearly polarized waves passes through circular polarizer. Circular polarizer produces left and right hand side polarized waves. Those two circularly polarized waves travels along the fiber optic cable around current carrying conductor. A mirror is placed at the end of fiber optic cable which reflects the waves back from the loop. Along the path taken around current carrying conductor, the circular polarized waves experiences a phase shift proportional to the current flowing through conductor. Phase shift is detected by photo detector which is located in the electronics part of the system.

Optical transducers are high technology equipments which provide high precision measurements. Besides advantages they have disadvantages. They are expensive equipments and not suitable to be mobile because of their size and weight. Optical Current transducers are

compared with other current measurement instruments in Table 2.1.

Hall Effect Transducers work by measuring Hall voltage built across a current carrying conductor. When charge carrying elements are exposed to a magnetic field which is perpendicular to the direction of motion, they experience a Lorentz force. Lorentz force draws charge carrying elements to a direction which is perpendicular to direction of motion and magnetic field which results in accumulation of elements on sides of conductor as depicted in Figure 2.10. This accumulation further causes a voltage difference between sides of conductor which is known as Hall voltage (Equation(2.9)).

$$V_H = R_H.I.B/t \tag{2.9}$$

Where V_H is the built Hall voltage, R_H is the Hall coefficient (cubic meters per Celsius), I is the current flowing through sensor which is held to be constant, B is the flux density (Tesla) and t is the thickness of sensor (meters). In this formula current flowing through main wire is not present. B is directly proportional to the main current which further affects Hall voltage built on the sensor.

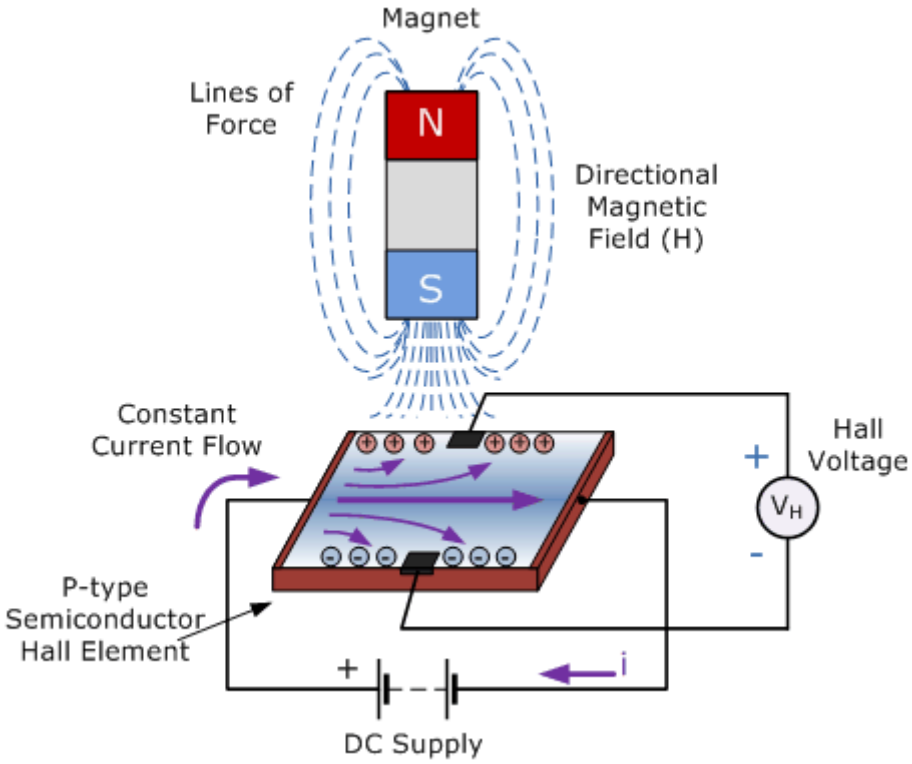

Figure 2.10: A conductor experiencing a magnetic field

Important result of Euation(2.9) is that Hall voltage is proportional to the product of flux density and flowing current. A typical Hall sensor is shown in Figure 2.11. VOUT is directly proportional to the flux induced in magnetic core and flux is directly proportional to the current flowing through conductor. Typically this output voltage is in the order of micro volts and should be amplified. Two types of Hall effect transducers can be found in the market; effect.png

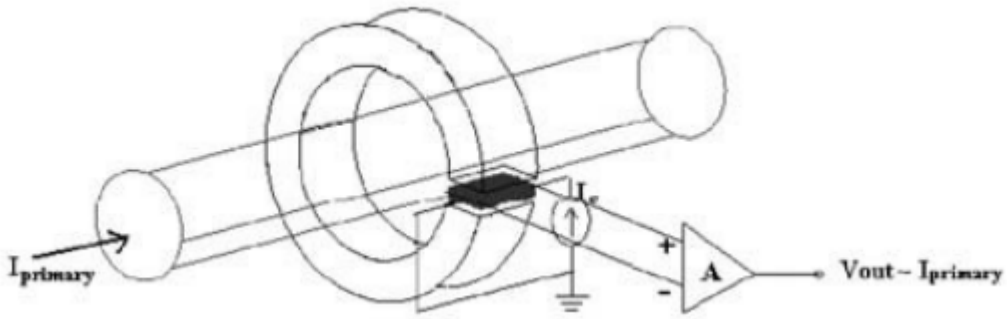

Figure 2.11: A Typical Hall effect transducer

closed loop and open loop Hall effect transducers. In open loop topology, transducer simply gives the amplified output voltage of Hall sensor. This output voltage is proportional to the measured current which is passed through transducer with the current carrying wire. Open loop Hall effect transducers are cheaper and consume less power than closed loop counterparts [35]. Topology of an open loop Hall effect sensor is shown in Figure 2.12(a). In closed

Figure 2.12: (a) An open loop Hall effect transducer (b) A closed loop Hall effect transducer

loop topology a secondary wire is present around the magnetic core. A closed loop Hall effect transducer compensates the flux generated in the secondary windings of transducer with the help of Hall sensor and necessary electronic circuit as depicted in Figure 2.12(b). Flux

generated by the primary current around the magnetic core is constantly made zero with the output current of Hall sensor and electronic circuit. Current given by the electronic circuit is directly proportional to the primary current flowing through conductor. This proportional current can be measured by connecting a proper value of resistance at the end of secondary winding. Closed loop topology which can be seen in Figure 2.12(b). has advantages and disadvantages when compared to open loop topology. Excellent linearity is ensured with this topology. Closed loop sensors have wide frequency range, good overall accuracy, fast response time, low temperature drift, and no insertion losses. They are more expensive than open loop types and not easy to be made split core [35].

Rogowski coils are similar to current transformers and used to measure AC current and current pulses. A Rogowski coil has an air core with a toroidal shape and a winding over the core. Winding starts on one end of toroid wounding helically over core and returns to start point through the center of toroid. Core is wound around current carrying conductor. When current passes through conductor a magnetic field H is created as shown in Figure 2.13. This

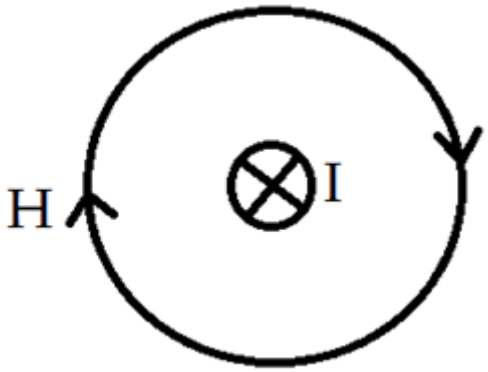

Figure 2.13: H field created around a current carrying conductor

magnetic field results a voltage difference between the ends of Rogowski coil which is given by Equation(2.10);

$$V_L(t) = -L.\frac{di(t)}{dt} \rightarrow i(t) = -\frac{1}{L}\int V_L(t)dt \tag{2.10}$$

Where L is mutual inductance of coil. Important result of this formula is that voltage built across terminals of Rogowski coil is directly proportional to current derivative. Output of an Rogowski coil is generally connected to an integrator circuit (Figure 2.14) whose output would be directly proportional to the flowing current.

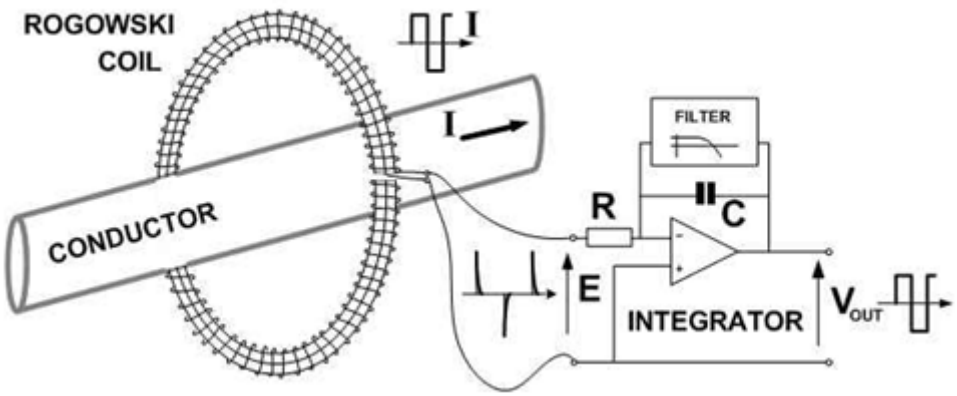

Figure 2.14: An example of Rogowski coil and integrator at the end

Rogowski coils are similar to current transformers but major differences and characteristics. Having an air core results in low inductance and coil can respond to rapid changes of current. Air core keeps Rogowski coil away from saturation which enables coil to be used in high currents. Rogowski coils have high frequency bandwidths. Wide measuring range enables to measure from milliamperes to million amperes.

Table 2.1 gives a comparison of mentioned current sensing devices by means of various specifications.

Table 2.1: Comparison of current sensing devices.

Specification	current Shunts	conventional Current Transformers	Optical Transducers	Hall effect Transducers	Rogowski Coils
AC,DC	AC,DC	AC	AC,DC	AC,DC	AC
Bandwith	Low	Low	High	High	High
Linearity	Good	Good	Good	Medium	Good
High Current Measurement	Bad	Medium	Good	Medium	Good
Saturation Problems	No	Yes	No	Yes	No
Power Consume	High	Low	Low	Low	Low
Cost	Very Low	Medium	Very High	High	Low

Those current sensing devices supply a proportion of actual current as an output. This output is then used as an input to a data acquisition device. There are various examples of data acquisition using a PC or an embedded electronic card [36-42]. Usage of a DSP or a micro-

controller is common in embedded electronic cards. After acquisition of data, analysis should be done to observe power quality events. Subsequent to data-acquisition data should be transferred to an analysis unit. Data Acquisition and analysis-performing parts can be combined in a single device or can be far apart from each other. Data or events can be stored according to needs. Analysis-performing part can receive data from one or more data acquisition devices. Another unit can be added for alarming personnel on duty. All of these possibilities brings in different types of monitoring systems. In this study, monitoring systems are examined in two groups according to architecture; monitoring systems working locally and monitoring systems working centrally. Background works are surveyed in this fashion.

Monitoring Systems Working Locally Those kind of monitoring systems are not operated from a center. Gathered data is only about the part of the electrical system where the monitoring system is located. Data acquisition parts can be many in number and connected to an analysis and display station.

Interconnection can be in miscellaneous ways. There are systems which communicate over RS-485, ZigBee and Local Area Network [66][1].

Figure 2.15 depicts an example of local monitoring system whose interconnection is provided by local area network. Another approach is using handheld devices for analysis performing as depicted in Figure 2.16 [2]. In those systems wireless communication is used as the interconnection method. Disadvantage of those kinds of systems is that system does not allow monitoring power quantities continuously and cannot alarm the operator in case of power fault events.

Monitoring Systems Working Centrally The main idea of this architecture is collected data is transferred to a central server. Control of the whole system is centralized in a server station. Figure 2.17 depicts an example of that kind of architecture. Because of its widespread communication infrastructure, internet is widely used in these systems between data acquisition - server and/or server-client communication. [43][44][45]. Broad usage of internet allows engineers to develop widespread even nationwide monitoring systems[46]. GSM infrastructure and GPRS communication- based architecture are also used in those applications. [47][48]. GPRS/3G, ADSL are suitable for large data transformation between server and

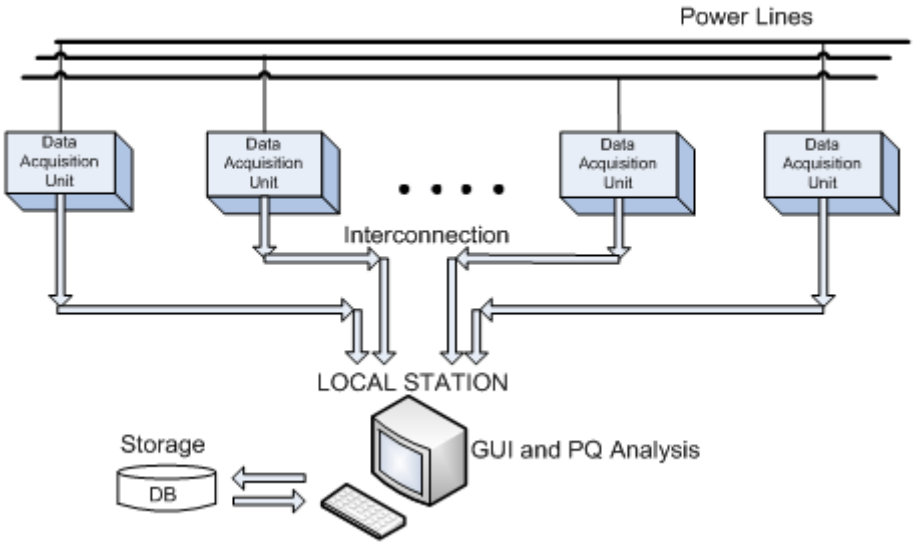

Figure 2.15: An example monitoring system block diagram

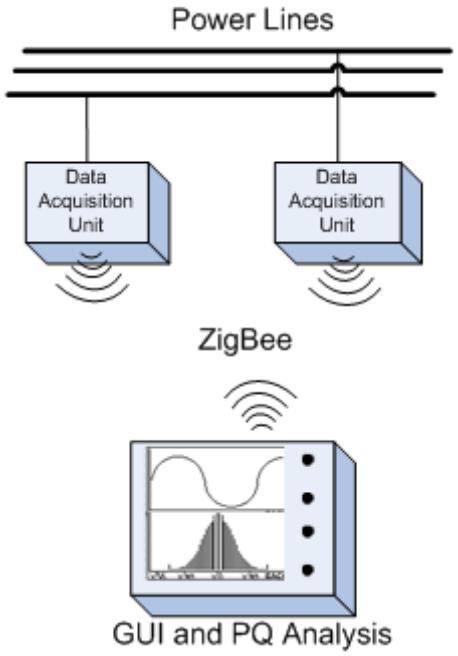

Figure 2.16: An Example handheld device monitoring system block diagram

client. Power line communication is also used while losing its popularity because of its short distance range [49]. Wireless sensor applications using networking standard ZigBee are suitable and common among data acquisition devices because of that protocol's conformity with working in harsh radio environments.

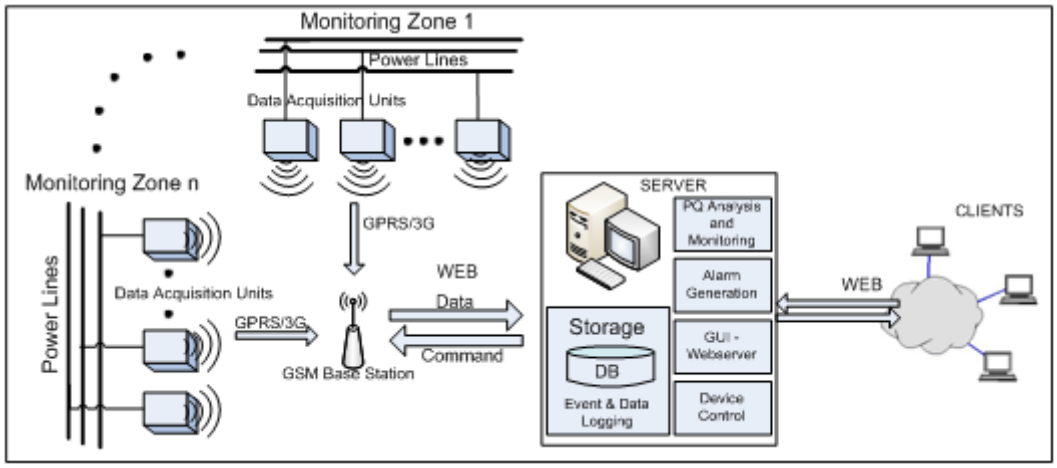

Figure 2.17: An example of centrally working monitoring systems

2.4 Total Harmonic Distortion

Total harmonic distortion (THD) is a power quality index for power systems. It is the proportion of undesired waveforms existent in the main signal waveform. These undesired waveforms are called harmonics. Harmonics are integer multiples of primary waveforms' main frequency. A power system initially designed to be purely sinusoidal by means of voltage and current waveform characteristics. A purely sinusoidal waveform is depicted in Figure 2.18(a). When some harmonics of main signal is injected into the system, current and voltage waveforms deviates from perfect shape. An example of a distorted sine wave can be seen in Figure 2.18(b). There are two kinds of loads; linear and non-linear. Linear loads have no harmful effect by means of injecting harmonics. They draw sinusoidal current and do not distort current and voltage waveforms. On the other hand non-linear loads like switched mode power supplies, uninterruptable power supplies, AC-DC drives, transformers and motors draw non-sinusoidal current from the system while distorting the current waveform which further results in voltage distortions. [50] Also, participation of distributed generation sources into the distribution network causes an increase in THD.

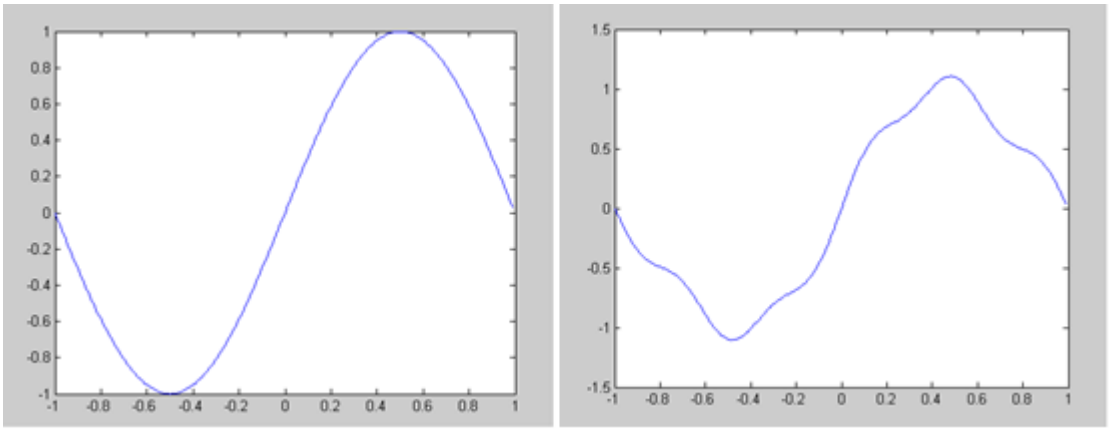

Figure 2.18: (a) A Pure sinusoidal wave (b) A Sinusoidal wave distorted with 2nd and 5th harmonics

THD is measured as the ratio of the sum of undesired harmonic components over main signal of voltage or current. THD of a voltage waveform is given by Equation (2.11).

$$THD = \frac{\sqrt{V_2^2 + V_3^2 + V_4^2 + ... + V_\infty^2}}{V_1} 100\% \tag{2.11}$$

THD is represented as percentage. If there is no harmonics present in the main signal, THD will be zero.

By similar, THD of current waveform is calculated in Equation (2.12) according to IEEE Standard 519-1992.

$$THD = \frac{\sqrt{I_2^2 + I_3^2 + I_4^2 + ... + I_\infty^2}}{I_1} 100\% \tag{2.12}$$

By means of power, THD is calculated as in Equation (2.13)

$$THD = \frac{P_2 + P_3 + P_4 + ... + P_\infty}{P_1} = \frac{\sum_{i=2}^{\infty} P_i}{P_1} 100\% \tag{2.13}$$

In this thesis study, THD is found as the current harmonics against main signal. FFT is used to find the magnitudes of all present frequencies. This FFT is performed on a 16-bit DSP. There are more accurate platforms like 40-bit DSP accumulators to calculate THD more correctly.[51] Also DSP- FPGA based systems can be used for this purpose[52].

Harmonic distortions cause various problems in power systems. Rapid ageing of insulation devices, malfunction of end-user IT devices, undesired temperature increase in the core of transformers, mechanic oscillations in electric motors, additional losses on power lines, affection of communication lines from high order harmonics of power lines are some results of harmonic distortion

To overcome the undesired results of harmonic distortion, first of all on-site measurements should be taken for analysis and diagnose. In some situations where performing measurements are not feasible, some predicting methods based on existing data, can be used [53].

2.5 Root Mean Square (RMS)

Root mean square is defined as statistical measure of magnitude a varying quantity in mathematics in mathematics. It is also known as quadratic mean. In electrical engineering RMS is used to define the effective value of a voltage or a current wave unless the wave is DC. RMS value for a function in the interval $T_1 \leq t \leq T_2$, is defined as:

$$f_{rms} = \sqrt{\frac{1}{T_1 - T_2} \int_{T_1}^{T_2} [f(t)^2]\, dt} \tag{2.14}$$

Above formula can be expanded for a continuous function all over the time as:

$$f_{rms} = \lim_{T \to \infty} \sqrt{\frac{1}{T} \int_{0}^{T} [f(t)^2]\, dt} \tag{2.15}$$

In this thesis study discrete values for current values are used. For a set of discrete values defined as x1,x2,....,xn, RMS value is calculated as:

$$x_{rms} = \sqrt{\frac{1}{n} x_1^2 + x_2^2 + x_3^2 + ... + x_n^2} \tag{2.16}$$

Parseval's theorem allows us to compute RMS in frequency domain also.

$$\sum_n x^2(t) = \frac{\sum_n |X(f)|^2}{n} \tag{2.17}$$

where X(f) is FFT of x(t) and n is number of data samples. Left side of equation (2.17) can be used in an analogous way described in Equation (2.16), yielding Equation(2.18):

$$RMS = \sqrt{\frac{1}{n} \sum_n x^2(t)} = \sqrt{\frac{1}{n^2} \sum_n |X(f)|^2} \tag{2.18}$$

which allows to use Fourier coefficients in calculation of RMS. As a summary Table 2.2 gives RMS of some common functions.

2.6 Fourier Transform

Fourier transform and Fourier series were both introduced by Joseph Fourier. Fourier introduced Fourier series to solve the heat equation on a metal plate in 1807. Fourier series are

Table 2.2: RMS of some common functions

Waveform	Equation	RMS
DC, constant	$y = a$	a
Sine wave	$y = a\sin(2\pi ft)$	$\frac{a}{\sqrt{2}}$
Square wave	$y = \begin{cases} a & \{ft\} < 0.5 \\ -a & \{ft\} > 0.5 \end{cases}$	a
Modified square wave	$y = \begin{cases} 0 & \{ft\} < 0.25 \\ a & 0.25 < \{ft\} < 0.5 \\ 0 & 0.5 < \{ft\} < 0.75 \\ -a & \{ft\} > 0.75 \end{cases}$	$\frac{a}{\sqrt{2}}$
Triangle wave	$y = \lvert 2a\{ft\} - a \rvert$	$\frac{a}{\sqrt{3}}$
Sawtooth wave	$y = 2a\{ft\} - a$	$\frac{a}{\sqrt{3}}$
Pulse train	$y = \begin{cases} a & \{ft\} < D \\ 0 & \{ft\} > D \end{cases}$	$a\sqrt{D}$

Notes:
t is time
f is frequency
a is amplitude (peak value)
D is the duty cycle or the percent(%) spent high of the period (1/*f*)
{r} is the fractional part of r

used to express a periodic signal with a sum of periodic signals. Those periodic signals are sinuses and cosines with phase angles. Fourier transform is a version of Fourier series with period of signal extended to infinity. Fourier series, Fourier transform and Fourier analysis are widely used in mathematics, physics and engineering. They allow working on frequency domain other than time domain. Inverse of the Fourier transform allow to bulid the time-domain signal from frequency-domain components. Outputs of a time domain signal are complex numbers which represents magnitude and phase angles of periodic signals.

A function f(t) can be approximated by Fourier series as in Equation (2.19);

$$g(t) = a_0 + \sum_{m=1}^{\infty} a_m cos(\frac{2\pi mt}{T}) + \sum_{n=1}^{\infty} b_n cos(\frac{2\pi mt}{T}) = \sum_{m=0}^{\infty} a_m cos(\frac{2\pi mt}{T}) + \sum_{n=1}^{\infty} b_n cos(\frac{2\pi mt}{T}) \tag{2.19}$$

Where T is the period of function. Actually this is the representation of function as a sum of sine and cosine functions. Fourier coefficients a_0, a_m and b_n are calculated as in Equation(2.20)

$$a_0 = \frac{1}{T}\int_0^T f(t)dt; \qquad a_m = \frac{2}{T}\int_0^T f(t)cos(\frac{2\pi mt}{t})dt; \qquad b_n = \frac{2}{T}\int_0^T f(t)sin(\frac{2\pi mt}{t})dt \tag{2.20}$$

Fourier transform F of an integrable non-discrete function $f : R \rightarrow C$ is given by Eqaution (2.21)

$$f(\xi) = \int_{-\infty}^{\infty} f(x)e^{-2\pi ix\xi}dx \tag{2.21}$$

for every real number ξ.

There are also discrete Fourier transform and discrete time Fourier transform. In this thesis study discrete Fourier transform with Cooley-Tukey algorithm is used to calculate harmonics of current waveform. Following two sections are dedicated to these subjects.

2.6.1 Discrete Fourier Transform (DFT)

In digital systems to process a signal, first of all sampling is done to get quantative values. Discrete Fourier transform (DFT) is a type of Fourier transform which is used when the input function is discrete and the duration is limited. The input of DFT can be real or complex numbers.

The Discrete Fourier Transform (DFT) of a signal is defined by Equation(2.22):

$$X_k = \sum_{n==0}^{N-1} x_n.e^{-i2\pi\frac{k}{N}n}. \tag{2.22}$$

Where $x_0...x_N - 1$ is the set of discrete sampled values and $X_0...X_N - 1$ are the Fourier series coefficients. This transform is usually denoted as

$$X = F(X)$$

or $F(x)$. Xk is found as a complex number after the transform. These complex numbers give magnitude and phase angle of every periodic component of the original signal. Magnitude and phase angle can be calculated according to equations (2.23) and (2.24). Frequency of sinusoidal components can be found as k/N cycles.

$$arg(X_k) = atan2(Im(X_k), Re(X_k)) \tag{2.23}$$

$$|X_k|/N = \sqrt{Re(X_k)^2 + Im(X_k)^2}/N \tag{2.24}$$

Obtained frequency components are limited in number because of sampling only a portion of the signal. Because of transforming only a window of the signal, inverse of DFT does not give the original signal completely. Inverse Discrete Fourier Transform (IDFT) is defined as equation (2.25):

$$x_n = \frac{1}{N}\sum_{k=0}^{N-1} X_k.e^{i2\pi\frac{k}{N}n} \tag{2.25}$$

2.6.2 Cooley - Tukey Algorithm

Computing DFT from its definition on computer based systems can be uneasy and slow. Computing a DFT of N number of samples from definition takes O (N2) operations. Increasing number of sample points brings in a heavy burden on the system. Fast Fourier Transform (FFT) is an algorithm to compute DFT and its inverse. FFTs can compute a DFT with O (N. log(N)) operations [54]. Prime-factor FFT algorithm, Bruun's FFT algorithm, Rader's FFT algorithm and Bluestein's FFT algorithm are examples of FFTs.

Cooley- Tukey is the most widely used FFT algorithm. This algorithm was introduced by James W. Cooley and John W. Tukey in 1965 for the ease of Machine calculation of FFT [55]. The reason for introducing this method is that this algorithm was used to perform FFT on DSPIC for harmonics analysis in the scope of thesis study.

This algorithm is a divide and conquer method. Let number of samples N be N=N1. N2, N is decomposed into its multipliers and smaller DFTs are obtained. Further N1 and N2 are decomposed and even smaller DFTs are obtained. Best efficiency is achieved when N = 2p.

If N is chosen to be as 2m, decomposition will continue until 2 point DFTs are obtained. This case is called radix-2 decimation-in-time (DIT) Cooley- Tukey FFT.

Formal definition of DFT is defined by Equation (2.26)

$$X_k = \sum_{k=0}^{N-1} x_n . e^{-i2\pi \frac{k}{N} n} \tag{2.26}$$

Where $N = 2^p$, $0 \leq k \leq N-1$.

According to Radix-2 DIT, this formula can be decomposed into two parts by even and odd numbered samples where even numbered samples are n = 2m and odd numbered samples are n = 2m+1. Then definition of DFT in Equation (2.26) can be decomposed as Equation (2.27);

$$X_k = \sum_{m=0}^{N/2-1} x_{2m} e^{-\frac{2\pi i}{N}(2m)k} + \sum_{m=0}^{N/2-1} x_{2m+1} e^{-\frac{2\pi i}{N}(2m+1)k} \tag{2.27}$$

If we use the symbol Ek for even indexed part and Ok for odd indexed part and factor out $e^{-\frac{2\pi i}{N}k}$ from Odd indexed part, we end up with Equation (2.28).

$$X_k = \underbrace{\sum_{m=0}^{N/2-1} x_{2m} e^{-\frac{2\pi i}{N/2}mk}}_{DFT\,of\,even-indexed\,part\,of\,x_m} + e^{-\frac{2\pi i}{N}k} \underbrace{\sum_{m=0}^{N/2-1} x_{2m+1} e^{-\frac{2\pi i}{N/2}mk}}_{DFT\,of\,odd-indexed\,part\,of\,x_m} = E_k + e^{-\frac{2\pi i}{N}k} O_k \tag{2.28}$$

The important result of Equation (2.28) is that now there are two DFTs to be calculated which are ranging from 0 to N/2-1. Periodicity of DFT tells us that outputs for $N/2 \leq k < N$ are identical to $0 \leq k < N/2$ for a DFT of length $N/2$. So, $E_k + N/2 = E_k$ and $O_{k+N/2} = O_k$. We can see that multiplier of O_k can be written as Equation (2.29).

$$exp[-2\pi i(k + N/2)/N] = e^{-\pi i} exp[-2\pi ik/N] = -exp[-2\pi ik/N] \tag{2.29}$$

Which converts the sign of $O_{k+N/2}$ to $-1.e^{-\frac{2\pi i}{N}k}$ is called twiddle factor. In machine computing, twiddle factors can be pre-calculated to decrease the burden of machine and increase the speed.

The formula (2.28) now can be expressed as in (2.30). Definitions (2.30) now can be expressed for half number of samples and necessary simplifications can be done as explained in (2.27),

(2.28) and (2.29) for every decomposition by two halves. DFT is progressed in this manner until 2 point DFT (butterfly DFT) is achieved. Stages for a 8 point DFT is illustrated in Figure 2.19.

$$X_k = \begin{cases} E_k + e^{-\frac{2\pi i}{N}k} O_k & \text{if } k < N/2 \\ E_{k-N/2} - e^{-\frac{2\pi i}{N}k-N/2} O_{k-N/2} & \text{if } k \geq N/2 \end{cases} \tag{2.30}$$

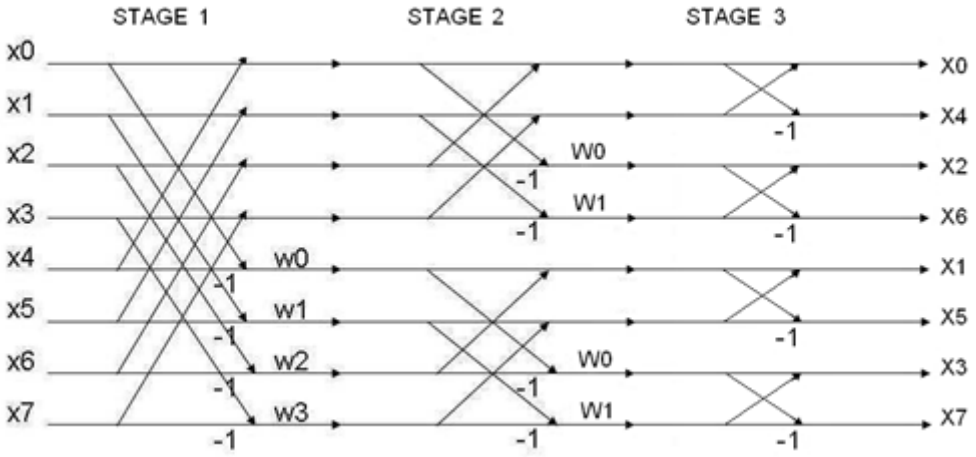

Figure 2.19: Butterfly Stages for a 8 point DFT

CHAPTER 3

SYSTEM DEVELOPED FOR CURRENT HARMONICS AND CURRENT MEASUREMENT

3.1 System Introduction

System developed for current harmonics and current measurement is composed of two parts namely data-acquisition card and control card. Those mentioned cards can be seen in Figure 3.1 and Figure 3.2. As seen by Figure 3.3, data-acquisition card works with a current sensor. This part of the system is intended to stay on the power line or at the secondary side of medium - voltage transformers for the duration of use. Second part of the system is control card. Control card is operated by the user person to start the process and obtain the results of the analysis process. Designed control card which can be seen in Figure 3.4, has a graphical

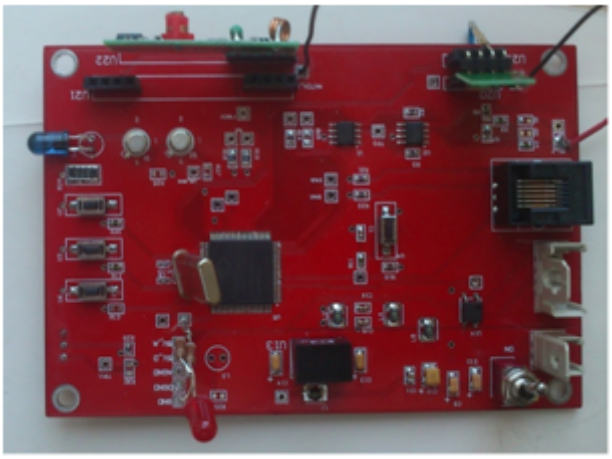

Figure 3.1: Data-acquisition card

LCD interface to give the ability to see the results drawn as a graph, on the screen. User can

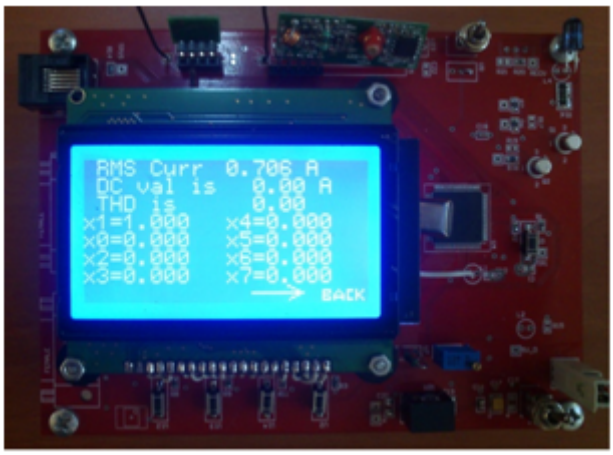

Figure 3.2: Control Card

control start-stop and repetition of process whenever needed.

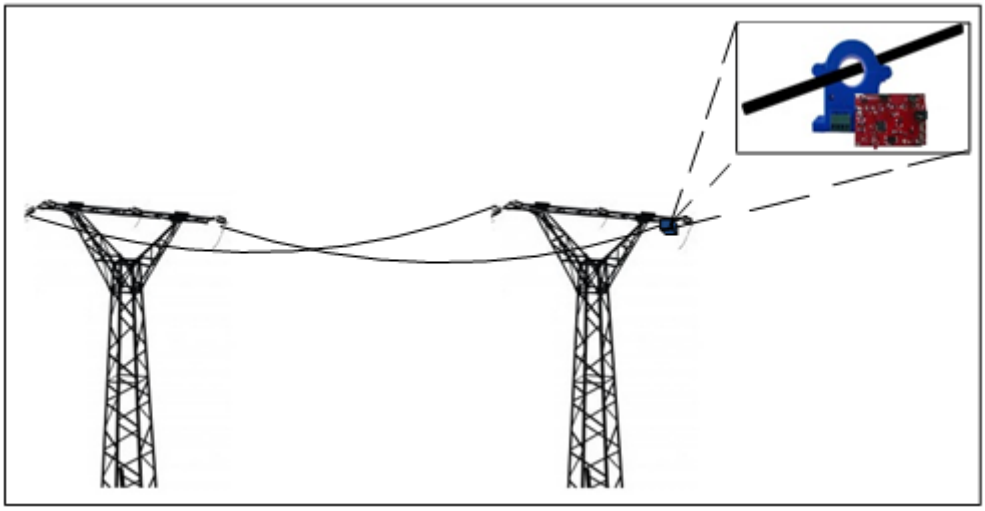

Figure 3.3: First part of the designed system: AC current sensor and developed data-acquisition card

There are various current sensors in the market which outputs AC voltages at the levels of $\pm 5V$. Designed Data-Acquisition Card accepts up to $\pm 5V$ swing of AC voltages. Output of the current sensor is a voltage waveform which is actually proportional to the value of the current that is passing through the conductor of the transmission line. This output waveform is used to take data samples by designed Data-Acquisition Card which stays with the current sensor. Sampling and analysis is triggered by Control Card with user's initiation.

Process starts with user's initiation. Start of the process message is sent from control card

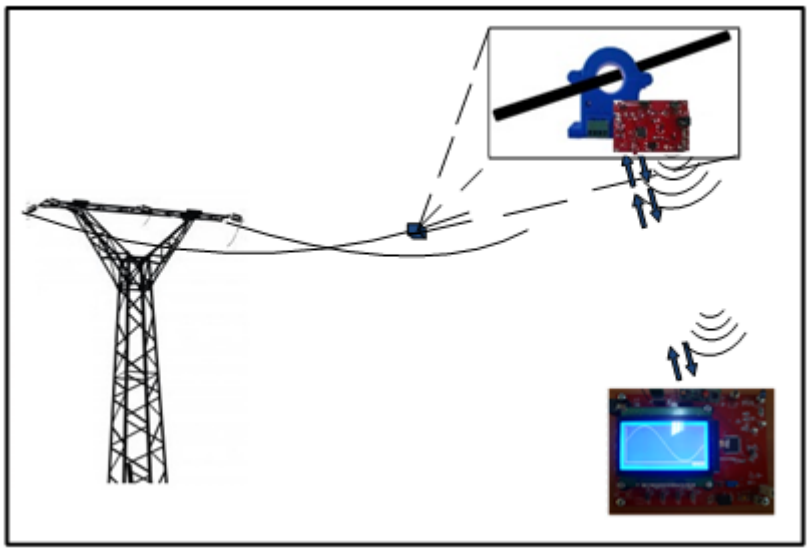

Figure 3.4: Illustration of the entire system

to the data-acquisition card. Data-Acquisition card starts sampling necessary number of data points by using analog to digital conversion on current sensor's output. By the end of sampling part data-acquisition card immediately sends data over demanded communication way. Upon receiving samples, control card performs DFT analysis to find out harmonic components of current waveform. Subsequent to harmonic analysis THD and RMS values are calculated. The stages of this process are illustrated in Figure 3.5. System specifications are found after

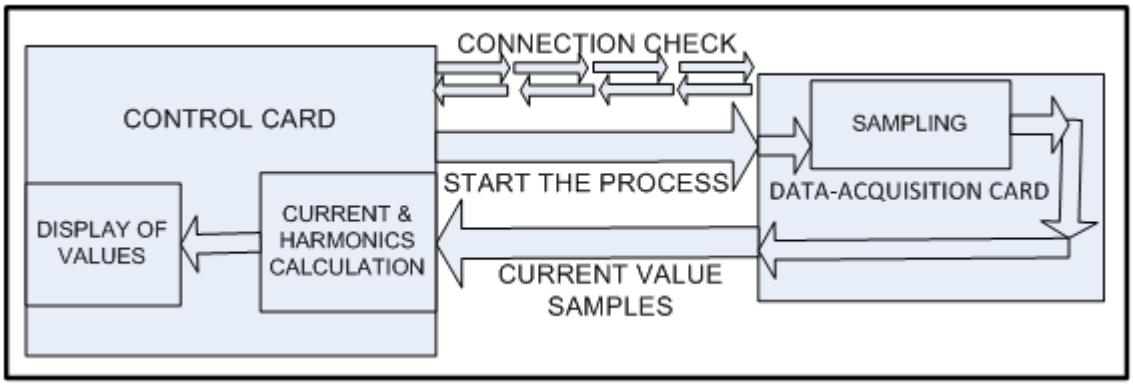

Figure 3.5: Block diagram explaining the processing stages of the system

performing various tests and given in Table 3.1.

Table 3.1: Data-acquisistion card and control card specifications

Specification	Data-Acquisition Card	Control Card
Input Voltage Range	$+6V - +35V$	$+6V - +35V$
Current Consumption	13 mA (Idle mode) 64mA (RF IR transmitting and receiving)	320 mA (Idle mode) 370 mA (RF IR transmitting and receiving)
Operating Temperature	-10 - +55	-10 - +55
RF Comm. Range	50 m	50 m
IR Comm. Range	6 m	6 m
Data sampling freq.	12.8kHz	-
Harmonic detection	-	35th

3.2 Data-Acquisition Card

Data-acquisition card is the part which is intended to stay on power line permanently. This part of the system has tasks such as: rectifying the supply voltage from sensor output, adjustment of sensor output voltage for ADC process, gathering waveform samples and communication with control card. Data-acquisition card is able to communicate over radio frequency and infrared. Functional block diagram of Data-Acquisition Card is given in Figure 3.6. Those functional parts will be examined from hardware and software aspects.

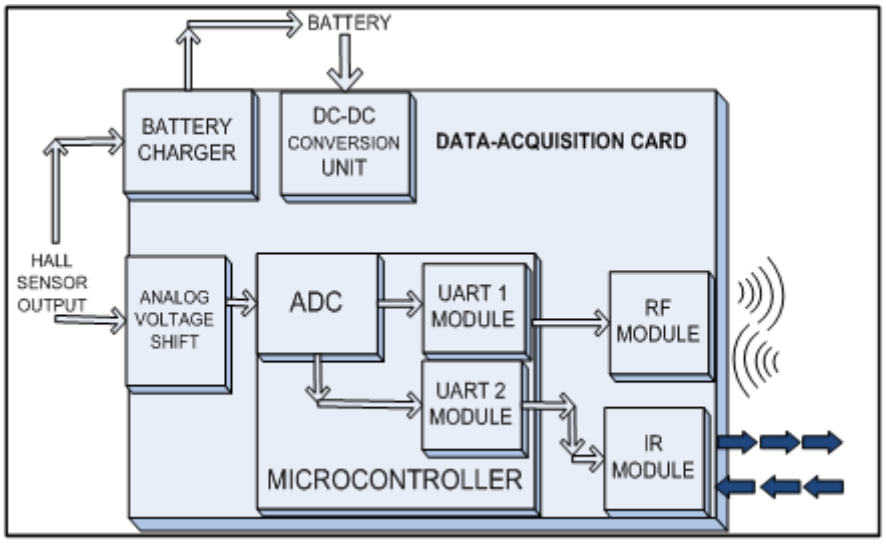

Figure 3.6: Functional block diagram of data-acquisition card

3.2.1 Hardware Definition of Data-Acquisition Card

Hardware of the Data-Acquisition Card is composed of battery charge unit, DC-DC voltage conversion unit, signal offset and analog voltage regulation part, DSP and peripherals, RF Communication Part and IR Communication Part.

3.2.1.1 Battery Charge Circuit

This part of the Data-acquisition Card is the key point for battery charging. As explained in the background section closed loop Hall effect sensors are fed from an external source to equalize created flux. Induced current is opposed by the feeding current of the external source which means that the more current induced from sensor, the more current drawn from the battery. In this case it is impossible to feed the battery from the sensor device.

Open loop Hall effect sensors with a conductor wound around the core for energy harvesting or current transducers can be used to feed battery of the system. Data acquisition card draws a current of 13 mA when not transmitting, 18mA while transmitting over RF and about 45mA with IR communication. A Hall sensor would draw around 10mA current to operate, yielding 55mA at maximum. Data transmission is performed rarely. Card can be kept waiting at sleep mode for power conservation. Also by using sleep functions of microcontroller, current draw can be reduced down to micro-amperes.

There are models of open loop Hall which can output more than its input by the help of induced current from magnetic field. Even a current transformer does not require external supply to operate. Induced current magnitude is related with the current flowing through primary conductor, of course. In the market, current transformers which can give 20mA output for 5A primary current can easily be found. Using the device where high currents are flowing would make the device to be able to charge the battery.

Figure 3.7 shows the components composing battery charge unit. ZXSBMR16P is a bridge rectifier which is rectifies the output signal of current transducer. Output of this transducer is connected to a series of capacitors to eliminate the ripples resided from former stage. Rectified and filtered DC current comes to DC-DC booster IE0312S-H which boosts the voltage up to $+12V$. Li-Ion battery charger integrated circuit LTC4008EGN receives output of booster as

an input. LTC4008EGN is able accept from $+6V$ up to $+28V$ where $+12V$ output of booster is acceptable for charger IC. Li-Ion charger drives the battery to full scale according to li-ion battery charge regulations.

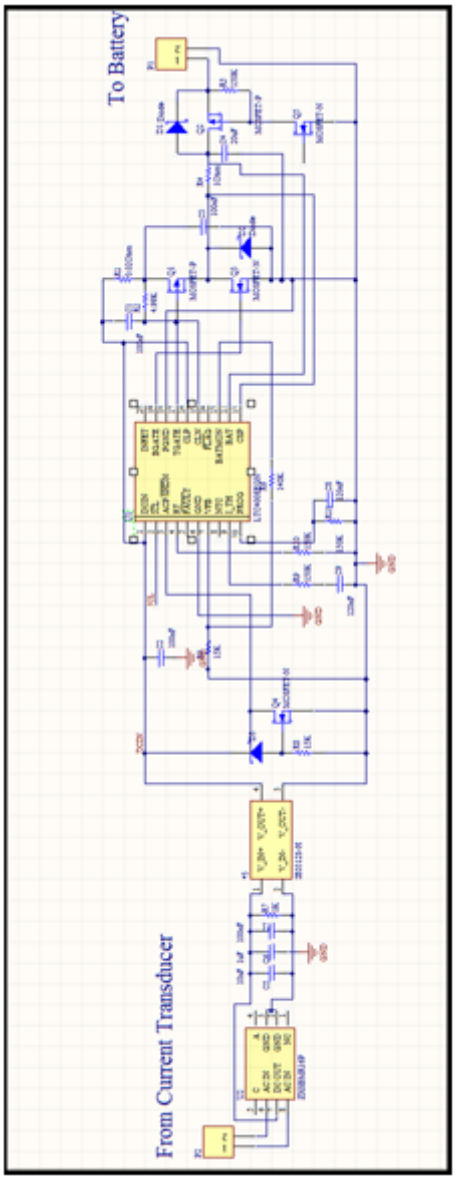

Figure 3.7: Battery charge unit schematic drawing of data-acquisition card

3.2.1.2 Power Unit

This part of the system includes all power related instruments. All of the components which take part in this section can be shown in Figure 3.8. Two power connectors are presented

in this part of the hardware. The connector KN2 is used for power input from battery. The second connector KN3 is used to transmit regulated power to current sensor if needed.

Two state switch U8 and a LED is added to the hardware. Two state switch allows the user to switch on or completely switch off the system. Either the system is switched on can be realized from the state of the LED also.

Data Acquisition Card is able to accept voltages from +6V up to +35V. This ability is gained from the XP Power SR05S05 converter. Power input from KN2 is bypassed by array of capacitors namely C9, C10, C11 and C12. Bypassing those capacitors input power is passed from converter's own capacitors and inductor. This DC-DC converter converts from voltages from $+6V$ to $+35V$ into $+5V$. All of the components in data-acquisition card are chosen to work with +5V.

AQY221R2S is a solid state relay to switch on and off in presence of a Hall sensor. This integrated circuit is controlled by DSP and switches on the sensor when needed and off when not needed for power saving reasons.

Three different ground layers are used for this card. The first ground layer GND is used for components from the beginning of input connector up to the output of DC-DC converter unit. Analog ground which has been named as AGND is used for analog part of the system. Analog part of DSP and signal offset and reduction part use AGND for ground purposes. DGND is prepared for digital part of the system. Digital part of DSP, RF and IR communication parts use digital ground. Those three ground layers are connected to each other with protection inductors. Data-acquisition card is intended to work on high voltage lines for future work. Around high voltage lines high electromagnetic field is created and corona currents passes by in the air. For safety reasons, isolating different functional parts from each other by means of grounding is a necessity. By isolating those layers a probable fault in any part of the system is inhibited from passing to the other parts. As well as in fault conditions, under normal operation, analog part shall be isolated from any other part. Analog part samples the voltage taken from current sensor which requires sensitivity and this part should not be affected from external interruptions.

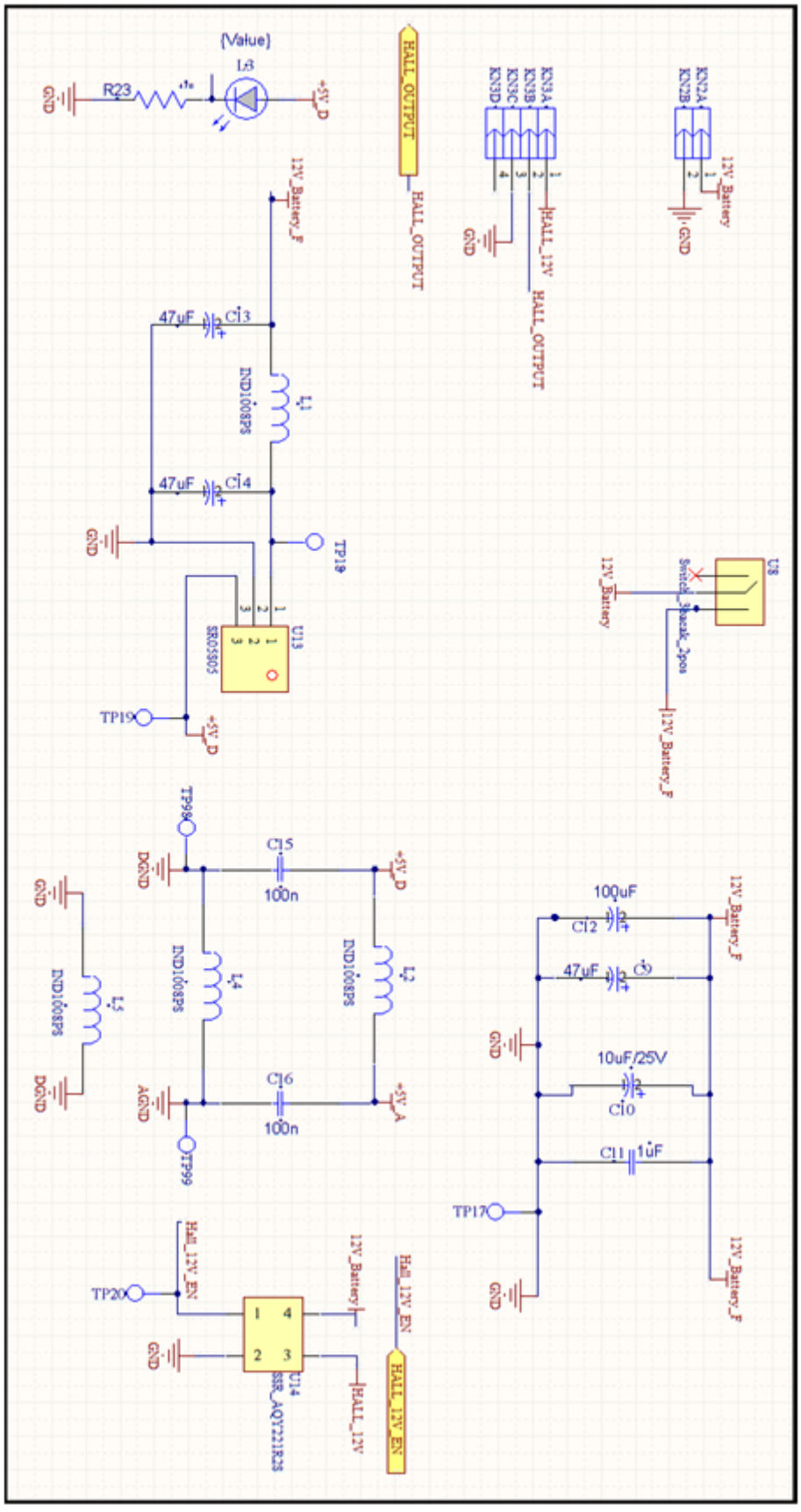

Figure 3.8: Power unit schematic drawing of data-acquisition card

3.2.1.3 Analog Voltage Regulation Part

Data - acquisition card is designed flexible to be adapted for different sensors. In the market various sensors with different output voltages can be found. DSPIC30f6010A digital signal processor used on the card accepts 0V up to +5V as analog input. Any output from sensor side to be sampled by DSP should be between 0V and +5V. For sensors with output other than 0V - 5V this part of the system works as a regulating part.

As can be seen from Figure 3.9 first OP191GS op-amp is connected to the output of sensor and to $+5V$ with a resistor arrangement. Test harmonic input is included in the system and connected to op-amp for test purposes. For outputs of $\pm 5V$ AC, setup in Figure 3.9 is used. The first op-amp sums $+5V$ DC and input at equal rates yielding a result of $0\text{V} - +10V$. This result is still not appropriate for DSP and this voltage is divided by two to obtain an input of $0V - +5V$. Second op-amp serves as a buffer between DSP and first op-amp for safety reasons.

Correctness of this part has been verified under tests and under simulations. Figure 3.10 shows the simulation results of this part on oscilloscope screen. Sinusoidal signal oscillating between $-5V$ - $+5V$ is given as input to the part and an output of $0V - +5V$ signal is obtained as a result.

This part can be modified to suit for other sensors by arranging R2, R3, R4, R7, R8, and R9 resistors.

3.2.1.4 DSP and peripherals

Data - acquisition card is driven by digital signal processor DSPIC30f6010A. This DSP is responsible for sampling of sensor data and communicating with control card. PWM output and one channel of UART of controller is connected to IR communication part while the other channel is reserved for RF communication.

7.37 MHz crystal oscillator is connected to the processor. This oscillation value is increased to 30 MHz internally by processor with the help of PLL to obtain high working rate.

KN1 which can be seen in Figure 3.11, is programming and debugging connector of the card.

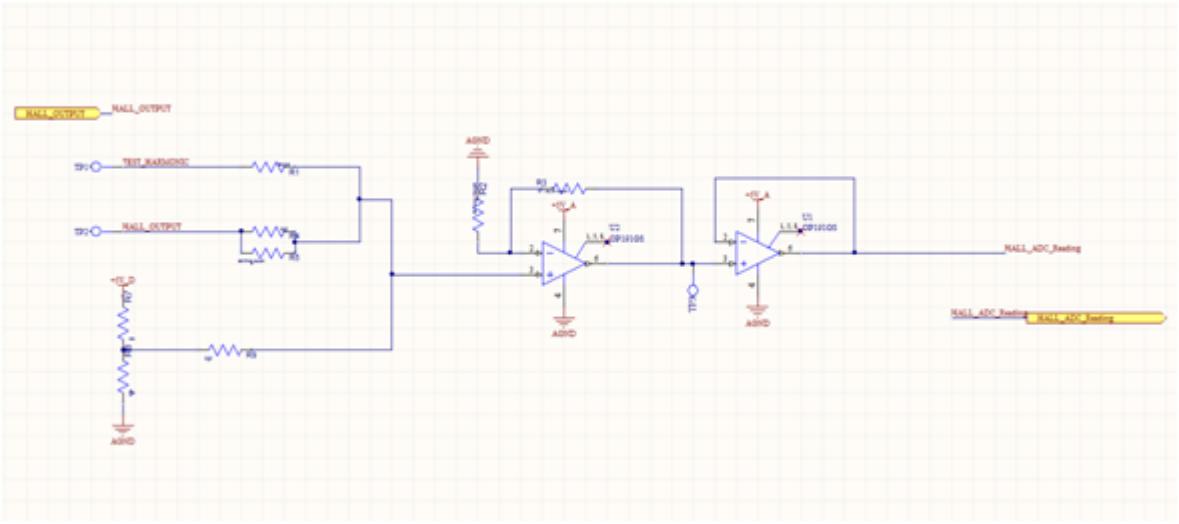

Figure 3.9: Analog voltage regulation part schematic drawing of data-acquisition card

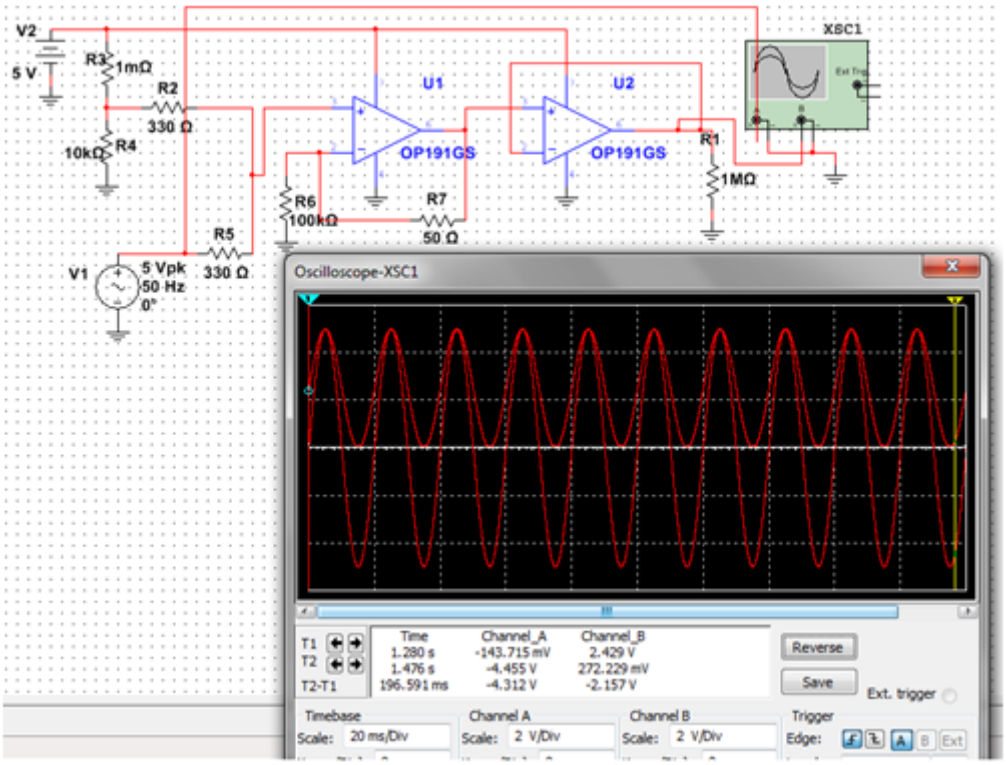

Figure 3.10: Simulation results for analog part

Software of processor can be updated any time without disassembling the processor or any integrated circuit. This in circuit programming part is designed to work with MPLAB ICD3.

Bypass capacitors for every power input of DSP are presented in this part. Three push buttons are added to this card for debug purposes. In order to switch on-off solid state relay and RF transmitter, necessary output pins are connected to the related integrated circuits.

This processor was chosen for this thesis for its features about digital signal processing capabilities and communication channels. Reasons for choosing this processor is explained in section 3.3.1.2 and some features of processor are given in Appendix A.

3.2.1.5 RF and IR Communication Part

Data-acquisition card is able to communicate over radio frequency and infrared wavelength. As can be seen from Figure 3.12, RF transmitter and receiver modules are used to enable RF communication. Two different patterns for receiver and transmitter are included in the design for different modules which can be found in the market. In this thesis study, U22 and U23 patterns are used for UDEA ARX34C and ATX34S modules. These modules can be seen in Figure 3.13(a) and (b). Those modules work at 433.930MHz and communicate up to 50 meters. Distance varies with conditions of surrounding. As transmitter and receiver antenna a cable about 17.3 cm is used. At 433.930MHz, Lambda/4 antenna length is about 17.3 cm. These modules are serially connected to processor by UART channels. A 2N2222A npn junction transistor is connected to the ground pin of transmitter module. This transistor enables to switch off transmitter module when not needed. When powered, transmitter module emits carrier signal regardless of transmitting data. If transmitter modules of two cards are powered, carrier signal conflict occurs resulting none of the cards can transmit, therefore switching off transmitter is necessary. Switching off the transmitter also helps to save energy. Infrared communication is maintained by IR transmitter LED and IR receiver LED. Receiver LED accepts data which is modulated with a PWM signal as can be seen from Figure 3.14. Output of receiver drops to zero when a burst is detected. Reverse logic of receiver and modulation is provided by two npn transistors named as Q1 and Q2 at the transmitter side. Output to transmitter and input from receiver IR LEDs is connected to tx and rx pins of UART channel, respectively.

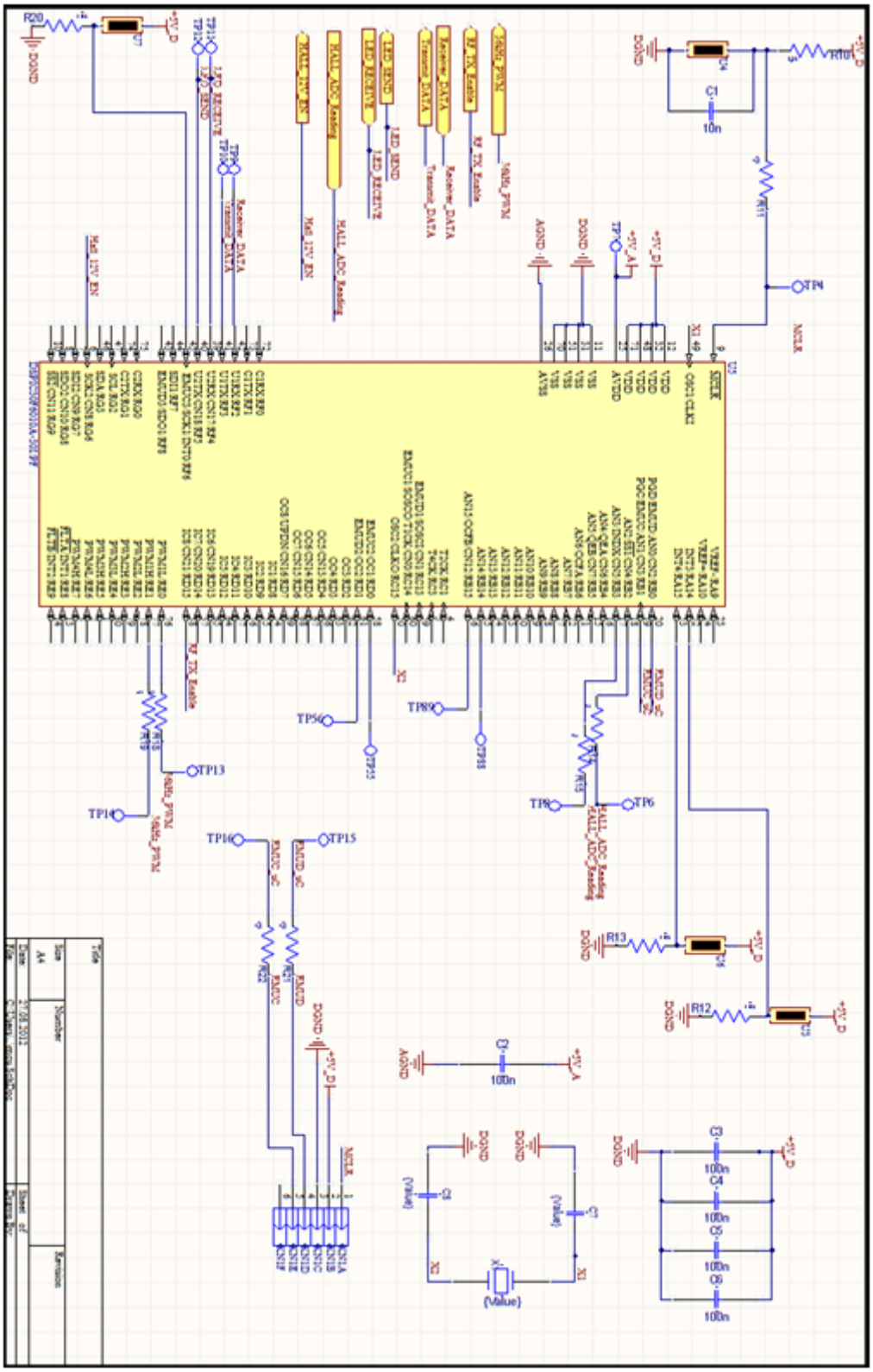

Figure 3.11: DSP and peripherals schematic drawing of data-acquisition card

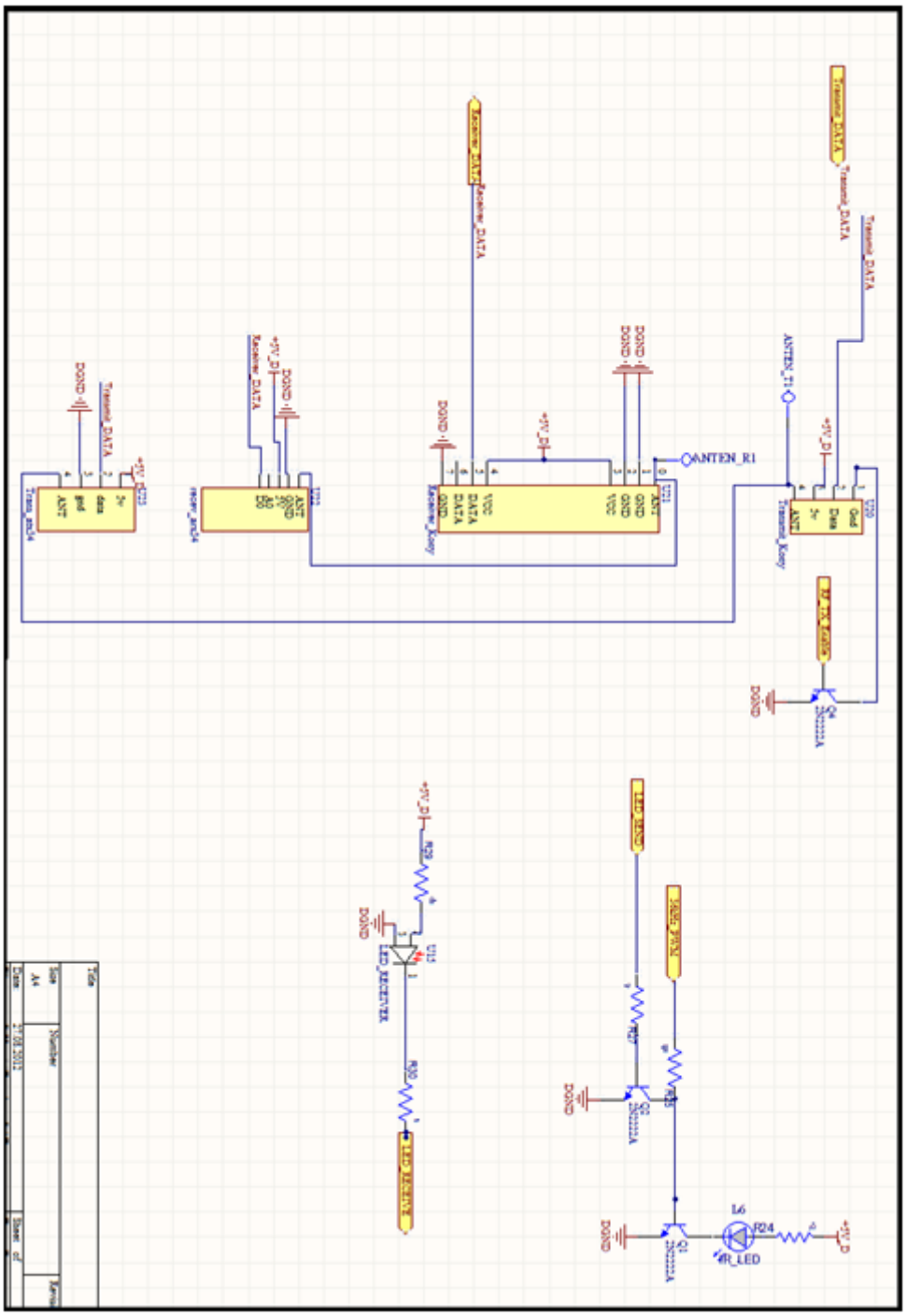

Figure 3.12: RF and IR communication unit schematic drawing of data-acquisition card

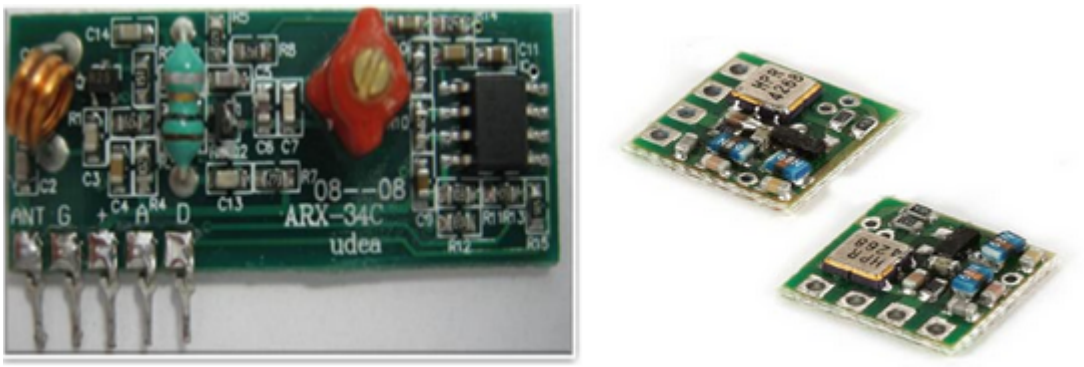

Figure 3.13: (a). UDEA ARX34C receiver (b) UDEA ATX34S transmitter

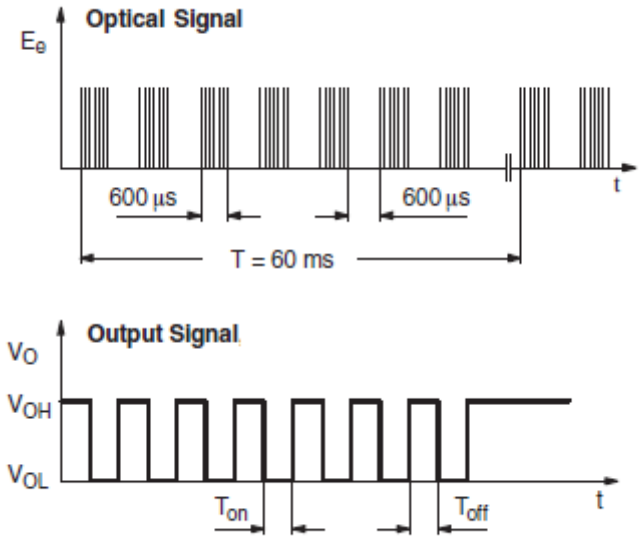

Figure 3.14: Infrared signal and corresponding output at the receiver side

3.2.2 Software Definition of Data-Acquisition Card

In this section software of data-acquisition card is inspected in details.

3.2.2.1 Software Module for ADC

Outputs of used current measuring devices used in this study are analog voltages which are directly proportional to the current flowing through main conductor. To study on those analog outputs, they should be transferred to digital platform using an analog-digital converter. Selected DSP has a 10-bits ADC module, which was used to digitalize sampled data. Sampled data about sensor output is expressed as a number between 0 and 210 for the use of digital operations. Wireless communication between electronic cards is based on 8-bit protocol therefore only eight of ten bits are used for DFT operations.

Analog reference voltage of DSPIC (AVDD) is 5 Volts and this voltage is expressed with 8 bits i.e. a number between 0 and 256. 5V/256 results 19.53 mV which is analog to digital conversion precision of controller.

Analog to digital conversion is done in two steps in DSP. Those steps are sampling and conversion phases. In sampling step, voltage level of analog signal is obtained at the moment of sampling. In conversion phase this corresponding voltage level is converted into digital number which is expressed as binary.

In this study, ADC timing is set such that in a period of 50Hz signal ADC module samples the signal 256 times. The reason for sampling the signal for 256 points is to obtain an appropriate number for DFT operation. DFT software in control card works with 2n number of samples for transforms. In DFT code samples are taken at just a period of signal. 1 period of 50 Hz signal is 1/50 = 20ms. In a time period of 20ms 256 ADC operation is completed; so that in every 20ms/256 = 0.078ms, one sample is obtained.

DSP allows to convert ADC data into integer, signed integer, fractional and signal fractional. Desired form is selected by the use of FORM bits which reside in ADCON1 register. In software of data-acquisition card, unsigned integer form is used as the return value of ADC. In DFT software fractional value is used so that integer to fractional transformation is done in control card.

ADC initialization and necessary software reside in adc.c file. adc_init and $get_samples$ functions are used for ADC operations. ADC module is turned on when ADC operations are needed to be done and turned off when operations are completed.

3.2.2.2 Software Module for RF Communication

Communication between data-acquisition card and control card are done by wireless methods. Radio frequency (RF) communication is the main method of communication for this system. RF system is faster and more reliable than infrared communication. As mentioned in hardware definition of data-acquisition card UDEA ARX34S and ATX34C modules are used for RF communication. Those modules are serially driven modules and in order to use benefits of ready serial module of DSP, universal asynchronous receive transmit (UART) channel is connected to those modules.

$uart_RF_init$, $U1RXInterrupt$ and RF_send functions residing in uart.c are the functions of radio communication. In $uart_RF_init$ function UART channel 1 is arranged so that communication baud rate is 1200. This adjustment is done by the help of U1BRG register taking into consideration crystal speed. 8 bit communication with 1 stop bit and no parity bit is set U1MODE bits. Upon receiving a byte from serial channel an interrupt request is desired so that interrupt request is enabled by setting IEC0 bits. Interrupt request is set so that for every character received, an interrupt request is generated. Generated receive interrupt request is served in U1RXInterrupt function. $COMM_FLAG$ character is a character which keeps the record of present communication type.

RF modules require hardware and software synchronization before communicating. As can be seen from Figure 3.15, preamble and synchronization is required before data trading. Preamble is sent for hardware synchronization. Preamble data is an array which is composed of consecutive 1's and 0's. In order to synchronize hardware's, 2 bytes of 0x55 are sent before software synchronization. Software synchronization data is composed of 1 byte of 0x00 and two bytes of 0x33 for data-acquisition card. Control card sends 1 byte of 0x00 and two bytes of 0x34. Before every data transfer hardware and software synchronization bytes are sent. This method decreases throughput but increases reliability. Two responses are returned from data-acquisition card when a byte is received from RF channel. If a byte of 0xAA is received 0xBB is returned in order to indicate that RF channel is active and cards can commu-

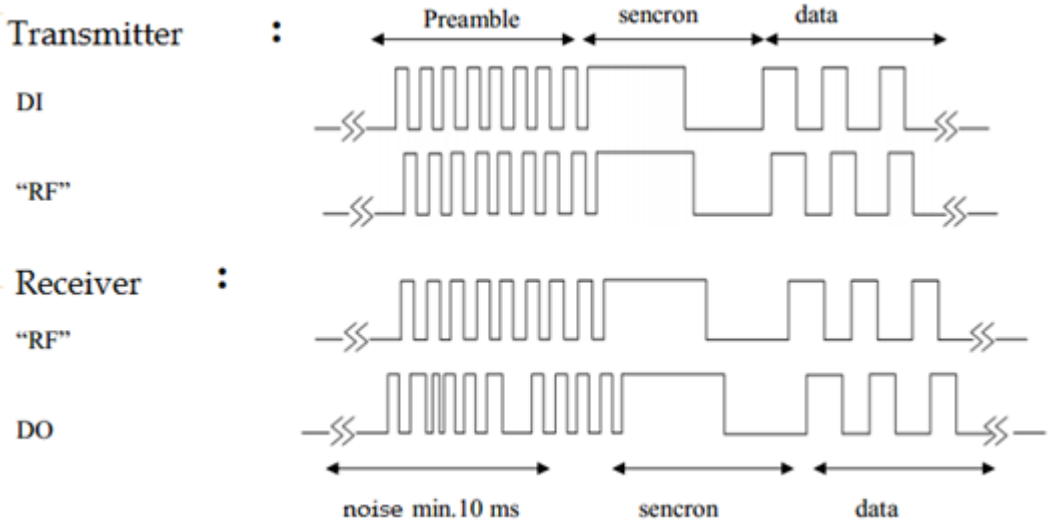

Figure 3.15: Transmitter and receiver data format for UDEA modules

nicate over RF. This check is done before every RF communication. Receiving 0xCC means that sampling should be done and sent over RF. Upon receiving 0xCC, data-acquisition card obtains 256 bytes of samples and sends over RF immediately.

Future work and improvement suggestions are done for RF part and can be found in conclusion and future works chapter.

3.2.2.3 Software Module for Infrared Communication

IR communication is the secondary communication method for designed system. As defined in the hardware part, IR receiver and transmitter transfer a modulated data. This is a simple modulation of square wave at 38 KHz. In order to make modulation, PWM feature of DSPIC is used. As the communication channel, UART2 is used. IR_init function is the initialization function of IR communication software. IR communication can not reach high speeds. U2BRG register is adjusted so that 400 baud rate is selected as the communication speed. By the help of U2MODE register, communication protocol is set so that packet size is 8 bits. Parity bit is not used and one stop bit is added at the end of every packet. Interrupt of UART2 channel is devoted to IR communication. For every received character through this channel, an interrupt is created.

$COMM_FLAG$ flag is an unsigned character which keeps the record of present communication type. Upon receiving a character over UART2, this flag is set to IR and necessary response is sent over IR.

In the software receiving some special bytes have some meanings. If a 0xAA byte is received over IR channel, it has a meaning that control card desires to check IR connection. Upon receiving this byte, 0xBB is sent to report that IR channel is active. Receiving 0xCC has a meaning that control card requests samples to be taken and sent. Upon receiving this command data-acquisition card samples 256 points of data and sent over IR channel immediately.

3.3 Control Card

Control Card is the user - system interface part. This part of the system has the tasks such as: Regulating power received from battery, providing the user menu to make user informed about the process, performing mathematical calculations and communication with the data-acquisition card. Functional block diagram of control card is given in Figure 3.16. Those functional parts will be examined from hardware and software aspects.

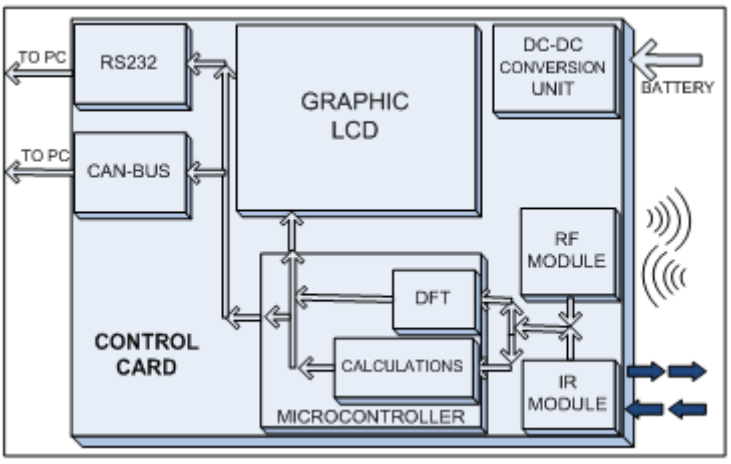

Figure 3.16: Functional block diagram of control card

3.3.1 Hardware Definition of Control Card

Hardware of control card is composed of power unit, DSP layer and communication part. In the following sections these parts will be described.

3.3.1.1 Power Unit

Power unit of control card is similar to the power unit of data-acquisition card. Schematic drawings of this unit is depicted in Figure 3.17. A two state switch is added to switch on and off the system. Either the system is powered can be seen from power state LED or from graphic LCD. Power from battery is taken from KN4 connector. For control card 9V PP3 batteries are chosen to work with. Current from battery is filtered by bypass capacitors C15, C16 and C17. These capacitors filters sparks which Filtered power reaches to dc-dc converter by passing C19, C20 capacitors and L3 inductor. DC - DC converter SR05S05 converts +9V input voltage to +5V for internal usage.

DGND is the ground of the system. As there are neither analog operations nor operations requiring precision, only one ground layer is sufficient for this system.

3.3.1.2 DSP and peripherals

DSP is the most important component of control card. DSPIC30F6010A is used as processor for both of the electronic cards. In control card DSP has following tasks as communicating with data-acquisition card, performing signal processing operations and operating user menu. Communication with other devices over RS232 or CAN-BUS are included in design but not implemented.

There are some reasons why this controller is chosen. Firstly, this controller is a DSP controller and have advantages making digital signal processing tasks over traditional microcontrollers. This controller has a DSP library which is prepared by Microchip. This library eases to make complex DSP operations by proper use of the library. Price of this controller is inexpensive and can be bought at a price of 8 euros. Single supply usage is an advantage for designer. Multiple voltage supply means several dc-dc converters and additional components in the embedded system which increases the complexity of the design. Two UART channels

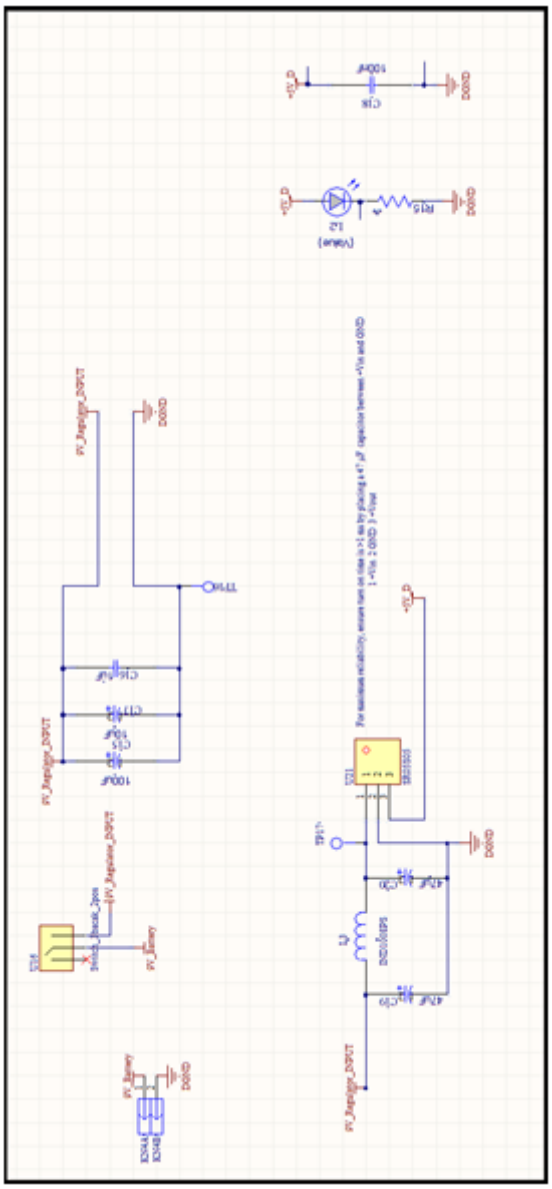

Figure 3.17: Power unit schematic drawing of control card

and PWM feature enables to implement RF and IR communication at the same time.

In Figure 3.18 and Figure 3.19, digital signal processor and its peripherals are presented. External crystal usage is chosen for timing accuracy reasons and 7.37 MHz crystal oscillator is connected as a clock source. This 7.37 MHz clocking rate is enhanced to 30 MIPS internally to gain processing speed. Four external interrupt pins are used for user push buttons. Those buttons are placed under graphic LCD to control user menu. Another button is used for reset operation. Button U23 is connected to MCLR to reset the card when needed.

Two two-state switches are used to switch UART1 channel between RS232 channel and RF communication modules. DSPIC30F6010A has two UART channels and control card has four serial communication ways as RF, IR, RS232 and CAN. CAN-BUS has its own communication channel on DSP. Two of remaining three serial ways are switched using those switches. RS232 communication was not been implemented by means of software and left as a future work .

In Figure 3.19, character and graphic LCDs are presented. $CAN - BUS$ and RS232 driver circuit and their connectors are shown in this figure. Control card use a 128x64 resolution graphic LCD to display graphics and writings. With more resolution one can show graphics more accurately. Increasing the resolution increases size or price of LCD. One of the goals of this study is to build a system at low costs. LCDs with this resolution are found in the market with ease at appropriate prices therefore chosen to be used in this study. Winstar WG12864B-TMI-VN model graphic LCD is used in this study. MAX232CPE is used as RS232 driver IC and a DSUB-9 is placed for connection. SN65HVD230M-EP is used as CAN-BUS driver and another DSUB-9 connector is placed on the card. RS232 and CAN- BUS communication parts were not implemented and left as a future work.

RJ-11 jack is used for MPLAB ICD3 programmer/debugger connection. Control card also has the ability to be programmed in circuit.

3.3.1.3 RF and IR Communication Part

For RF and IR communication, exactly the same components with data-acquisition card are used for the control card. Connections and design logic is same therefore schematic drawings are not given again. Design is explained for data-acquisition card in section 3.3.1.5.

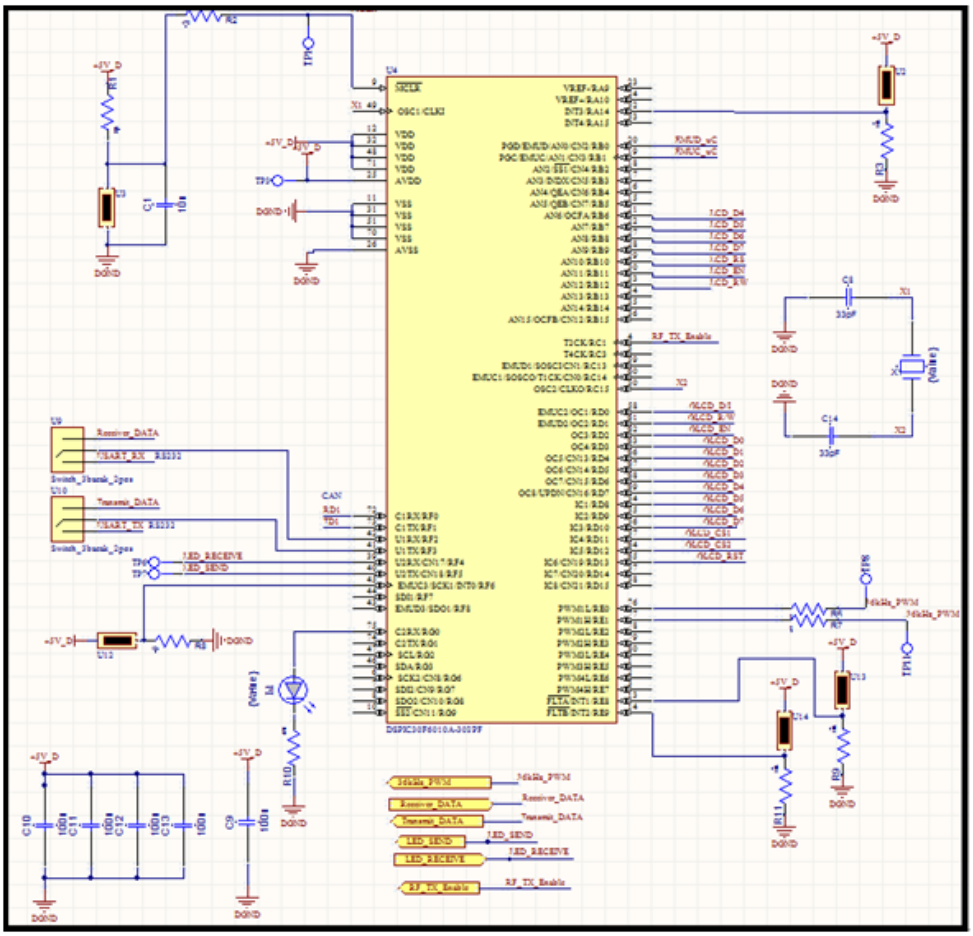

Figure 3.18: DSPIC30F6010A and peripherals schematic drawing of control card

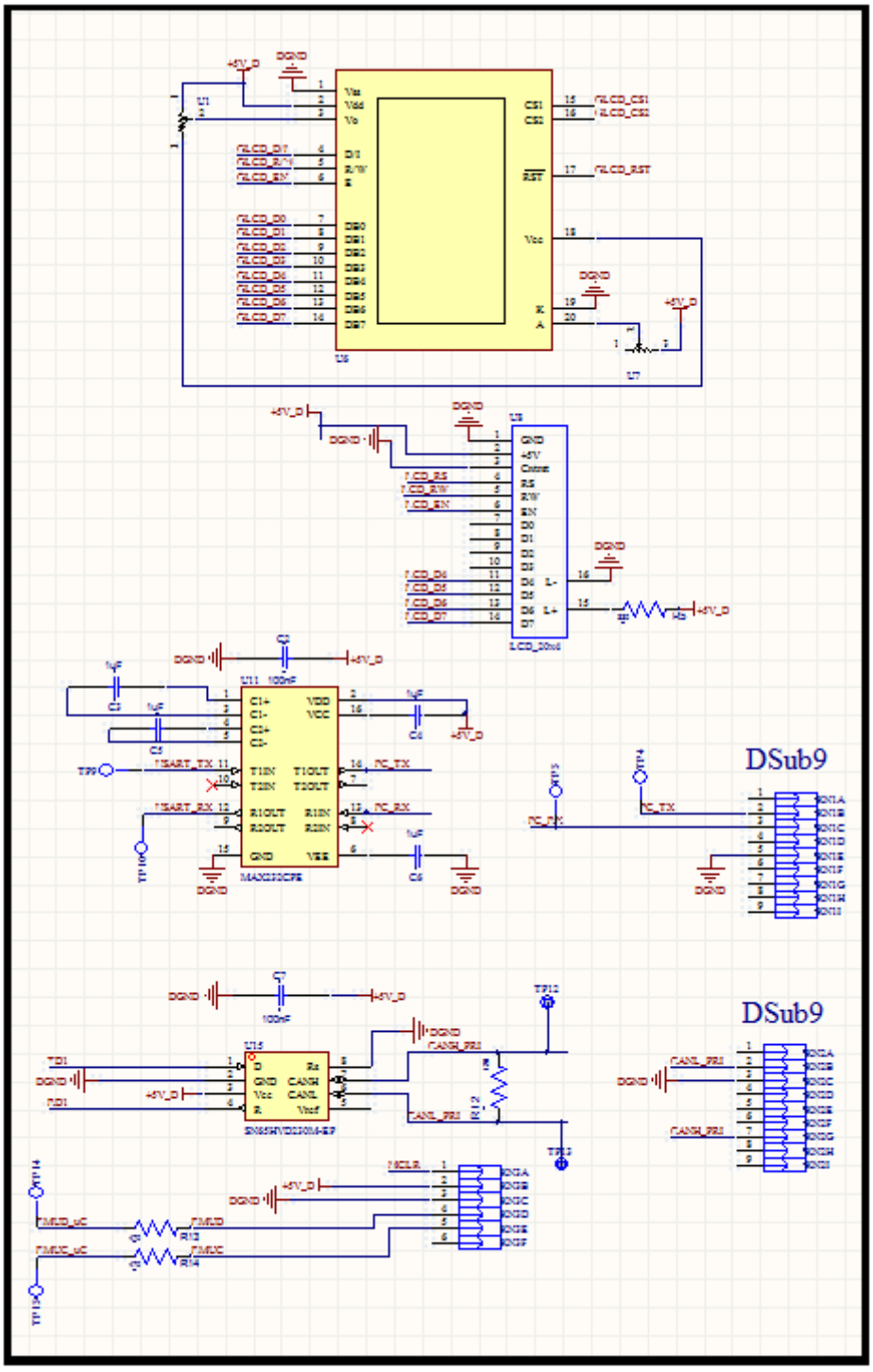

Figure 3.19: Character LCD, Graphic LCD and serial communication peripherals of control card

3.3.2 Software Definition of Control Card

3.3.2.1 Software Module for Fast Fourier Transform

Fast Fourier transform (FFT) software is one of the important part in control card software. A fast Fourier transform (FFT) is an algorithm to compute the discrete Fourier transform (DFT). This part of the software is used to decompose sinusoidal components of signal at different frequencies i.e. harmonics of the signal.

FFT functions residing in dsp.h library of Microchip are used to calculate some steps of transform. FFT software takes samples in fractional format. Samples which are taken from data-acquisition card are in integer format with a length of 1 byte. Functions in char2frac.c and frac2char are used to make conversations between fractional and integer. FFT software can work with 64, 128, 256 and 512 samples. In this study 256 samples are chosen to be work with. FFT_BLOCK_LENGTH in fft.h is set as 256 to set necessary variables to work with 256 samples. $LOG2_BLOCK_LENGTH$ is set to 8, where 256 is 28.

In butterfly stages FFT needs Twiddle coefficients. Those coefficients are defined in program memory. FFT process is performed in several steps:

- Samples are converted from integer format to fractional format. This operation is performed by $convert_char2frac$ function which is in char2frac.c file. Received samples are stored in sigCmpx array which is a fractcomplex array. A fractcomplex data type is defined as a combination of real fractional and an imaginary fractional data.
- Received samples are scaled to express fractional numbers between $[-0.5, +0.5]$. Samples are initially numbers which are between $[-1, +1]$. Shifting 1 bit to right scales these numbers between $[-0.5, +0.5]$. Scaled data is written into real part of sigCmpx array
- Imaginary part of sigCmpx array is initialized as 0.
- FFTComplexIP function is called to process butterfly stages. This function is called from dsp.h library of Microchip. Results which are obtained at the end of FFT process are stored in signal data array to save memory.
- BitReverseComplex function reorders the results which are residing in sigCmpx as most

significant bit is reordered as least significant and, so on. Results are reverse ordered after FFTComplexIP function.

- SquareMagnitudeCplx function calculates magnitudes of complex results residing in sigCmpx array.

At the completion of those steps, harmonic components of signal is obtained. Every harmonic value including DC value are found in sigCmpx array in order. 0th element shows the DC value of signal. Main signal which is assumed to be 50 Hz is found in 1st element. For example 5th element which is 250 Hz can be found in 5th place.

Obtained results are used to display harmonic values on graphic LCD. Those values are listed in harmonics table and drawn on a spectrum.

A digital signal processor has advantages over conventional processors. DSPs have built-in hardware for dsp operations which provide helps to perform those operations in a higher-speed fashion. Required number of cycles for dsp operations for dsPIC30F6010A is given in Table 3.1.

3.3.2.2 Software Module for Radio Frequency Communication

RF communication for control card is similar to that of data-acquisition card. Control card sends 0x34 before every byte to introduce itself to the data-acquisition card and to synchronize software. Like data acquisition card software, necessary RF communication functions reside in uart.c file. Those functions are $uart_RF_init,_U1RXInterrupt$, RF_send and $rf_receive_samples$.

3.3.2.3 Software Module for Infrared Communication

Software for IR communication part for control card is very similar to that of data-acquisition card. For connection check control card sends 0xAA and expects to receive 0xBB. Demanding the samples is done by sending 0xCC to data-acquisition card.

Table 3.2: Required number of cycles for DSP Operations [56]

Function	Cycle Count Equation	Conditions*	Number of Cycles	Execution Time @30 MIPS
Complex FFT**	—	N=64	3739	124.6 µs
Complex FFT**	—	N=128	8485	282.8 µs
Complex FFT**	—	N=256	19055	635.2 µs
Single Tap FIR	—	—	1	33 ns
Block FIR	53+N(4+M)	N=32, M=32	1205	40.2 µs
Block FIR Lattice	41+N(4+7M)	N=32, M=32	7337	244.6 µs
Block IIR Canonic	36+N(8+7S)	N=32, S=4	1188	39.6 µs
Block IIR Lattice	46+N(16+7M)	N=32, M=8	2350	78.3 µs
Matrix Add	20+3(C*R)	C=8, R=8	212	7.1 µs
Matrix Transpose	16+C(6+3(R-1))	C=8, R=8	232	7.7 µs
Vector Dot Product	17+3N	N=32	113	3.8 µs
Vector Max	19+7(N-2)	N=32	229	7.6 µs
Vector Multiply	17+4N	N=32	145	4.8 µs
Vector Power	16+2N	N=32	80	2.7 µs
PID Loop Core	—	—	7	231 ns
*C= #columns, N=# samples, M=#taps, S=#sections, R=#rows **Complex FFT routine inherently prevents overflow				
1 cycle = 33 nanoseconds @ 30 MIPS				

3.3.2.4 Software Module for Graphical LCD Menu

Running the control card and governing the process is done with the help of user menu which is displayed on a graphic LCD placed on control card. This LCD is 128 pixels wide and 64 pixels height and driven with parallel data. Necessary initialization and drawing functions are gathered in glcd.c file. This file holds many useful functions like drawing circle, square, rectangle, bar and text writing.

Drawing picture function is useful by means of drawing complex pictures. Some screen images and some part of various screen images are produced by drawing picture function. Those pictures are prepared under MS-paint as 128x64 screen resolution and saved as bitmap images. In order to transfer these bitmap images into hexadecimal numbers, Bmp2asm program is used. Upon a function call for $draw_picture$ with related hexadecimal array, desired image is constructed on the screen.

Menu of control card is generated by connecting states of menu in a logical form. Figure 3.20 shows logical states of menu and state transitions. A state machine is constructed to manage those transitions and $menu_state$ function is assigned to execute transitions. This function takes button press event as input. There are four push buttons under graphic LCD for user to interact with control card. When user pushes a button, an external interrupt is generated in DSP. Interrupt service routine immediately deactivates external interrupts in order to inhibit undesired external interrupt created from voltage bouncing arising from button push. In service routine $menu_state$ function is called with related button press event information. This function keeps the record of last menu stage and decides next stage by taking into account last stage and last button press event. Going back between stages is provided by ”back” option in stages which can be seen in Figure MENU.

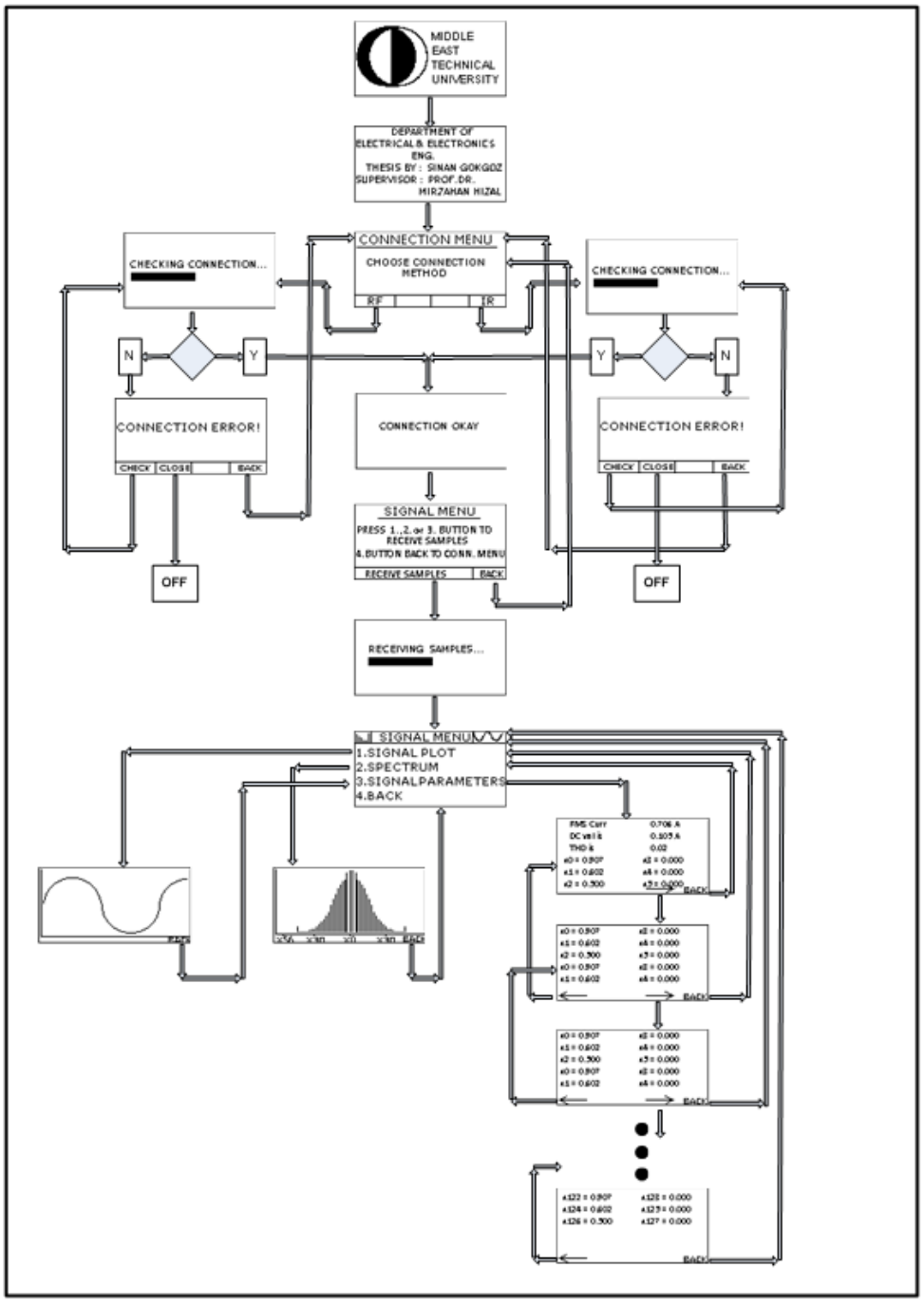

Figure 3.20: Software flow diagram for control card menu

CHAPTER 4

RESULTS AND OBSERVATIONS ABOUT PERFORMED TESTS

4.1 Tests Conducted with Different Signal Types in Laboratory Environment

Those tests are performed with software produced signals and signal generator generated signals. Tests in this section are useful to test validity of FFT software of control card, menu and communication between cards. In the following section, tests conducted with current transformers and Hall effect sensors are presented.

In those software tests, $\pm 5V$ output of current sensor is accepted that it corresponds to 1A peak primary current through current carrying conductor. Samples are arranged so that one period of main signal is samples in every case.

4.1.1 50 Hz Pure Sinusoidal Wave

This test is software based. 256 samples of a 50 Hz sinusoidal which has a 5V peak is produced in data-acquisition card with the following code snippet;

```
for(i=0;i<256;i++)
{
samples[i] =1*sin((double)(PI*2*(i*256/360)/180));
}
```

Created sinus waveform can be considered as $sin(2.\pi.f.t)$, where f is 50Hz.

In order to verify obtained values same data is processed with MATLAB, harmonic values are found by the help of FFT with the following code snippet:

```
t=0:1/128:2-1/128;
s_t=1*sin(1*pi*t);
plot(t,s_t);
x=fft(s_t);
x=fftshift(x);
y=abs(x);
y = y/128;
figure;
plot(y);
```

Produced samples are transferred to control card and results are observed. In Figure 4.1(a) and (b), obtained signal waveform from system and MATLAB can be seen. Figure 4.1(a) shows a sinus which has no harmonic component which is an expected result for this test.

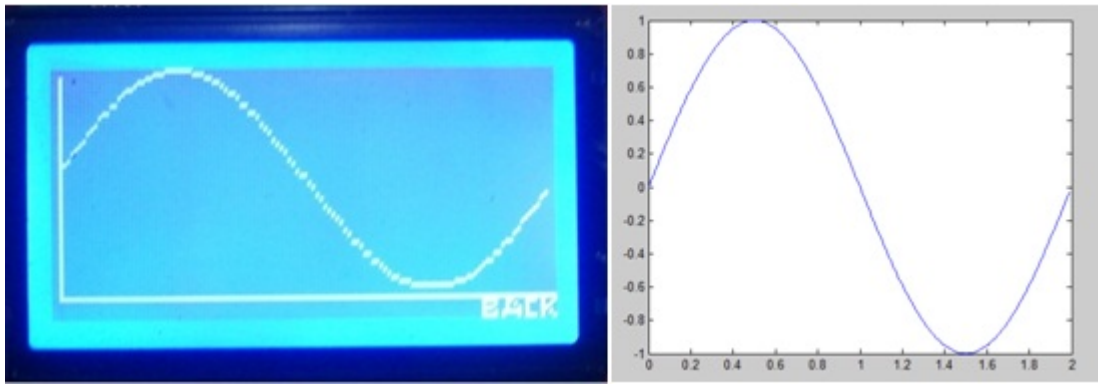

Figure 4.1: (a) Signal Waveform -control card (b)signal waveform- MATLAB

Figure 4.2 shows harmonic components of the signal. In this menu, greater values are adjusted to be presented to be at the beginning of the list. x1 is the first harmonic as being 50 Hz component. This component of the signal which is found to be 1 and others as 0. Result can easily be seen to be true. This is a 5V peak sinus signal with only one component which is signal itself. DC value is found to be 0 which is a correct result also.

Root mean square (RMS) value of the signal is found to be 0.706 A. As explained in section 2.5, for a unity peak sinus RMS is calculated as$Vpeak/2$simply, which is about $1/1.4142$ =

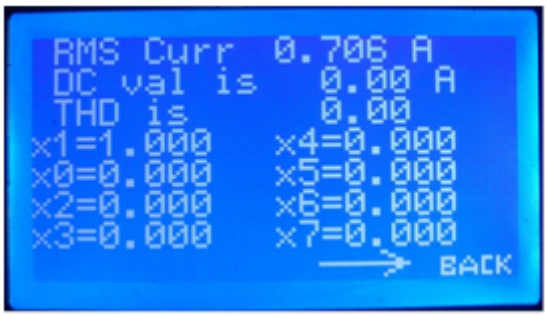

Figure 4.2: Signal parameters found in test

Table 4.1: Comparison of found values between control card and MATLAB

Parameter	Control Card Results	MATLAB Results	Absolute Error%
THD	0.0	0.0	0%
RMS	0.706	0.707	0.14%
1st Harmonic	1.00	1.00	0%

0.707. This is a theoretical study and 5V peak sinus input can be interpreted as 1A primary current. In this situation obtained value 0.706 A is pretty close to the expected result.

As explained in section 2.4, THD is calculated using current magnitudes:

$$THD = \sqrt{0^2 + 0^2 + 0^2 + ...}/1 = 0.0$$

which is found to be 0 by control card also.

Spectrum screen is arranged so that harmonic components are aligned symmetrically around 0^th component. As can be seen from Figure 4.3(a), DC component of the signal is zero and there are only two bars (actually one, two bars because of symmetry) around DC component. Figure 4.3(b) shows spectrum obtained from MATLAB. As can be seen from figure, obtained spectrum is same with the one found with control card. There is only one harmonic component around DC value which is 1st harmonic and DC value is 0.

4.1.2 50Hz Sinusoidal Signal with 4th Harmonic

In this test, same setup is utilized with the one in 4.1.1. 256 data samples are produced where 1st harmonic signal with 4th harmonic signal is summed by software with the code snippet written in data-acquisition card:

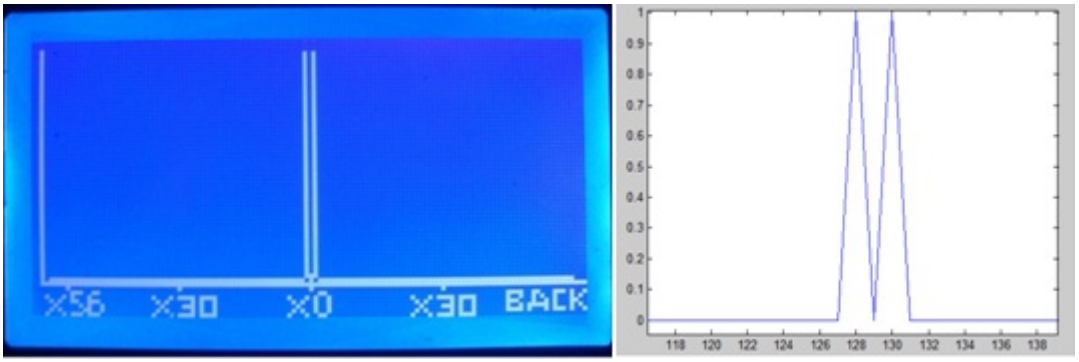

Figure 4.3: (a) Spectrum - control card (b) Spectrum- MATLAB

```
for(i=0;i<256;i++)
{
    samples[i]=
    0.5*sin((double)(1*PI*2*(i*256/360)/180)) +
    0.4*sin((double)(4*PI*2*(i*256/360)/180));
}
```

Created sinus waveform can be considered as $0.5 * sin(2.\pi.f.t) + 0.4 * sin(2.\pi.4.f.t)$ where f is 50 Hz.

In order to verify data to be obtained same signal is produced with MATLAB with the following code snippet:

```
t=0:1/128:2-1/128;
s_t=0.5*sin(1*pi*t)+0.4*sin(4*pi*t);
plot(t,s_t);
x=fft(s_t);
x=fftshift(x);
y=abs(x);
y = y/128;
figure;
plot(y);
```

Data is transferred to control card and obtained signal waveform is drawn as shown in Figure 4.4(a). Obtained signal waveform is very realistic and very close to the one obtained with

MATLAB which can be seen in Figure 4.4(b).

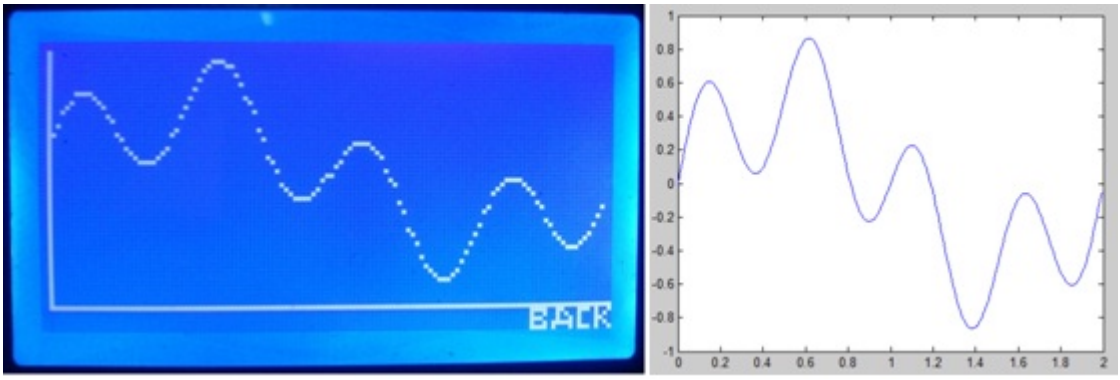

Figure 4.4: (a) Signal Waveform - control card (b) Signal Waveform - MATLAB

After performing FFT operation, coefficients are found to be 0.499 for the 1st harmonic and 0.398 for the 4th harmonic, as shown in Figure 4.5. Comparing results with MATLAB results shows that, obtained values are very close to the values which would actually be. Coefficients found in MATLAB analysis can be seen in Appendix C. DC value of the signal is found to

Figure 4.5: Signal parameters found in test

be 0 and this result is exactly correct. As defined in section 2.5, after calculating RMS value for a set of discrete values with MATLAB data, it is found as 0.456 which is nearly same with values found with control card. Values for 1st harmonic and 4th harmonic are expected to be 0.5 and 0.4, respectively. Values found with control card is very close to the expected values. Set of data produced by MATLAB for this sinusoidal waveform and FFT coefficients can be found in Appendix C.

Section 2.4 explains calculating THD for current values. Coefficients found after FFT analysis are magnitudes of currents. Using coefficients found from MATLAB THD is found as;

$$THD = 0.400/0.500 = 0.8$$

where it is the result found with control card. This result is shown on the display of control card and can be seen in Figure 4.5.

Figure 4.6(a) and (b) show the spectrum of this signal drawn with control card and MATLAB, respectively.

Table 4.2: Comparison of found values between control card and MATLAB

Parameter	Control Card Results	MATLAB Results	Absolute Error%
THD	0.8	0.8	0%
RMS	0.454	0.452	0.44%
1st Harmonic	0.499	0.500	0.2%
4th Harmonic	0.398	0.400	0.5%

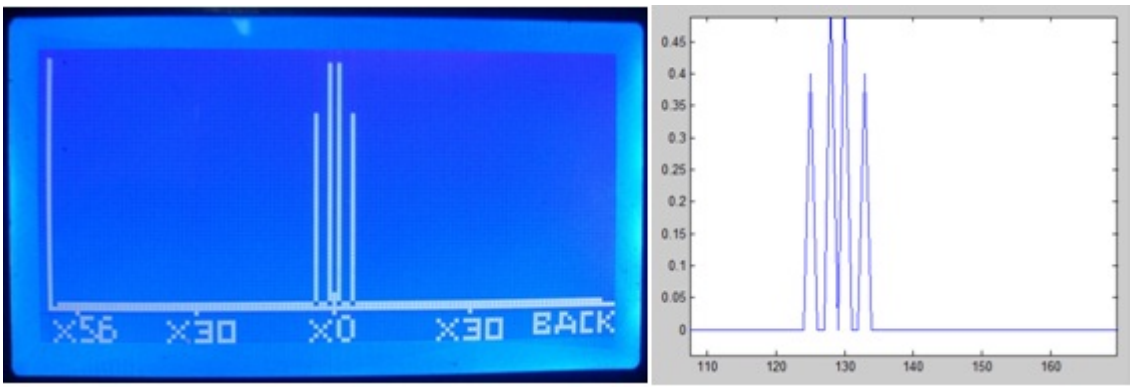

Figure 4.6: (a) Spectrum - control card (b)Spectrum - MATLAB

4.1.3 50Hz Sinusoidal Signal with 35th Harmonic

In this test, another software test is arranged with sum of a 50Hz frequency and 1,75 kHz frequency (35th harmonic) signals. 256 data samples are produced where 1st harmonic signal with 35th harmonic signal is summed by software with the code snippet written in data-acquisition card:

```
for(i=0;i<256;i++)
{
```

```
samples[i]=0.8*sin((double)(1*PI*2*(i*256/360)/180)) +
0.1*sin((double)(35*PI*2*(i*256/360)/180));
}
```

Created sinus waveform can be considered as $0.8 * sin(2.\pi.f.t) + 0.1 * sin(2.\pi.35f.t)$.

In order to verify data to be obtained same signal is produced with MATLAB with the following code snippet;

```
t=0:1/128:2-1/128;
s_t =0.8* sin(1*pi*t)+0.1* sin(35*pi*t);
plot(t,s_t);
x=fft(s_t);
x=fftshift(x);
y=abs(x);
y = y/128;
figure;
plot(y);
```

A signal waveform which is shown in Figure 4.7(a), is observed. Signal waveform obtained from MATLAB is shown in Figure 4.7(b) to compare with Figure 4.7(a). By comparing Figure 4.7 (a) and (b), it can be seen that waveform obtained from control card is similar to the one shown in Figure 4.7 (b). The reason for obtaining a signal waveform composed of dots about screen resolution of control card.

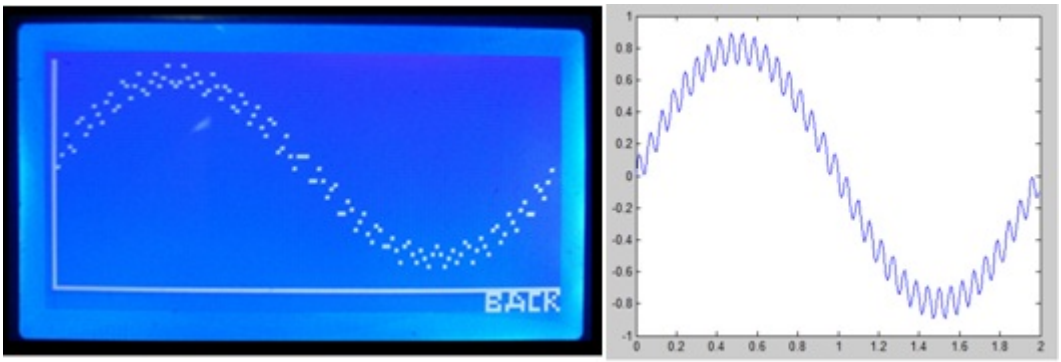

Figure 4.7: (a)Signal waveform- control card (b)Signal waveform - MATLAB

Figure 4.8: Signal parameters found in test

After performing FFT operation, coefficients are found to be 0.795 for the 1st harmonic and 0.095 for the 35th harmonic, as shown in Figure 4.8(a). Coefficients found in MATLAB analysis can be found in Appendix C. At 130th column first harmonic can be seen with a value of 0.8 and at 164th column, 35th harmonic with a value of 0.1. DC values are found to be 0 at both sides. In this test, control card find harmonics with some errors. At 1st harmonic, error is;

$$((0.800 - 0.795)/0.800) * 100 = 0.6$$

At 35th harmonic error is found as;

$$((0.1 - 0.095)/0.1) * 100 = 5$$

which is a greater error than the one found at 1st harmonic. Control card also finds another coefficient which is 39th harmonic and 0.031. This result shows us that, at higher frequencies reliability of FFT software decreases but still can be accepted.

THD is found from MATLAB coefficients as;

$$THD = 0.1/0.8 = 0.125$$

where it would be displayed as 0.12. Control card also finds THD as 0.12 which means that errors in harmonic coefficients do not sum up to make THD incorrect, in this case.

As defined in Section 2.5, after calculating RMS value for a set of values, it is found as 0.573 for MATLAB. Set of data and coefficients produced by MATLAB for this sinusoidal waveform can be found in Appendix C. Figure 4.9(a) and (b) show the spectrum of this signal drawn with control card and MATLAB, respectively.

Table 4.3: Comparison of found values between control card and MATLAB

Parameter	Control Card Results	MATLAB Results	Absolute Error%
THD	0.12	0.80	0%
RMS	0.567	0.570	0.52%
1st Harmonic	0.795	0.800	0.62%
35th Harmonic	0.095	0.100	0.5%
39th Harmonic	0.031	0.000	-

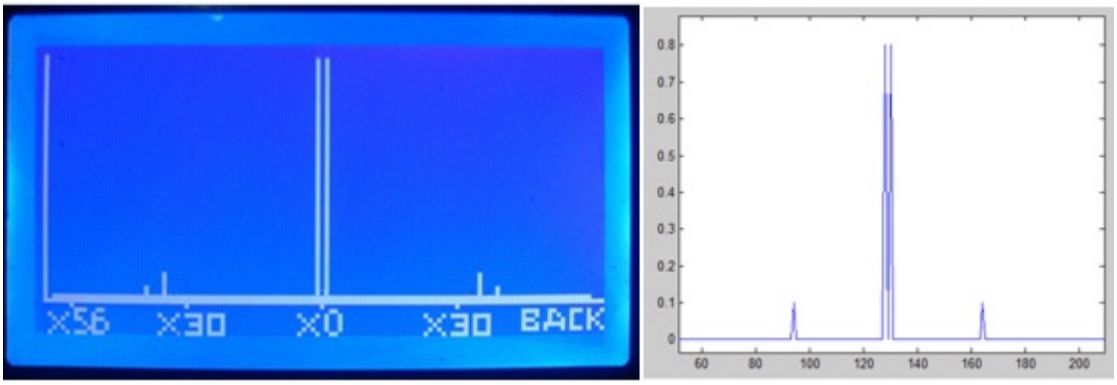

Figure 4.9: (a)Spectrum - control card (b)Spectrum - MATLAB

4.1.4 100Hz Sinusoidal Signal with Phase Shift and DC Offset

In this test case, 256 data samples are produced where 100 Hz signal with a phase angle is summed with a DC value. This signal is produced in data-acquisition card with the following code snippet;

```
for(i=0;i<256;i++)
{
samples1[i] =0.4 + 0.5*sin((double)(2*PI*2*(i*256/360)/180) + PI/2);
}
```

Created sinus waveform can be considered as $0.4 + 0.5 * sin(2.\pi.2.f.t + \pi/2)$.

In order to verify data to be obtained same signal is produced with MATLAB with the following code snippet;

```
t=0:1/128:2-1/128;
```

```
s_t=0.4+0.5*sin((2*pi*(t+1/4)));
plot(t,s_t);
x=fft(s_t);
x=fftshift(x);
y=abs(x);
y = y/128;
figure;
plot(y);
```

Signal waveforms are obtained by the help of using those code snippets. Those waveforms can be seen in Figure 4.10(a) and (b). The reason for seeing two periods of a sinusoidal waveform is that: Control card is programmed to draw 1/50 of one second. Produced signal is a 100 Hz signal and this signal completes two periods in 1/50 of one second. It can be seen that effect of 900 phase shift and DC is successfully reflected in Figure 4.10(a).

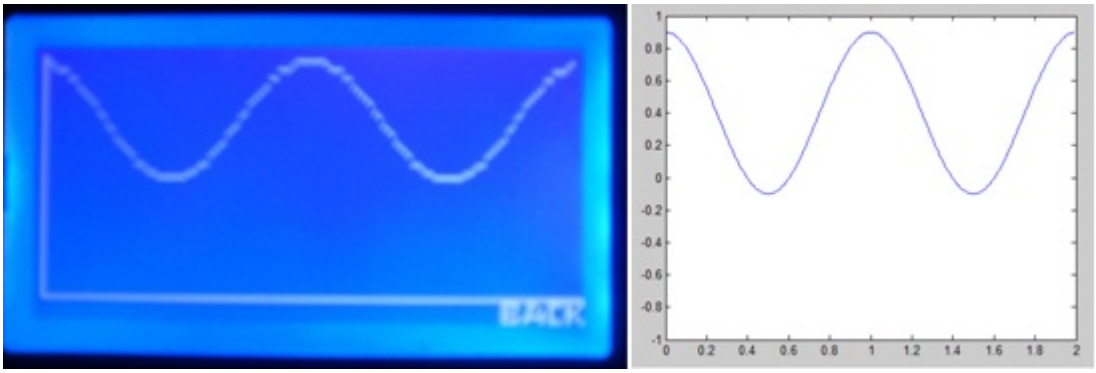

Figure 4.10: (a) Signal Waveform - control card (b) signal waveform - MATLAB

Figure 4.11 shows the coefficients obtained from control card. Control card finds 0th harmonic as 0.798 which should be 0.8. Error percentage for 0th harmonic is calculated as;

$$((0.800 - 0.798)/0.800) * 100 = 0.25$$

2nd harmonic is found to be 0.497 which would be 0.500. Error percentage in this coefficient is;

$$((0.500 - 0.497)/0.500) * 100 = 0.6$$

DC value is found to be 0.39 which is half of 0th coefficient actually. This is very close to the expected result which is 0.4. As defined in Section 2.5, after calculating RMS value for a

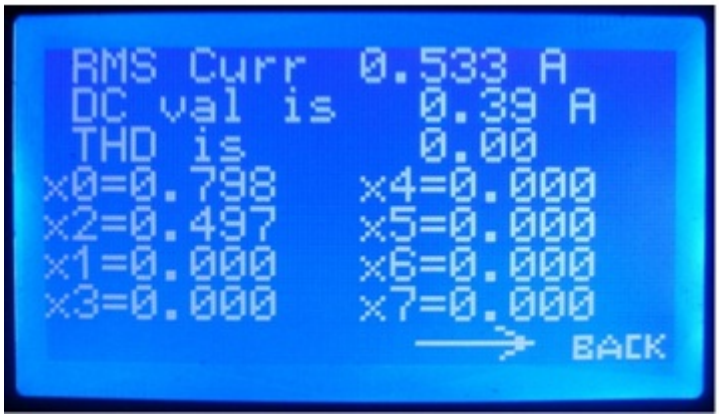

Figure 4.11: Signal parameters found in test

Table 4.4: Comparison of found values between control card and MATLAB

Parameter	Control Card Results	MATLAB Results	Absolute Error%
THD	0.00	0.00	0%
RMS	0.533	0.533	0.0%
DC	0.39	0.40	2.5%
2nd Harmonic	0.497	0.500	0.6%

set of values, it is found as 0.454. Set of data produced for this sinusoidal waveform can be found in Appendix C.

In this test no periodic signal is summed with the main signal. As a result THD is expected to be 0 and it is found as 0 as can be seen from Figure 4.11.

Figure 4.12 shows the spectrum of this signal drawn with control card and MATLAB, respectively.

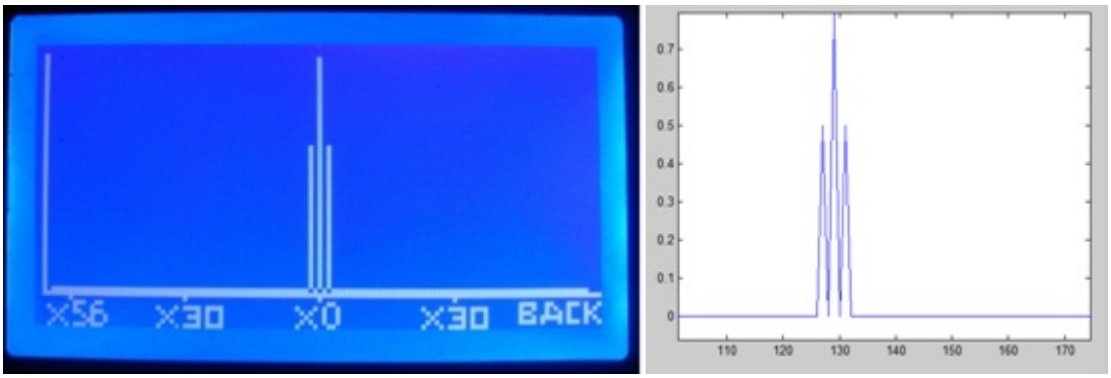

Figure 4.12: (a)Spectrum - control card (b)Spectrum - MATLAB

4.1.5 50Hz Square Wave

Square wave is a waveform which is composed of many sinusoidal signals. Square wave is a good choice if a signal with many harmonics is to be observed. In this test case, 256 data samples are produced to create a square wave. This signal is produced in data-acquisition card with the following code snippet:

```
for(i=0;i<128;i++)
{
samples [i] =-1;
}
for(i=128;i<256;i++)
{
samples[i] =1;
}
```

In order to verify data to be obtained same signal is produced with MATLAB with the following code snippet;

```
t = 0:1/128:2-1/128;
s_t= -1:1/128:1-1/128;
i=0;
       s_t(1:64)    =  -1;
       s_t(65:128)  = -1;
       s_t(128:192) = 1;
       s_t(192:256) = 1;
plot(t,s_t);
x=fft(s_t);
x=fftshift(x);
y=abs(x);
y = y/128;
figure;
plot(y);
```

A square wave with a unity peak value is obtained at the control card side and MATLAB. Signal waveforms are obtained and depicted in Figure 4.13 (a) and (b).

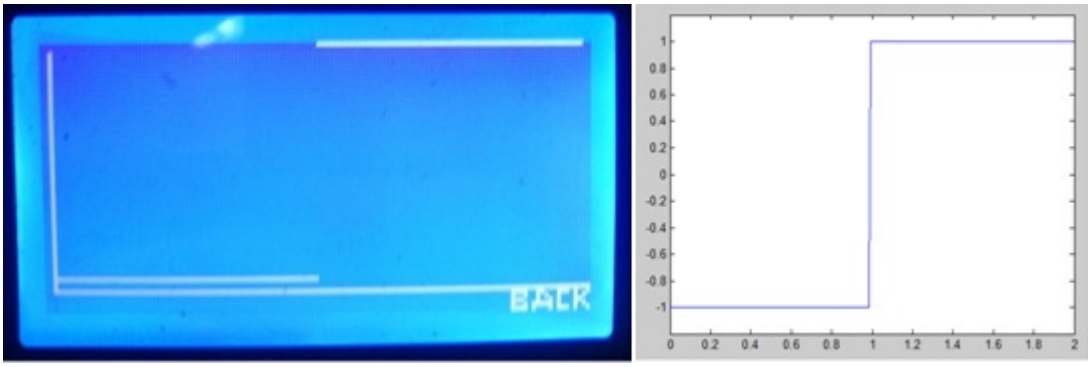

Figure 4.13: (a) Signal waveform - control card (b)Signal Waveform - MATLAB

FFT coefficients are obtained after performing transform operation. Correct values for a unity peak square wave and found values can be seen in Figure 4.14 (a) and (b). In this case, various coefficients are in interest. Table 4.2 lists coefficients with greater values for control card and MATLAB. Error rates in percentage for control card are also listed in this table.

Table 4.5: Comparison of found harmonic values between control card and MATLAB

Parameter	Control Card Values	MATLAB Values	Absolute Error%
THD	0.53	0.48	10.41%
RMS	0.992	1.000	0.8%
1st Harmonic	1.270	1.2732	0.07%
3 rd Harmonic	0.423	0.4242	0.23%
5th Harmonic	0.254	0.2543	0.11%
7th Harmonic	0.182	0.1814	0.33%
9th Harmonic	0.115	0.1409	1.83%
11th Harmonic	0.097	0.1150	15.65%
13rd Harmonic	0.083	0.0971	14.43%
15th Harmonic	0.074	0.0839	10.84%
17th Harmonic	0.074	0.0738	0.27%
19th Harmonic	0.067	0.0658	1.79%
21st Harmonic	0.059	0.0593	0.50%
23rd Harmonic	0.054	0.0539	0.18%
25th Harmonic	0.050	0.0493	1.40%

According to section 2.5, correct RMS value would be peak value itself, which is unity. Obtained value is 0.992 which implies that (1.000-0.992)/1*100 = 0.8 error is done by control

Figure 4.14: Signal parameters found in test

card. Calculating the THD from sample values gives a result of 0.46. Control card finds THD as 0.53, which has an error value of 10.41%.

Figure 4.15(a) and (b) show the spectrum of this signal drawn with control card and MATLAB, respectively.

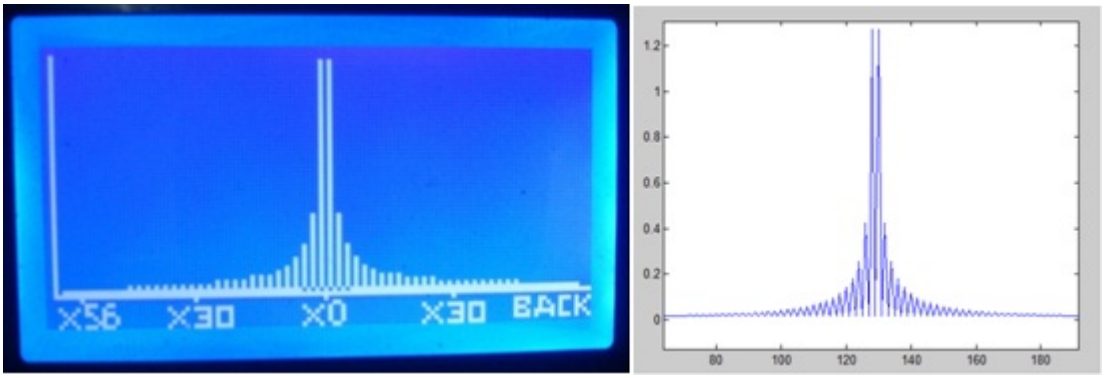

Figure 4.15: (a)Spectrum - control card (b) Spectrum - MATLAB

4.1.6 50Hz Triangular Wave

Triangle wave is also a waveform which is composed of many sinusoidal signals like square wave. In this test case, 256 data samples are produced to create a triangle wave. This signal is produced in data-acquisition card with the following code snippet:

```
for(i=0;i<64;i++)
{
samples[i] =(double)i*(double)1/64;
```

```
}
for(i=64;i<127;i++)
{
samples[i] =-(double)i*(double)1/64+2;
}
for(i=127;i<192;i++)
{
samples[i] =-(double)i*(double)1/64+2;
}
for(i=192;i<256;i++)
{
samples[i] =(double)i*(double)1/64-4;
}
```

In order to verify data to be obtained same signal is produced with MATLAB with the following code snippet;

```
t = -1:1/128:1-1/128;
s_t= -1:1/128:1-1/128;
s_t(1:64)    =  2*t(1:64)+2;
s_t(65:128)  = -2*t(65:128);
s_t(129:192) = -2*t(129:192);
s_t(193:256) =  2*t(193:256)-2;
plot(t,s_t);
x=fft(s_t);
x=fftshift(x);
y=abs(x);
y = y/128;
figure;
plot(y);
```

Figure 4.16(a) and (b) depict the signal waveforms observed at the control card side and MATLAB. Control card successfully gathers samples and draws the waveform on graphic interface.

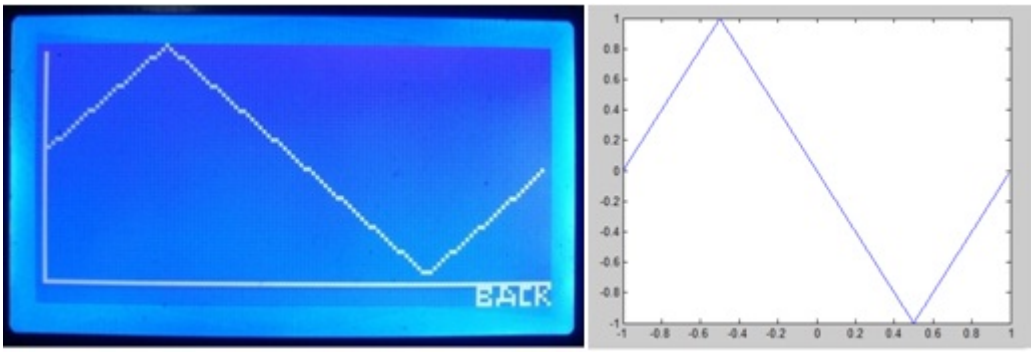

Figure 4.16: (a)Signal waveform - control card (b) Signal waveform - MATLAB

FFT coefficients obtained from MATLAB and control card can be seen in Figure 4.17. Table 4.6 also lists the values and gives the results of absolute error calculation between those values.

Table 4.6: Comparison of found harmonic values between control card and MATLAB

Parameter	Control Card Values	MATLAB Values	Absolute Error%
THD	0.11	0.14	21.42%
RMS	0.581	0.578	0.51%
1st Harmonic	0.815	0.8106	0.62%
3 rd Harmonic	0.092	0.0901	2.06%
5th Harmonic	0.031	0.0325	4.61%
7th Harmonic	0.022	0.0166	24.54%
9th Harmonic	0.000	0.0100	-%
11th Harmonic	0.000	0.0067	-%
13rd Harmonic	0.000	0.0048	-%
15th Harmonic	0.000	0.0036	-%

According to section 2.5, correct RMS value would be $1/\sqrt{3} = 0.578$. Obtained value is 0.581 which implies that (0.581-0.578)/0.581*100 = 0.3 error is done by control card. Calculating the THD from sample values gives a result of 0.14. Control card finds THD as 0.11, which has an error value of 21.42%.

Figure 4.18 shows the spectrum of this signal drawn with control card and MATLAB, respectively.

Figure 4.17: Signal parameters found in test

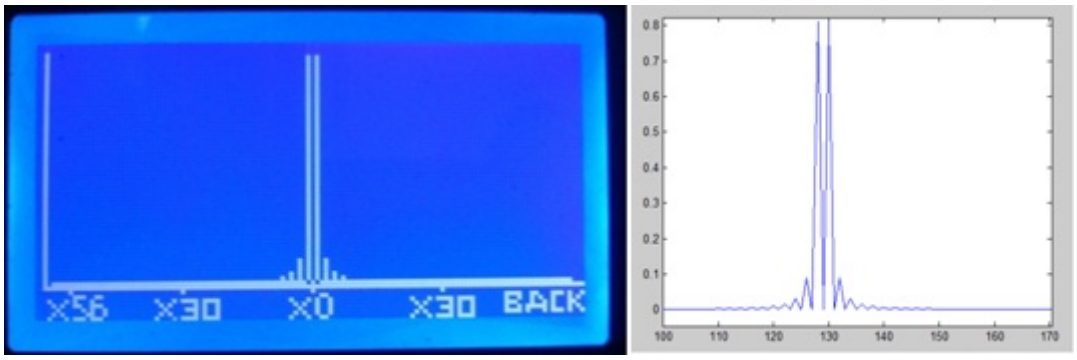

Figure 4.18: (a)Spectrum - control card (b)Spectrum - MATLAB

4.2 Tests Conducted with Household Appliances

Those tests are performed in house environment. Devices which work with mains (household electricity i.e. 220 Volts and 50 Hz) are tested. Data acquisition card along with Magnelab current transformer is inserted between the device and wall plug. Magnelab current transformer and test set up are shown in Figure 4.19(a) and (b).

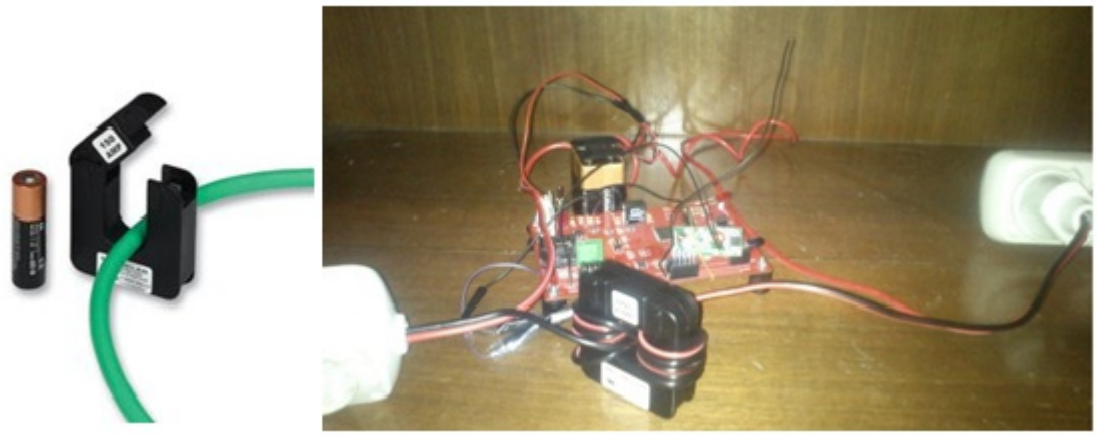

Figure 4.19: (a) Magnelab SCT0750-005 current transformer (b) CT with data-acquisition card

4.2.1 Washing Machine

In this case, system is tested with a 2000W washing machine which is fed from mains power. System setup is shown in Figure 4.20. When the motor is not running, machine draws nearly no current. Sampling of drawn current by the machine is performed when the motor starts. Figure 4.21(a), (b) and (c) show obtained waveform, spectrum and signal parameters respectively.

RMS value of drawn current is found to be around 9A and this is an expected result. Washing machine has an AC motor and this motor has nearly linear characteristic.

Figure 4.20: Test setup for testing washing machine current harmonics

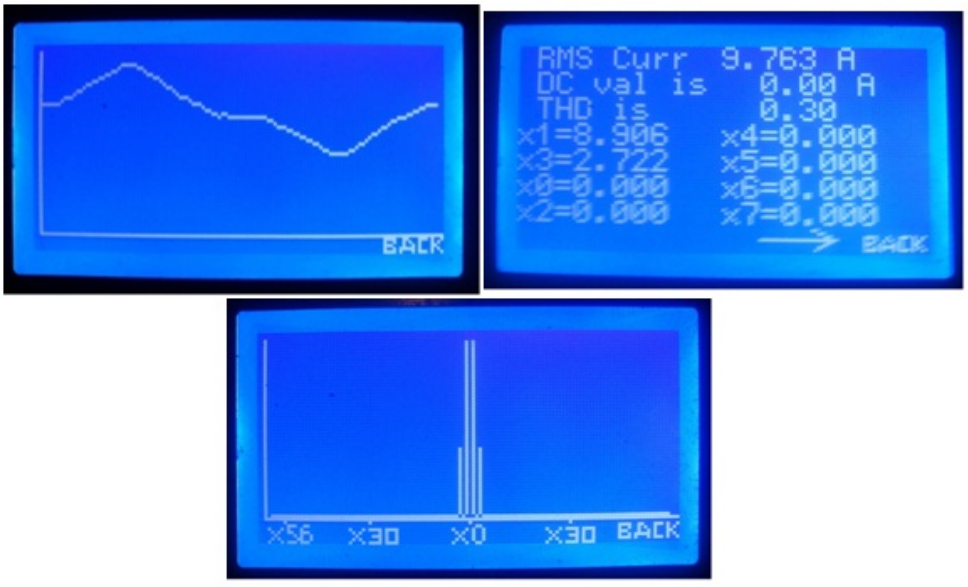

Figure 4.21: Obtained (a)waveform (b) parameters (c) spectrum plot

4.2.2 Vacuum Cleaner

A 1200W washing machine which is fed from mains power is tested. Current transformer is inserted between machine and wall plug and necessary samplings are obtained. System setup is shown in Figure 4.22. While the machine is running samplings are obtained by data-acquisition card and results are observed with control card. Figure 4.23 (a), (b) and (c) show obtained waveform, spectrum and signal parameters respectively.

Figure 4.22: Test setup for testing vacuum cleaner current harmonics

RMS value of drawn current is found to be around 7.3 amperes and this is somewhat higher than the expected result. This vacuum cleaner also has an AC motor and this motor is found to have more non-linear characteristics than washing machine.

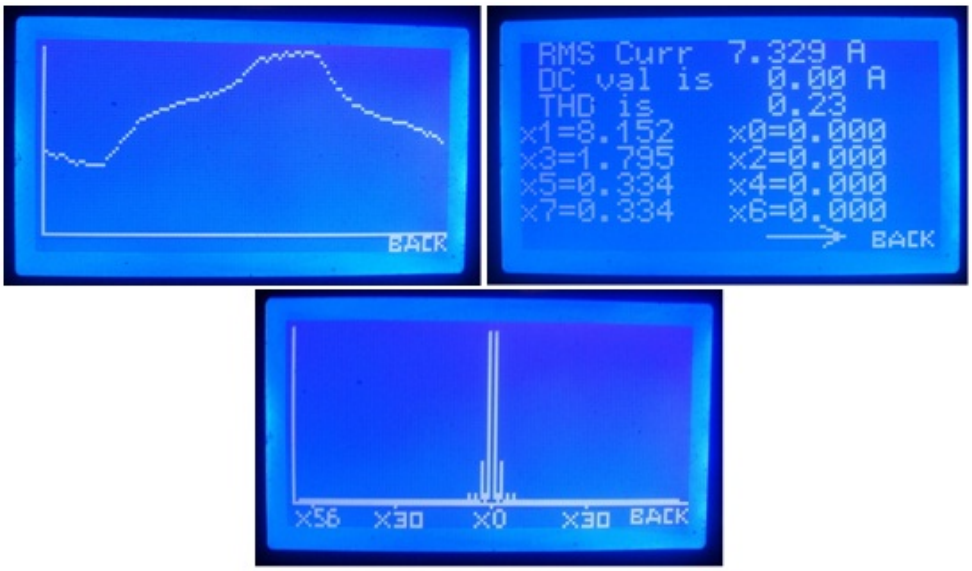

Figure 4.23: Obtained (a)waveform (b) parameters (c) spectrum plot

4.2.3 Electric Heater

System is tested with a 1500W electric heater in this test case as shown in Figure 4.24. Obtained results after performing the test are shown in Figure 4.25(a),(b) and (c).

Figure 4.24: Test setup for electric heater current harmonics

Electric heater has a basic principle of working. It only converts electricity power into heat by heating up resistors. A undistorted sinusoidal signal waveform is expected for drawn current. Drawn current waveform is almost perfect excluding the small 3rd harmonic.

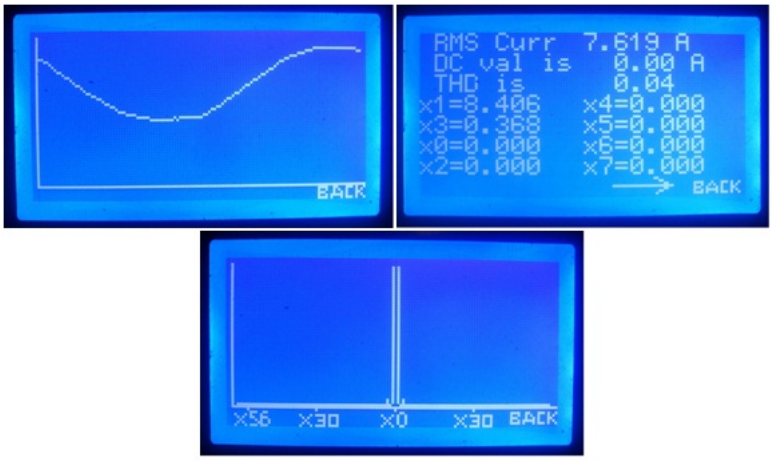

Figure 4.25: Obtained (a)waveform (b) parameters (c) spectrum plot

4.3 Tests in Medium and High Voltage Environments

Those tests are performed in high voltage laboratory environment in HIZAL Electro Erozyon San. Tic. Ltd. Sti. company. Three tests are performed under 18 kV, 36 kV and 54 kV respectively. Figure 4.26 shows the test setup used in those tests and Figure 4.27 shows metal boxing around data-acquisition card.

As shown in Figure 4.26, a high voltage transformer, voltage divider, variacs for current and voltage, voltage measurement tools and a transformer for current adjustment are used. Voltage transformer and voltage divider are used to supply necessary voltage which is applied on the Faraday caging as shown in Figure 4.27. Around 10 amperes of current is allowed with the help of a transformer and a variac, to flow through main wire which crosses through the windows of Faraday caging. Obtained results are given in the following sections.

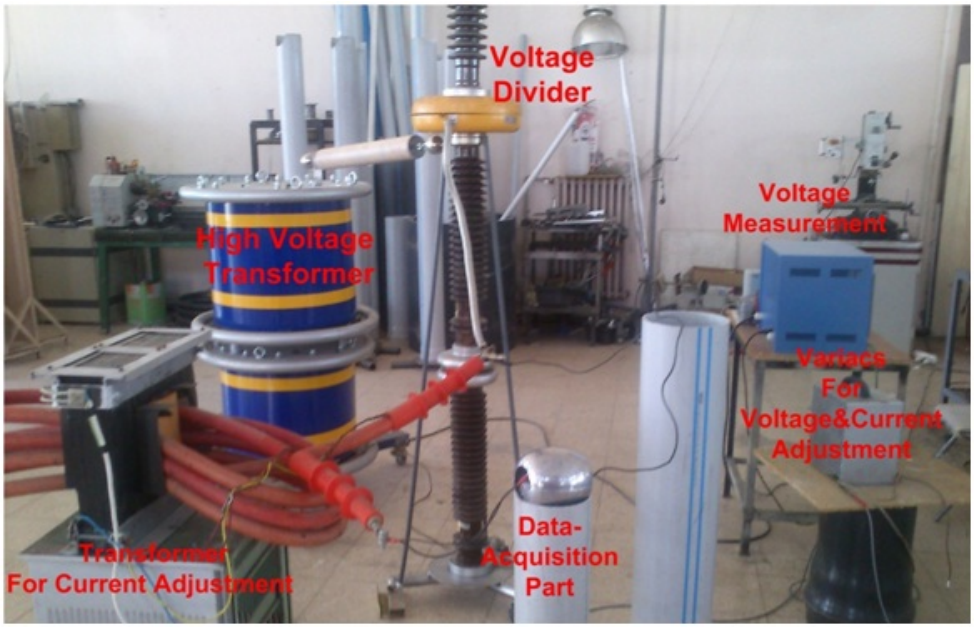

Figure 4.26: Test setup for MV and HV tests

Figure 4.27: Faraday caging around data-acquisition card

4.3.1 Test in 18 kV Environment

Current in the main cundoctor is measured with the help of a clamp-on probe and found to be 10 Amperes. This current flowing through main conductor is measured to be 10.268 A under 18kV. Error may result from that probe, system under test or heating up of equipment. Obtained waveform, parameters and spectrum plot are given in Figure 4.28(a), (b) and (c). Harmonics are not found in current supplying transformer.

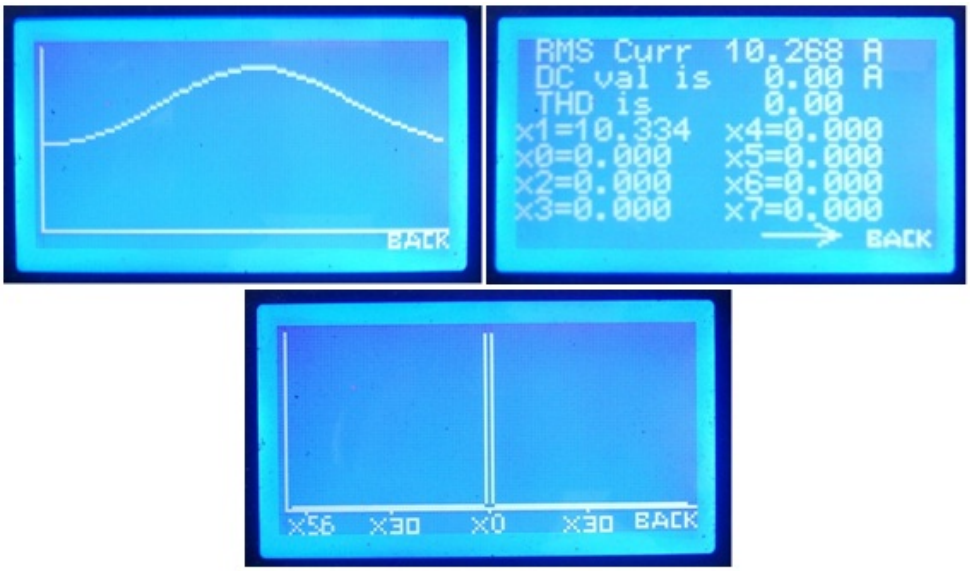

Figure 4.28: Obtained (a)waveform (b) parameters (c) spectrum plot

4.3.2 Test in 36 kV Environment

10 Amperes flowing through main conductor is measured to be 10.169A under 36kV. Obtained waveform, parameters and spectrum plot are given in Figure 4.29(a), (b) and (c). Again, harmonics are not found in current supplying transformer.

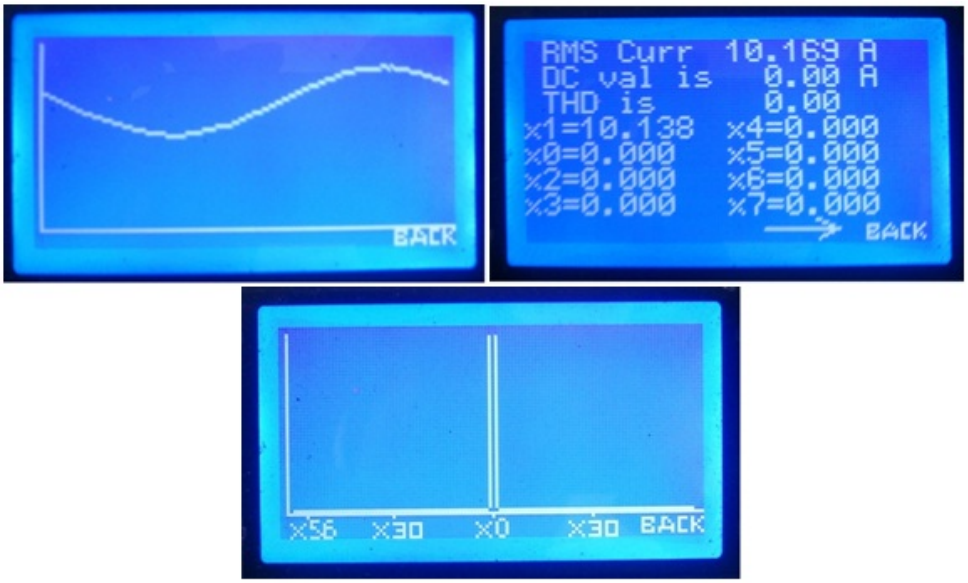

Figure 4.29: Obtained (a)waveform (b) parameters (c) spectrum plot

4.3.3 Test in 54 kV Environment

10 Amperes flowing through main conductor is measured to be 9.874 A under 54kV. Current in the main cundoctor is measured with the help of a clamp-on probe Obtained waveform, parameters and spectrum plot are given in Figure 4.30(a), (b) and (c). Harmonics are not found in current supplying transformer.

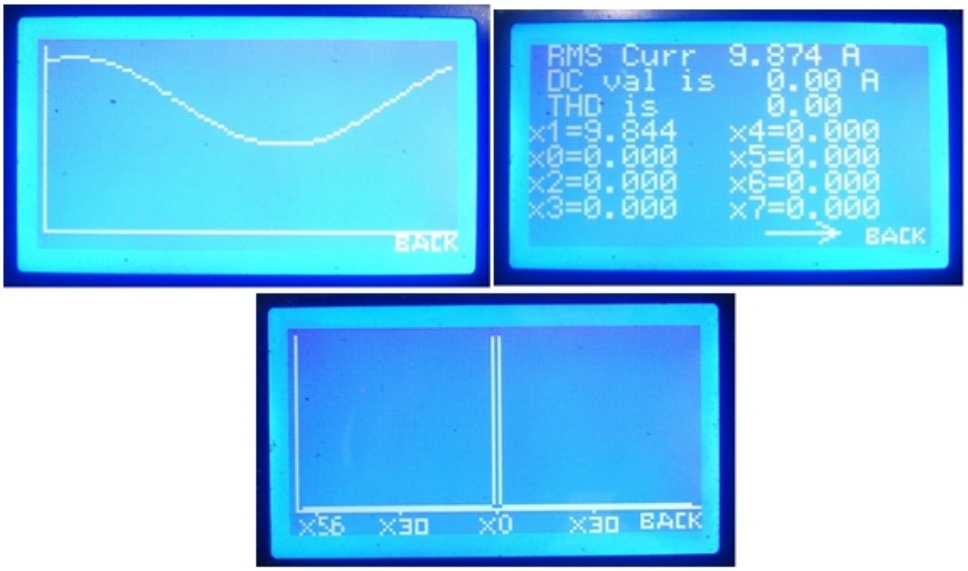

Figure 4.30: Obtained (a)waveform (b) parameters (c) spectrum plot

4.4 Conclusions About Performed Tests

Those conducted software tests are useful to see system performance. Tests performed with current measurement instruments, bring in errors created by instrument itself. Before analyzing results of following tests, following conclusions can be made:

- System can measure AC and DC both. Utilization of Hall effect sensors or optical transducers with this system bring the ability of DC measurement.
- Phase shift does not affect results of DFT analysis which implies that in real cases, start instance of sampling is not important and system can be used confidently.
- In low order of harmonics system is reliable and has error rates which are under 1%. In higher order of harmonics, error rates tend to grow. This situation can be overcome by working with greater number of samples and improving precision of floating point numbers.
- Error rates in THD calculations can deviate from expected results greatly. This is caused by accumulation of harmonic errors throughout frequency spectrum. More precise harmonic calculation would result more accurate THD calculation.
- In some cases, high order harmonics can not be calculated or false harmonics are found. This situation can also be improved by the methods suggested in conclusions.
- System proves itself that it can work under MV conditions. In tests, it is found that as we increase the voltage, measured RMS value decreases. System may require calibration for enviromental conditions.

CHAPTER 5

CONCLUSION AND FUTURE WORKS

In this thesis study, importance of power quality hence power quality measurement is explained. Instruments used for current measurement and power quality monitoring devices are examined. A stand-alone induction powered current RMS value and current harmonics measurement system for medium voltage and low voltage systems is designed and implemented. Designed system is tested in various ways. Some tests are conducted in laboratory environment to verify the software of the system. Tests done in laboratory prove that system would be used in ready to work under medium voltage and low voltage systems with water resistant boxing.

System is tested with clamp-on and non clamp-on current sensors however suggested to work with clamp-on sensors. Usage of those kinds of sensor eliminates the need for cutting energy lines which brings in many burden.

The result of making researches about the products in the market and about the studies of other researchers helps to gain insight about methodologies and tendencies in technology. Designing and implementing such a system help gaining know-how about devising more accurate and more stable systems. With the experience gained in this study and literature survey, improvement suggestions can be made which are listed below:

- Frequency of a power system is also an important parameter for power quality analysis. Frequency measurement property can be employed on this system by making improvements on hardware and software. There are various frequency measurement techniques in science of engineering. The most suitable technique for this system would be using FFT analysis. By working with greater number of samples, one can easily detect fre-

quency of the system by inspecting FFT coefficients. Also employing DCT gives twice frequency resolution compared to FFT with the same number of samples. The more number of samples yields more precise frequency measurement. Working with greater number of samples bring in burden of processing and data transfer problems. Solutions for those problems are suggested in the following bullets.

- Employing a more powerful microcontroller enables to analyze greater number of data points in shorter times. There are various kinds of digital signal processors which offer different advantages. In the market DSPs with a 2.5 GHz DSP cores, ultra low power consumptions and DSP operations up to 64 bit type devices can be found [57][58][59]. Results of test show that error tend to increase with increasing number of harmonics. This is the result of working with a limited number of samples which are 8-bit numbers. By employing a powerful DSP, working with greater number of samples which have 64-bit precision would increase the accuracy of analysis, greatly.

- Wireless communication speed is important if working with more number of samples is essential. In this study, 256 bytes of data is transferred in a time of 17 seconds with RF communication. In IR communication, this speed decreased down to 256 bytes/30 seconds. Also, in order to maintain the security of communication, instead of 10bits, 8-bit packets of data are transferred. By increasing the speed, error handling capability and packet size of communication protocol, precision of analyses can be improved. Protocols like ZigBee with a speed up to 900 Kbit/s and with a range up to 75 meters or IEEE 802.11 standard Wifi with a speed up to 300Mbit/s and with a range up to 90 meters can easily be employed with products which can be found in the market [60][61]. Monitoring systems in the coverage area of GSM can also use GPRS and 3G/4G protocols to communicate with the analysis center over internet. There are also easy to use modules in the market for GPRS and 3G/4G [62] [63]. Outside of coverage area of GSM operators, internet communication over satellites is possible. Communication modules for Iridium and Globalstar satellites are found in the market easily [64][65]. Those modules are designed for embedded products and can be employed with power monitoring systems.

- In tests it is observed that, screen resolution is important to display complicated signals and high order harmonics. For control card a graphical LCD with higher screen resolution can be employed. A touch-screen would be also elegant to use and provide ease of

use for the user.

- IR communication range is 6 meters for the designed system. For high voltage lines this range would not be sufficient. As the system is improved for high voltage applications, IR range should be improved also.

- Data storage is a desirable feature for those kind of systems. By simply employing an external flash memory or a SD-card to data-acquisition card, monitoring results can be stored on the card. Also deploying a storage element on control card enables the card to hold the data permanently and to transfer to a computer.

- RS-232 and CAN bus communication integrated circuits and necessary passive components are included in the schematics of control card. In order to enable the system to communicate with other devices, those proposed components can be put in the design. In the case of employing storage elements on control card, communicating with a computer feature would be useful.

- In this study, a solution for battery charging is suggested and a proper design is explained. For a future work, this design can be implemented and can be tested with different current measurement instruments. For environments where flowing current is not enough to charge the battery, solar charging system can be considered. In such cases batteries with enough capacity should be used in order to keep the system going when there is no sunlight for hours.

One goal of this thesis is to make the system to be able to work on high voltage lines. Some issues should be taken into account because of electromagnetic field and corona currents around those lines:

- Metal boxing or Faraday caging around data-acquisition part is essential to protect the electronic parts. Antenna for wireless communication would be stretched out from a small hole through this boxing. If infrared communication is to be used with this system a small conducting and transparent window can be installed on metal boxing. Screens of cathode ray tube (CRT) televisions and surface-conduction electron-emitter display (SED) televisions are covered with a thin layer of aluminum. Those screens are not only transparent but also conductive for the electrons to return to ground. A

small window made of this kind of material would do the desired task. Also, current measurement instrument should have a metal exterior container to keep the discharging outside of the instrument. Going one step further, current measuring instrument can also be contained in the Faraday caging. Figure 5.1(a),(b) and (c) illustrate an example of this design which is described in this bullet. This design is a clamp-on device for ease of installation.

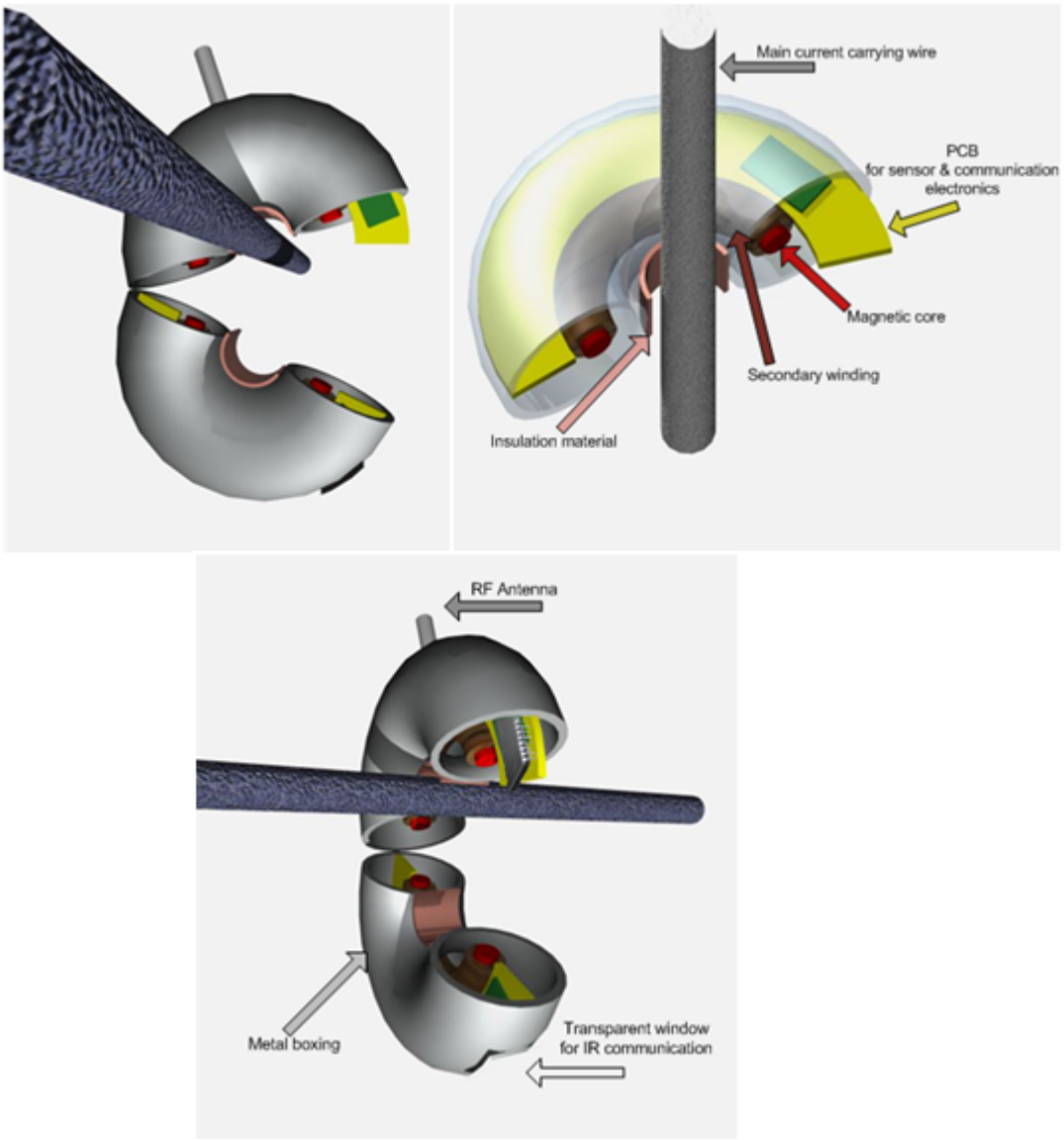

Figure 5.1: (a) Proposed design of (b) Interior structure of proposed design (c) Exterior structure of proposed design

Employment of magnetic core based current measurement instrument brings in errors because of core magnetization current and magnetic reluctance caused by the cutting of the core mate-

rial. Those errors can be compansated by electronic feedback through a magnetic circuit [72]. Hall effect based structure or a rogowski coil with a D.C. electronic transducer would bring in the ability of measuring DC [73]. RF antenna brings in risk of sparking high currents into the system which may cause break-down of the system irreversibly. RF antenna design can be thought in other methods or shall be excluded from the design and communication can be performed through IR only.

REFERENCES

[1] I.Y. Chung, D.J. Won, J.M. Kim, S.J. Ahn, S.J. Moon, J.C. Seo and J.W. Choe, "Development of Power Quality Diagnosis System for Power Quality Improvment," in Power Engineering Society General Meeting IEEE, pp. 1256-1261, 2003

[2] AC Enersis, VarCorder ile 69kV Kadar olan Hatlardan Kablosuz Veri Okuyabilme[Online]. Available: http://www.acenersis.com/varcorder.html [Accessed: 4 August, 2012]

[3] C. Zhu, M. Hu, Z. Wu, X. Dou and S. Zhao, "Design and realization of regional power quality monitoring system," in Electric Utility Deregulation and Restructuring and Power Technologies, 2008. DRPT 2008. Third International Conference on, pp. 2023-2027, 2008

[4] C.A. Turkmen, "Calibration of Conventional Measurement Transformers Against Harmonic Components by Using Field Measurements of Optical Transducers and Resistive-Capacitive Voltage Transformers," Master of Science Thesis, METU, 2010

[5] D. Gezer, "A Proposed Rule for Interconnection of Distributed Generation and its Economic Justification," Master of Science Thesis, METU, 2009

[6] CIRED Working Group on Dispersed Generation, Preliminary for Discussion on Dispersed Generation, Nice: June 1999

[7] H. A. Gil and G. Joos, ?Models for quantifying the economic benefits of distributed generation,? IEEE Trans. Power Syst., vol. 23, no. 2, pp. 327-335, May 2008

[8] IEEE Standards, IEEE 1547 Standard for Interconnecting Distributed Resources with Electric Power System, New York: July 2003

[9] R.C. Dugan, M.F. McGranaghan, S. Santosa, H.W. Beaty, "Electric power systems quality", McGraw-Hill, New York, 2002. Chapter 9: Distributed generation and power quality.

[10] N. Jenkins, R. Allan, P. Crossley, D. Kirschen,G. Strbac, "Embedded generation", Institution of Electrical Engineers, London, 2000. Chapter 5: Power quality.

[11] F. Noor, R. Arumugam, M. Vaziri, Unintentional Islanding and Comparison of Prevention Techniques Proceedings of the 37th Annual IEEE NAPS (North American Power Symposium) 0-7803-9255-8105, October 23 -25, 2005. Iowa State University

[12] R. A. Walling, Senior Member, IEEE, and N. W. Miller, Fellow, IEEE, "Distributed Generation Islanding - Implications on Power System Dynamic Performance." Proceedings of the IEEE/PES Summer Power Meeting, Chicago, July, 2002.

[13] G. Kaur, M. Vaziri Y., " Effects of Distributed Generation (DG)Interconnections on Protection of Distribution Feeders," Power Engineering Society General Meeting IEEE, 2006.

[14] C. J. Mozina, "A Tutorial on the Impact of Distributed Generation (DG) on Distribution Systems," Protective Relay Engineers, 61st Annual Conference for, pp. 591-609, 2008

[15] M.H.J. Bollen, F. Sollerkvist, The Hosting Capacity of Distribution Networks against High-Frequency Harmonics Emitted by Distributed generation, Int Conf on Harmonics and Quality of Power (ICHQP); Cascais, Portugal, October 2006.

[16] M.H.J. Bollen, P.F. Ribeiro, E.O.A. Larsson, C.M. Lundmark, Limits for voltage distortion in the frequency range 2-9 kHz, IEEE Transactions on Power Delivery, accepted for publication.

[17] M. Lindholm and T. Rasmussen, "Harmonic analysis of doubly fed induction generators," vol. 2. The 5th International Conference on Power Electronics and Drive Systems, PEDS, pp. 837-841, nov 17-20 2003

[18] P. Jorgensen, J. O. Tande, A. Vikkelso, P. Norgard, J. S. Christensen,P. Sorensen, J. D. Kledal and L. Sondergard, "Power quality and grid connection of wind turbines," no. 438. Lisbon, Portugal: CRIED Conference Publication, Jun 2-5 1997.

[19] A. Latheef, M. Negnevitsky, K. Muttaqi and S Perera, "Present Understanding of the Impact of Distributed Generation on Power Quality," Power Engineering Conference, AUPEC '08. Australasian Universities, 2008

[20] S. Kazemi, "Reliability Evaluation of Smart Distribution Grids," Phd. Thesis, Department of Electrical Engineering, Aalto University, 2011

[21] Energy Informative, What is the Smart Grid [Online]. Available: http://energyinformative.org/what-is-the-smart-grid/ixzz20ox0u5Oc, [Accessed: 18 June,2012]

[22] "System View of the Modern Grid", Document Preparedby the National Energy Technology Laboratory for the U.S. Department of Energy, Office of Electricity Delivery and Energy Reliability, January 2007, [online]. Available: http://www.netl.doe.gov/smartgrid/refshelf.html [Accessed: 8 August, 2012]

[23] B. SHENG and W. ZHOU, "Ultra-low Power Wireless-Online-Monitoring Platform for Transmission Line in Smart Grid," High Voltage Engineering and Application (ICHVE), International Conference on, pp. 244-247, 2010

[24] D.g Gan, F. Liu, L. Du and Y. Liu, "Research and Implementation of On-line Monitoring Techniques for High Voltage Equipments in Smart Grid," High Voltage Engineering and Application (ICHVE), 2010 International Conference on, pp. 236-239, 11-14 Oct. 2010.

[25] Fan Cai, David J.Chung, Evangelos Farantatos, A.P. Sakis Meliopoulos, John Papapolymerou, " Self- powered Advanced Meter Design for Smart Grid," Microwave Conference Proceedings (APMC), 2010 Asia-Pacific, pp. 1380-1383, 7-10 Dec. 2010

[26] H Jin Sim, Member, IEEE and David L Harris," Current practices on Power Transformer Monitoring and Controls for Smart Grid Applications," Power and Energy Society General Meeting, 2011 IEEE, pp. 1-5, 24-29 July 2011

[27] Standardfor Interconnecting Distributed Resources with Electric Power Systems, IEEE Standard C21.1547-2003, Jul. 2003.

[28] Lin Haixue. Voltage dip and short supply interruption in power systems, Distribution Utilization, vol. 19, pp. 9-13, Feb. 2002.

[29] B. H. Chowdhury, "Power Quality, " IEEE Potentials, Vol.20, Issue:2, Apr/May pp. 5-11,2001

[30] D.O. Koval, R.A. Bocencea and K. Yao et al. Canadian national power quality survey: frequency and duration of voltages sags and surges at industrial sites, IEEE Trans. on IA,1998, Vol.34, No.5.

[31] J. B. Hoover, "The Changing World of Power Monitoring", Telecommunications Energy Conference, 2000. INTELEC. Twenty-second International, pp. 103-108, 2000

[32] D. Raskovic, "Energy-efficient Hierarchical Processing in the Network of Wireless Intelligent Sensors," Ph.D. Thesis, ECE Dept., University of Alabama in Huntsville, 2004.

[33] Y. C. Kang, T. Y. Zheng, S. H. So, H. G. Kang, S. I. Jang and Y. G. Kim, "Compensating Algorithm for the Secondary Current of a Measurement CT Considering the Hysteresis Characteristic," Transmission Distribution Conference Exposition: Asia and Pacific, 2009, pp.1-4, 26-30 Oct. 2009.

[34] NxtPhase T D Corporation Presentation, January 2006

[35] Y. Wang, J. G. Liu, Jing Zhao and Y. Yang, "Split Core Closed Loop Hall Effect Current Sensors and Applications," PCIM EUROPE International Exhibition and Conference for Power Electronics, Intelligent Motion, Power Quality, Nuremberg, Germany, pp.1633-1638, 8-10 May 2012

[36] L.F. Auler and R. d'Amore, "Power Quality Monitoring and Control Using Ethernet Networks," IEEE International Conference on Harmonics and Quality of Power, 10th, vol. 1, pp. 208-213, 2002.

[37] J. Batista, J. L. Alfonso, and J. S. Martins, "Low-Cost Power Quality Monitor Based on a PC," IEEE International Symposium on Industrial Electronics. vol. 1, pp 323-328, 2003.

[38] A. Rahim bin Abdullah and A. Zuri bin Sha'ameri, "Real-Time Power Quality Monitoring System Based On TMS320CV5416 DSP Processor," IEEE International Conference on Power Electronics and Drive Systems, vol. 2, pp. 1668-1672, November 2005.

[39] D. Hong, J. Lee, and J. Choi, "Power Quality Monitoring System Using Power Line Communication," IEEE International Conference on Information, Communications and Signal Processing, 5th, pp. 931-935, December 2005.

[40] A. So, N. Tse, W. L. Chan, and L. L. Lai, "A Low-Cost Power Quality Meter for Utility and Consumer Assessments," IEEE International Conference on Electric Utility Deregulation and Restructuring and Power Technologies, pp. 96-100, April 2000.

[41] G. H. Yang, and B. Y. Wen, "A Device for Power Quality Monitoring Based on ARM and DSP," IEEE Conference on Industrial Electronics and Applications,1st, pp. 1-5, May 2006.

[42] M. E. Salem, A. Mohamed, S.Abd. Samad, and R. Mohamed, "Development of a DSP-Based Power Quality Monitoring Instrument for Real-Time Detection of Power Disturbances," IEEE International Conference on Power Electronics and Drives Systems, vol. 1, pp. 304 - 307, January 2006.

[43] BRUCE G. BAILEY, "Power System Protection - Power Monitoring - Data Logging - Remote Interrogation System," IEEE - IXPS PANEL DISCUSSION, pp.65-68, 30 Apr-1 May 1990

[44] M. H. Hung, J. Y. Cheng, P. N. Chen and S. S. Lin, "Development of a ZigBee-based Distributed Power Monitoring and Control Platform with Easy-Deployment and Flexible-Extension Considerations", 2011 International Conference on Instrumentation, Measurement, Computer, Communication and Control, pp. 345-348, 21-23 Oct. 2011

[45] M. Zhang and K. Li, "A Power Quality Monitoring System over the Internet," The 1st International Conference on Information Science and Engineering (ICISE2009,), pp.1577-1580, 2009

[46] D. Divan, G. A. Luckjiff, W. E. Brumsickle, J. Freeborg, and A. Bhadkamkar, " A Grid Information Resource for Nationwide Real-Time Power Monitoring", IEEE TRANSACTIONS ON INDUSTRY APPLICATIONS, VOL. 40, NO. 2, MARCH/APRIL 2004

[47] R. V. P. Yerra, A. K. Bharathi, P. Rajalakshmi, U.B.Desai," WSN Based Power Monitoring in Smart Grids," Intelligent Sensors, Sensor Networks and Information Processing (ISSNIP), 2011 Seventh International Conference on, 2011

[48] Z. Sun, T. Zhao and C. Che, " Design Of Electric Power Monitoring System Based On ZigBee And GPRS", Computer Network and Multimedia Technology, 2009. CNMT 2009. International Symposium on, pp. 1-4, 2009.

[49] Zhang Donglai, Sun Baokui, Fan Hong, " Remote Online Power System Monitoring System Based on Multi-Information Acquisition Technology," 2004 lntemationat Conference on Power System Technology - POWERCON 2004 Slngapore, 21-24 November 2004, pp. 1147-1151, 2004.

[50] Associated Power Technologies, Total Harmonic Distortion and Effects in Electrical Power Systems.

[51] G. E. Mog and E. P. Ribeiro, " Total Harmonic Distortion Calculation by Filtering for Power Quality Monitoring", 2004 IEEHPES Transmission 8 Distribution Conference Exposition: Latin America, pp.629-632, 2004.

[52] A. Ortiz, C. Gherasim, M. Mañana, C. J. Renedo, L. I. Eguíluz, and R. J. M. Belmans, " Total Harmonic Distortion Decomposition Depending on Distortion Origin", EEE TRANSACTIONS ON POWER DELIVERY, VOL. 20, NO. 4, pp. 2651-2656, OCTOBER 2005.

[53] T. Türker, N. Yörükeren, M.?engül, B. Alboyac?, "An Artificial Neural-Net Based Method for Predicting Distribution Transformer's Total Harmonic Distortions," 2nd IEEE International Conference on Power and Energy (PECon 08), Johor Baharu, Malaysia, pp.1194-1197, December 1-3, 2008.

[54] The Wikipedia Free Encyclopedia, Fast Fourier transform[Online]. Available : http://en.wikipedia.org/wiki/Fast-Fourier-transform. Accessed: 21 July, 2012.

[55] J. W. Cooley and J. W. Tukey, " An algorithm for the machine calculation of complex Fourier series," Journal: Math. Comp. 19 (1965), 297-301, 1965.

[56] Microchip Technology, dsPIC30F DSP Library [Online]. Available: http://ww1.microchip.com/downloads/en/devicedoc/70148a-19.pdf [Accessed: 12 August,2012].

[57] Texas Instruments, TMS320C6672 Mutticore Fixed and Floating-Point Digital Signal Processor [Online]. Available: http://www.ti.com/product/tms320c6672description [Accessed:12 August,2012].

[58] Texas Instruments, TMS320VC5510A Fixed Point Digital Signal Processor [Online]. Available: http [Accessed: 12 August,2012].

[59] Texas Instruments, TMS320C6726B Floating Point Digital Signal Processor [Online]. Available: http://www.ti.com/product/tms320c6726b [Accessed: 12 August,2012].

[60] Atmel Corporation, ZigBit Modules MCU Wireless [Online]. Available: http://www.atmel.com/products/microcontrollers/wireless/modules.aspx [Accessed: 13 August,2012].

[61] Sagrad Inc, Java Wi-fi Modules [Online]. Available: http://www.sagrad.com/index.php?option=com-contentview=articleid=105Itemid=63 [Accessed: 14 August,2012].

[62] Sierra Wireless, AirPrime Q2686 GPRS Module [Online]. Available: http://www.sierrawireless.com/en/productsandservices/AirPrime/Wireless-Modules/Smart/Connectorized/Q2686.aspx [Accessed: 14 August,2012].

[63] Sierra Wireless, High Speed 3G/4G Modules [Online]. Available: http://www.sierrawireless.com/MC-Series [Accessed: 14 August,2012].

[64] Iridium Communications, Modems and Modules [Online]. Available: http://www.iridium.com/ProductList.aspx?productCategoryID=2[Accessed: 17 August,2012].

[65] Round Solutions GmbH and Co.KG, Combined satellite M2M modem ORBCOMM/Globalstar/GPS/GSM/GPRS [Online]. Available: http://www.roundsolutions.com/shop/products/en/Modules-and-accessories/Satellite-Module/Combined-satellite-M2M-modem-ORBCOMM-Globalstar-GPS-GSM-GPRS.html [Accessed: 15 August,2012].

[66] Z. Balorda and P. Suhel, "Electro-optical transmission line current monitor", Industrial Electronics, 1999. ISIE '99. Proceedings of the IEEE International Symposium on, vol. 3, pp. 1229 - 1231, 1999

[67] Z. Gang, L. Shaohui, Z. Zhipeng, and C. Wei, "A Novel Electro-Optic Hybrid Current Measurement Instrument for High-Voltage Power Lines", Ieee Transactions On Instrumentation And Measurement, vol. 50, no. 1, pp.59 - 62, February 2001

[68] E. Nishiyama, K. Kuwanami, M. Kawano, T. Matsuda, and I. Oota, "Development of Monitoring Equipment of Currents and Voltages of Power-Transmission Lines ", Industrial Electronics, 2002. ISIE 2002. Proceedings of the 2002 IEEE International Symposium on, vol.3, pp. 964 - 969, 2002

[69] S. J. Petricevic, Z. Stojkovic, and J. B. Radunovic," Practical Application of Fiber-Optic Current Sensor in Power System Harmonic Measurement", Ieee Transactions On Instrumentation And Measurement, vol. 55, no. 3, pp.923 - 930, June 2006

[70] H. WeiBing, L. KaiCheng, and L. JianFeng, "Research On Digital Optics Fiber Current Transformer", Universities Power Engineering Conference, 2007. UPEC 2007. 42nd International, pp. 509 - 512, 2007

[71] Southern States, llc., Current Measurement Device (CMD II)[Online]. Available: http://www.southernstatesllc.com/productcategories/21/products/21-CMDII- [Accessed: 22 September, 2012]

[72] J. D. Ramboz, " A Highly Accurate, Hand-Held Clamp-On Current Transformer", Ieee Transactions 01'4 Instrumentation And Measurement, vol. 45, no. 2,Pp. 445- 448, April 1996

[73] A.M.Luciano (1) and M.Savastano (2), " Wide Band Transformer based on a Split-Conductor current Sensor and a Rogowski coil for High Current Measurement", Instrumentation and Measurement Technology Conference, 1995. IMTC/95. Proceedings. 'Integrating Intelligent Instrumentation and Control'., IEEE, 23-25 Apr. 1995

APPENDIX A

DSPIC30F6010A FEATURES

dsPIC30F6010A/6015

Analog Features:

- 10-bit Analog-to-Digital Converter (ADC) with 4 S/H Inputs:
  - 1 Msps conversion rate
  - 16 input channels
  - Conversion available during Sleep and Idle
- Programmable Brown-out Reset

Special Microcontroller Features:

- Enhanced Flash program memory:
  - 10,000 erase/write cycle (min.) for Industrial temperature range, 100K (typical)
- Data EEPROM memory:
  - 100,000 erase/write cycle (min.) for Industrial temperature range, 1M (typical)
- Self-reprogrammable under software control
- Power-on Reset (POR), Power-up Timer (PWRT) and Oscillator Start-up Timer (OST)
- Flexible Watchdog Timer (WDT) with on-chip, low-power RC oscillator for reliable operation
- Fail-Safe Clock Monitor operation detects clock failure and switches to on-chip, low-power RC oscillator
- Programmable code protection
- In-Circuit Serial Programming™ (ICSP™)
- Selectable Power Management modes
  - Sleep, Idle and Alternate Clock modes

CMOS Technology:

- Low-power, high-speed Flash technology
- Wide operating voltage range (2.5V to 5.5V)
- Industrial and Extended temperature ranges
- Low-power consumption

dsPIC30F Motor Control and Power Conversion Family*

Device	Pins	Program Mem. Bytes/ Instructions	SRAM Bytes	EEPROM Bytes	Timer 16-bit	Input Cap	Output Comp/Std PWM	Motor Control PWM	A/D 10-bit 1 Msps	Quad Enc	UART	SPI	I²C™	CAN
dsPIC30F2010	28	12K/4K	512	1024	3	4	2	6 ch	6 ch	Yes	1	1	1	—
dsPIC30F3010	28	24K/8K	1024	1024	5	4	2	6 ch	6 ch	Yes	1	1	1	—
dsPIC30F4012	28	48K/16K	2048	1024	5	4	2	6 ch	6 ch	Yes	1	1	1	1
dsPIC30F3011	40/ 44	24K/8K	1024	1024	5	4	4	6 ch	9 ch	Yes	2	1	1	—
dsPIC30F4011	40/ 44	48K/16K	2048	1024	5	4	4	6 ch	9 ch	Yes	2	1	1	1
dsPIC30F5015	64	66K/22K	2048	1024	5	4	4	8 ch	16 ch	Yes	1	2	1	1
dsPIC30F5016	80	66K/22K	2048	1024	5	4	4	8 ch	16 ch	Yes	1	2	1	1
dsPIC30F6010A	80	144K/48K	8192	4096	5	8	8	8 ch	16 ch	Yes	2	2	1	2
dsPIC30F6015	64	144K/48K	8192	4096	5	8	8	8 ch	16 ch	Yes	2	2	1	1

* This table provides a summary of the dsPIC30F peripheral features. Other available devices in the dsPIC30F Motor Control and Power Conversion Family are shown for feature comparison.

dsPIC30F6010A/6015 Enhanced Flash 16-bit Digital Signal Controller (DSC)

Note: This data sheet summarizes features of this group of dsPIC30F devices and is not intended to be a complete reference source. For more information on the CPU, peripherals, register descriptions and general device functionality, refer to the "*dsPIC30F Family Reference Manual*" (DS70046). For more information on the device instruction set and programming, refer to the "*dsPIC30F/33F Programmer's Reference Manual*" (DS70157).

High-Performance Modified RISC CPU:

- Modified Harvard architecture
- C compiler optimized instruction set architecture with flexible Addressing modes
- 83 base instructions
- 24-bit wide instructions, 16-bit wide data path
- 144 Kbytes on-chip Flash program space (instruction words)
- 8 Kbytes of on-chip data RAM
- 4 Kbytes of nonvolatile data EEPROM
- Up to 30 MIPS operation:
  - DC to 40 MHz external clock input
  - 4 MHz-10 MHz oscillator input with PLL active (4x, 8x, 16x)
  - 7.37 MHz internal RC with PLL active (4x, 8x, 16x)
- 44 interrupt sources:
  - 5 external interrupt sources
  - 8 user selectable priority levels for each interrupt source
  - 4 processor trap sources
- 16 x 16-bit working register array

DSP Engine Features:

- Dual data fetch
- Accumulator write-back for DSP operations
- Modulo and Bit-Reversed Addressing modes
- Two, 40-bit wide accumulators with optional saturation logic
- 17-bit x 17-bit single-cycle hardware fractional/integer multiplier
- All DSP instructions single cycle
- ±16-bit single-cycle shift

Peripheral Features:

- High-current sink/source I/O pins: 25 mA/25 mA
- Timer module with programmable prescaler:
  - Five 16-bit timers/counters; optionally pair 16-bit timers into 32-bit timer modules
- 16-bit Capture input functions
- 16-bit Compare/PWM output functions
- 3-wire SPI modules (supports 4 Frame modes)
- I^2C™ module supports Multi-Master/Slave mode and 7-bit/10-bit addressing
- 2 UART modules with FIFO Buffers
- 2 CAN modules, 2.0B compliant (dsPIC306010A)
- 1 CAN module, 2.0B compliant (dsPIC306015)

Motor Control PWM Module Features:

- 8 PWM output channels:
  - Complementary or Independent Output modes
  - Edge and Center-Aligned modes
- 4 duty cycle generators
- Dedicated time base
- Programmable output polarity
- Dead-Time control for Complementary mode
- Manual output control
- Trigger for A/D conversions

Quadrature Encoder Interface Module Features:

- Phase A, Phase B and Index Pulse input
- 16-bit up/down position counter
- Count direction status
- Position Measurement (x2 and x4) mode
- Programmable digital noise filters on inputs
- Alternate 16-bit Timer/Counter mode
- Interrupt on position counter rollover/underflow

APPENDIX B

PCB LAYOUT of DATA-ACQUISITUON CARD and CONTROL CARD

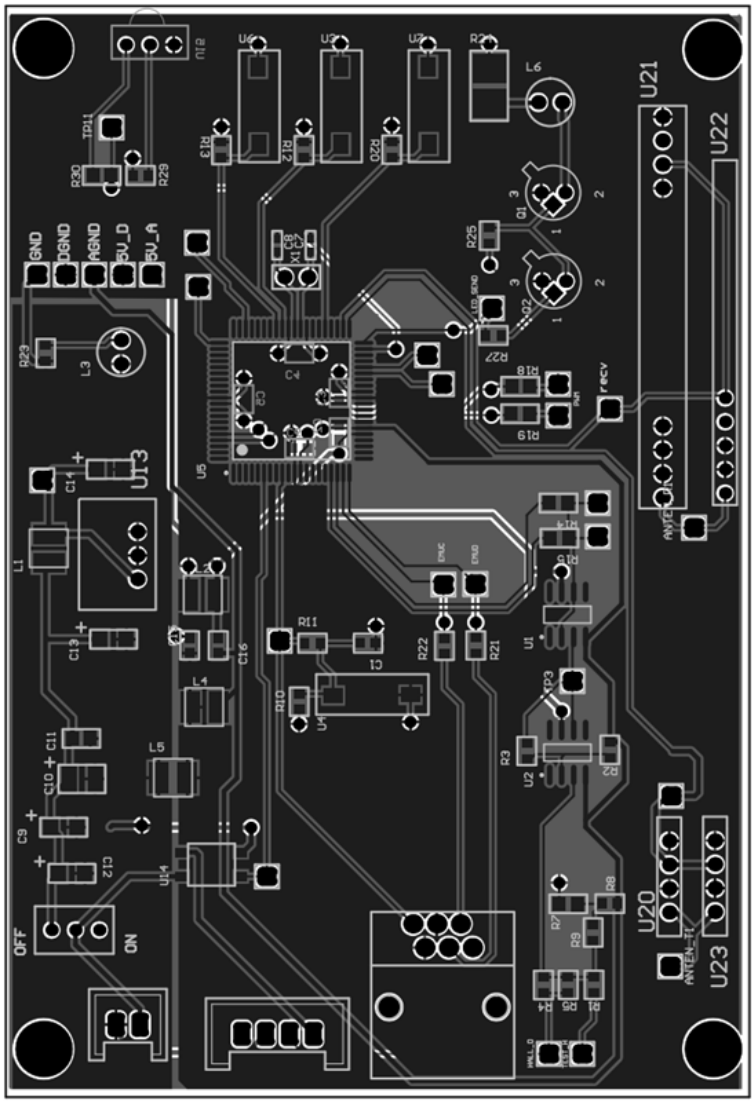

Figure B.1: PCB LAYOUT of DATA-ACQUISITUON CARD

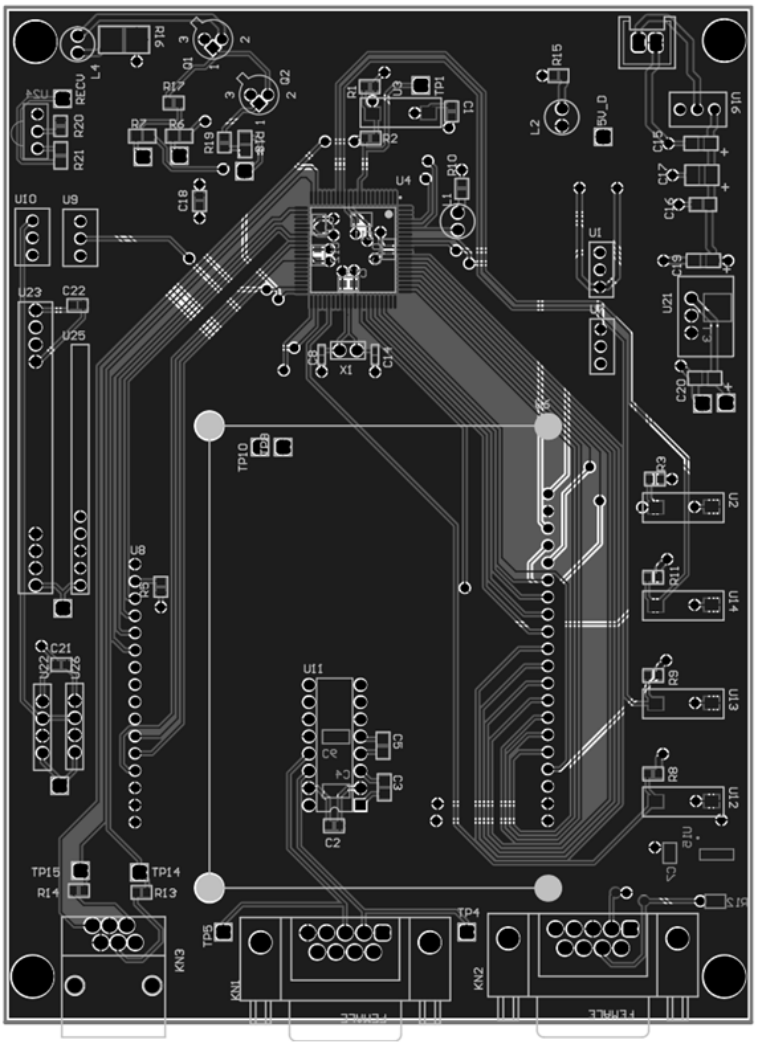

Figure B.2: PCB LAYOUT of CONTROL CARD

APPENDIX C

VALUES OBTAINED FROM MATLAB ANALYSIS FOR CHAPTER 4 TEST CASES

50 Hz Pure Sinusoidal Wave
Signal Samples

0.0000	0.0245	0.0491	0.0736	0.0980	0.1224	0.1467	0.1710	0.1951
0.2191	0.2430	0.2667	0.2903	0.3137	0.3369	0.3599	0.3827	0.4052
0.4276	0.4496	0.4714	0.4929	0.5141	0.5350	0.5556	0.5758	0.5957
0.6152	0.6344	0.6532	0.6716	0.6895	0.7071	0.7242	0.7410	0.7572
0.7730	0.7883	0.8032	0.8176	0.8315	0.8449	0.8577	0.8701	0.8819
0.8932	0.9040	0.9142	0.9239	0.9330	0.9415	0.9495	0.9569	0.9638
0.9700	0.9757	0.9808	0.9853	0.9892	0.9925	0.9952	0.9973	0.9988
0.9997	1.0000	0.9997	0.9988	0.9973	0.9952	0.9925	0.9892	0.9853
0.9808	0.9757	0.9700	0.9638	0.9569	0.9495	0.9415	0.9330	0.9239
0.9142	0.9040	0.8932	0.8819	0.8701	0.8577	0.8449	0.8315	0.8176
0.8032	0.7883	0.7730	0.7572	0.7410	0.7242	0.7071	0.6895	0.6716
0.6532	0.6344	0.6152	0.5957	0.5758	0.5556	0.5350	0.5141	0.4929
0.4714	0.4496	0.4276	0.4052	0.3827	0.3599	0.3369	0.3137	0.2903
0.2667	0.2430	0.2191	0.1951	0.1710	0.1467	0.1224	0.0980	0.0736
0.0491	0.0245	0.0000	-0.0245	-0.0491	-0.0736	-0.0980	-0.1224	-0.1467
-0.1710	-0.1951	-0.2191	-0.2430	-0.2667	-0.2903	-0.3137	-0.3369	-0.3599
-0.3827	-0.4052	-0.4276	-0.4496	-0.4714	-0.4929	-0.5141	-0.5350	-0.5556
-0.5758	-0.5957	-0.6152	-0.6344	-0.6532	-0.6716	-0.6895	-0.7071	-0.7242
-0.7410	-0.7572	-0.7730	-0.7883	-0.8032	-0.8176	-0.8315	-0.8449	-0.8577
-0.8701	-0.8819	-0.8932	-0.9040	-0.9142	-0.9239	-0.9330	-0.9415	-0.9495
-0.9569	-0.9638	-0.9700	-0.9757	-0.9808	-0.9853	-0.9892	-0.9925	-0.9952
-0.9973	-0.9988	-0.9997	-1.0000	-0.9997	-0.9988	-0.9973	-0.9952	-0.9925
-0.9892	-0.9853	-0.9808	-0.9757	-0.9700	-0.9638	-0.9569	-0.9495	-0.9415
-0.9330	-0.9239	-0.9142	-0.9040	-0.8932	-0.8819	-0.8701	-0.8577	-0.8449
-0.8315	-0.8176	-0.8032	-0.7883	-0.7730	-0.7572	-0.7410	-0.7242	-0.7071
-0.6895	-0.6716	-0.6532	-0.6344	-0.6152	-0.5957	-0.5758	-0.5556	-0.5350
-0.5141	-0.4929	-0.4714	-0.4496	-0.4276	-0.4052	-0.3827	-0.3599	-0.3369
-0.3137	-0.2903	-0.2667	-0.2430	-0.2191	-0.1951	-0.1710	-0.1467	-0.1224

-0.0980	-0.0736	-0.0491	-0.0245

Obtained Coefficients

0.0000	0.0000	0.0000	0.0000	0.0000	0.0000	0.0000	0.0000	0.0000
0.0000	0.0000	0.0000	0.0000	0.0000	0.0000	0.0000	0.0000	0.0000
0.0000	0.0000	0.0000	0.0000	0.0000	0.0000	0.0000	0.0000	0.0000
0.0000	0.0000	0.0000	0.0000	0.0000	0.0000	0.0000	0.0000	0.0000
0.0000	0.0000	0.0000	0.0000	0.0000	0.0000	0.0000	0.0000	0.0000
0.0000	0.0000	0.0000	0.0000	0.0000	0.0000	0.0000	0.0000	0.0000
0.0000	0.0000	0.0000	0.0000	0.0000	0.0000	0.0000	0.0000	0.0000
0.0000	0.0000	0.0000	0.0000	0.0000	0.0000	0.0000	0.0000	0.0000
0.0000	0.0000	0.0000	0.0000	0.0000	0.0000	0.0000	0.0000	0.0000
0.0000	0.0000	0.0000	0.0000	0.0000	0.0000	0.0000	0.0000	0.0000
0.0000	0.0000	0.0000	0.0000	0.0000	0.0000	0.0000	0.0000	0.0000
0.0000	0.0000	0.0000	0.0000	0.0000	0.0000	0.0000	0.0000	0.0000
0.0000	0.0000	0.0000	0.0000	0.0000	0.0000	0.0000	0.0000	0.0000
0.0000	0.0000	0.0000	0.0000	0.0000	0.0000	0.0000	0.0000	0.0000
0.0000	1.0000	0.0000	1.0000	0.0000	0.0000	0.0000	0.0000	0.0000
0.0000	0.0000	0.0000	0.0000	0.0000	0.0000	0.0000	0.0000	0.0000
0.0000	0.0000	0.0000	0.0000	0.0000	0.0000	0.0000	0.0000	0.0000
0.0000	0.0000	0.0000	0.0000	0.0000	0.0000	0.0000	0.0000	0.0000

0.0000	0.0000	0.0000	0.0000	0.0000	0.0000	0.0000	0.0000	0.0000
0.0000	0.0000	0.0000	0.0000	0.0000	0.0000	0.0000	0.0000	0.0000
0.0000	0.0000	0.0000	0.0000	0.0000	0.0000	0.0000	0.0000	0.0000
0.0000	0.0000	0.0000	0.0000	0.0000	0.0000	0.0000	0.0000	0.0000
0.0000	0.0000	0.0000	0.0000	0.0000	0.0000	0.0000	0.0000	0.0000
0.0000	0.0000	0.0000	0.0000	0.0000	0.0000	0.0000	0.0000	0.0000
0.0000	0.0000	0.0000	0.0000	0.0000	0.0000	0.0000	0.0000	0.0000
0.0000	0.0000	0.0000	0.0000	0.0000	0.0000	0.0000	0.0000	0.0000
0.0000	0.0000	0.0000	0.0000	0.0000	0.0000	0.0000	0.0000	0.0000
0.0000	0.0000	0.0000	0.0000	0.0000	0.0000	0.0000	0.0000	0.0000
0.0000	0.0000	0.0000	0.0000					

50Hz Sinusoidal Signal with 4th Harmonic
Signal Samples

0.0000	0.0515	0.1026	0.1529	0.2021	0.2498	0.2956	0.3392	0.3804
0.4188	0.4541	0.4861	0.5147	0.5396	0.5608	0.5780	0.5913	0.6007
0.6061	0.6076	0.6053	0.5992	0.5896	0.5767	0.5606	0.5417	0.5201
0.4962	0.4703	0.4427	0.4138	0.3840	0.3536	0.3229	0.2924	0.2625
0.2334	0.2056	0.1794	0.1550	0.1329	0.1132	0.0963	0.0823	0.0714

0.0638	0.0597	0.0590	0.0619	0.0684	0.0785	0.0920	0.1089	0.1291
0.1524	0.1786	0.2075	0.2389	0.2724	0.3077	0.3445	0.3825	0.4214
0.4606	0.5000	0.5391	0.5774	0.6148	0.6507	0.6848	0.7168	0.7464
0.7732	0.7971	0.8176	0.8347	0.8480	0.8575	0.8631	0.8646	0.8619
0.8552	0.8443	0.8294	0.8105	0.7878	0.7615	0.7316	0.6986	0.6625
0.6238	0.5827	0.5396	0.4947	0.4485	0.4013	0.3536	0.3056	0.2577
0.2105	0.1641	0.1191	0.0756	0.0341	-0.0051	-0.0417	-0.0755	-0.1063
-0.1339	-0.1580	-0.1785	-0.1955	-0.2087	-0.2181	-0.2239	-0.2259	-0.2244
-0.2194	-0.2111	-0.1997	-0.1853	-0.1683	-0.1489	-0.1274	-0.1041	-0.0793
-0.0535	-0.0269	-0.0000	0.0269	0.0535	0.0793	0.1041	0.1274	0.1489
0.1683	0.1853	0.1997	0.2111	0.2194	0.2244	0.2259	0.2239	0.2181
0.2087	0.1955	0.1785	0.1580	0.1339	0.1063	0.0755	0.0417	0.0051
-0.0341	-0.0756	-0.1191	-0.1641	-0.2105	-0.2577	-0.3056	-0.3536	-0.4013
-0.4485	-0.4947	-0.5396	-0.5827	-0.6238	-0.6625	-0.6986	-0.7316	-0.7615
-0.7878	-0.8105	-0.8294	-0.8443	-0.8552	-0.8619	-0.8646	-0.8631	-0.8575
-0.8480	-0.8347	-0.8176	-0.7971	-0.7732	-0.7464	-0.7168	-0.6848	-0.6507
-0.6148	-0.5774	-0.5391	-0.5000	-0.4606	-0.4214	-0.3825	-0.3445	-0.3077
-0.2724	-0.2389	-0.2075	-0.1786	-0.1524	-0.1291	-0.1089	-0.0920	-0.0785
-0.0684	-0.0619	-0.0590	-0.0597	-0.0638	-0.0714	-0.0823	-0.0963	-0.1132
-0.1329	-0.1550	-0.1794	-0.2056	-0.2334	-0.2625	-0.2924	-0.3229	-0.3536
-0.3840	-0.4138	-0.4427	-0.4703	-0.4962	-0.5201	-0.5417	-0.5606	-0.5767
-0.5896	-0.5992	-0.6053	-0.6076	-0.6061	-0.6007	-0.5913	-0.5780	-0.5608
-0.5396	-0.5147	-0.4861	-0.4541	-0.4188	-0.3804	-0.3392	-0.2956	-0.2498
-0.2021	-0.1529	-0.1026	-0.0515					

Obtained Coefficients

0.0000	0.0000	0.0000	0.0000	0.0000	0.0000	0.0000	0.0000	0.0000
0.0000	0.0000	0.0000	0.0000	0.0000	0.0000	0.0000	0.0000	0.0000
0.0000	0.0000	0.0000	0.0000	0.0000	0.0000	0.0000	0.0000	0.0000
0.0000	0.0000	0.0000	0.0000	0.0000	0.0000	0.0000	0.0000	0.0000
0.0000	0.0000	0.0000	0.0000	0.0000	0.0000	0.0000	0.0000	0.0000
0.0000	0.0000	0.0000	0.0000	0.0000	0.0000	0.0000	0.0000	0.0000
0.0000	0.0000	0.0000	0.0000	0.0000	0.0000	0.0000	0.0000	0.0000
0.0000	0.0000	0.0000	0.0000	0.0000	0.0000	0.0000	0.0000	0.0000
0.0000	0.0000	0.0000	0.0000	0.0000	0.0000	0.0000	0.0000	0.0000
0.0000	0.0000	0.0000	0.0000	0.0000	0.0000	0.0000	0.0000	0.0000
0.0000	0.0000	0.0000	0.0000	0.0000	0.0000	0.0000	0.0000	0.0000
0.0000	0.0000	0.0000	0.0000	0.0000	0.0000	0.0000	0.0000	0.0000
0.0000	0.0000	0.0000	0.0000	0.0000	0.0000	0.0000	0.0000	0.0000
0.0000	0.0000	0.0000	0.0000	0.0000	0.0000	0.0000	0.4000	0.0000
0.0000	0.5000	0.0000	0.5000	0.0000	0.0000	0.4000	0.0000	0.0000
0.0000	0.0000	0.0000	0.0000	0.0000	0.0000	0.0000	0.0000	0.0000
0.0000	0.0000	0.0000	0.0000	0.0000	0.0000	0.0000	0.0000	0.0000
0.0000	0.0000	0.0000	0.0000	0.0000	0.0000	0.0000	0.0000	0.0000
0.0000	0.0000	0.0000	0.0000	0.0000	0.0000	0.0000	0.0000	0.0000

0.0000	0.0000	0.0000	0.0000	0.0000	0.0000	0.0000	0.0000	0.0000
0.0000	0.0000	0.0000	0.0000	0.0000	0.0000	0.0000	0.0000	0.0000
0.0000	0.0000	0.0000	0.0000	0.0000	0.0000	0.0000	0.0000	0.0000
0.0000	0.0000	0.0000	0.0000	0.0000	0.0000	0.0000	0.0000	0.0000
0.0000	0.0000	0.0000	0.0000	0.0000	0.0000	0.0000	0.0000	0.0000
0.0000	0.0000	0.0000	0.0000	0.0000	0.0000	0.0000	0.0000	0.0000
0.0000	0.0000	0.0000	0.0000	0.0000	0.0000	0.0000	0.0000	0.0000
0.0000	0.0000	0.0000	0.0000	0.0000	0.0000	0.0000	0.0000	0.0000
0.0000	0.0000	0.0000	0.0000	0.0000	0.0000	0.0000	0.0000	0.0000
0.0000	0.0000	0.0000	0.0000					

50Hz Sinusoidal Signal with 35th Harmonic
Signal Samples

0.0000	0.0954	0.1382	0.1124	0.0494	0.0065	0.0270	0.1101	0.2116
0.2745	0.2685	0.2109	0.1549	0.1524	0.2181	0.3193	0.3985	0.4135
0.3663	0.3021	0.2776	0.3219	0.4162	0.5068	0.5425	0.5099	0.4429
0.3989	0.4193	0.5006	0.5968	0.6514	0.6364	0.5720	0.5124	0.5082
0.5713	0.6667	0.7367	0.7411	0.6847	0.6144	0.5863	0.6271	0.7153
0.7963	0.8202	0.7763	0.7008	0.6514	0.6675	0.7425	0.8290	0.8710
0.8432	0.7683	0.7015	0.6918	0.7486	0.8345	0.8918	0.8823	0.8137
0.7344	0.7000	0.7344	0.8137	0.8823	0.8918	0.8345	0.7486	0.6918
0.7015	0.7683	0.8432	0.8710	0.8290	0.7425	0.6675	0.6514	0.7008
0.7763	0.8202	0.7963	0.7153	0.6271	0.5863	0.6144	0.6847	0.7411
0.7367	0.6667	0.5713	0.5082	0.5124	0.5720	0.6364	0.6514	0.5968
0.5006	0.4193	0.3989	0.4429	0.5099	0.5425	0.5068	0.4162	0.3219
0.2776	0.3021	0.3663	0.4135	0.3985	0.3193	0.2181	0.1524	0.1549
0.2109	0.2685	0.2745	0.2116	0.1101	0.0270	0.0065	0.0494	0.1124
0.1382	0.0954	0.0000	-0.0954	-0.1382	-0.1124	-0.0494	-0.0065	-0.0270
-0.1101	-0.2116	-0.2745	-0.2685	-0.2109	-0.1549	-0.1524	-0.2181	-0.3193
-0.3985	-0.4135	-0.3663	-0.3021	-0.2776	-0.3219	-0.4162	-0.5068	-0.5425
-0.5099	-0.4429	-0.3989	-0.4193	-0.5006	-0.5968	-0.6514	-0.6364	-0.5720
-0.5124	-0.5082	-0.5713	-0.6667	-0.7367	-0.7411	-0.6847	-0.6144	-0.5863
-0.6271	-0.7153	-0.7963	-0.8202	-0.7763	-0.7008	-0.6514	-0.6675	-0.7425
-0.8290	-0.8710	-0.8432	-0.7683	-0.7015	-0.6918	-0.7486	-0.8345	-0.8918
-0.8823	-0.8137	-0.7344	-0.7000	-0.7344	-0.8137	-0.8823	-0.8918	-0.8345
-0.7486	-0.6918	-0.7015	-0.7683	-0.8432	-0.8710	-0.8290	-0.7425	-0.6675
-0.6514	-0.7008	-0.7763	-0.8202	-0.7963	-0.7153	-0.6271	-0.5863	-0.6144
-0.6847	-0.7411	-0.7367	-0.6667	-0.5713	-0.5082	-0.5124	-0.5720	-0.6364
-0.6514	-0.5968	-0.5006	-0.4193	-0.3989	-0.4429	-0.5099	-0.5425	-0.5068
-0.4162	-0.3219	-0.2776	-0.3021	-0.3663	-0.4135	-0.3985	-0.3193	-0.2181
-0.1524	-0.1549	-0.2109	-0.2685	-0.2745	-0.2116	-0.1101	-0.0270	-0.0065
-0.0494	-0.1124	-0.1382	-0.0954					

Obtained Coefficients

0.0000	0.0000	0.0000	0.0000	0.0000	0.0000	0.0000	0.0000	0.0000
0.0000	0.0000	0.0000	0.0000	0.0000	0.0000	0.0000	0.0000	0.0000
0.0000	0.0000	0.0000	0.0000	0.0000	0.0000	0.0000	0.0000	0.0000
0.0000	0.0000	0.0000	0.0000	0.0000	0.0000	0.0000	0.0000	0.0000
0.0000	0.0000	0.0000	0.0000	0.0000	0.0000	0.0000	0.0000	0.0000
0.0000	0.0000	0.0000	0.0000	0.0000	0.0000	0.0000	0.0000	0.0000
0.0000	0.0000	0.0000	0.0000	0.0000	0.0000	0.0000	0.0000	0.0000
0.0000	0.0000	0.0000	0.0000	0.0000	0.0000	0.0000	0.0000	0.0000
0.0000	0.0000	0.0000	0.0000	0.0000	0.0000	0.0000	0.0000	0.0000
0.0000	0.0000	0.0000	0.0000	0.0000	0.0000	0.0000	0.0000	0.0000
0.0000	0.0000	0.0000	0.1000	0.0000	0.0000	0.0000	0.0000	0.0000
0.0000	0.0000	0.0000	0.0000	0.0000	0.0000	0.0000	0.0000	0.0000
0.0000	0.0000	0.0000	0.0000	0.0000	0.0000	0.0000	0.0000	0.0000
0.0000	0.0000	0.0000	0.0000	0.0000	0.0000	0.0000	0.0000	0.0000
0.0000	0.8000	0.0000	0.8000	0.0000	0.0000	0.0000	0.0000	0.0000
0.0000	0.0000	0.0000	0.0000	0.0000	0.0000	0.0000	0.0000	0.0000
0.0000	0.0000	0.0000	0.0000	0.0000	0.0000	0.0000	0.0000	0.0000
0.0000	0.0000	0.0000	0.0000	0.0000	0.0000	0.0000	0.0000	0.0000
0.0000	0.1000	0.0000	0.0000	0.0000	0.0000	0.0000	0.0000	0.0000
0.0000	0.0000	0.0000	0.0000	0.0000	0.0000	0.0000	0.0000	0.0000
0.0000	0.0000	0.0000	0.0000	0.0000	0.0000	0.0000	0.0000	0.0000

0.0000	0.0000	0.0000	0.0000	0.0000	0.0000	0.0000	0.0000	0.0000
0.0000	0.0000	0.0000	0.0000	0.0000	0.0000	0.0000	0.0000	0.0000
0.0000	0.0000	0.0000	0.0000	0.0000	0.0000	0.0000	0.0000	0.0000
0.0000	0.0000	0.0000	0.0000	0.0000	0.0000	0.0000	0.0000	0.0000
0.0000	0.0000	0.0000	0.0000	0.0000	0.0000	0.0000	0.0000	0.0000
0.0000	0.0000	0.0000	0.0000	0.0000	0.0000	0.0000	0.0000	0.0000
0.0000	0.0000	0.0000	0.0000	0.0000	0.0000	0.0000	0.0000	0.0000
0.0000	0.0000	0.0000	0.0000					

100Hz Sinusoidal Signal with Phase Shift and DC Offset
Signal Samples

0.9000	0.8994	0.8976	0.8946	0.8904	0.8850	0.8785	0.8708	0.8619
0.8520	0.8410	0.8289	0.8157	0.8016	0.7865	0.7705	0.7536	0.7358
0.7172	0.6978	0.6778	0.6571	0.6357	0.6138	0.5913	0.5684	0.5451
0.5215	0.4975	0.4734	0.4490	0.4245	0.4000	0.3755	0.3510	0.3266
0.3025	0.2785	0.2549	0.2316	0.2087	0.1862	0.1643	0.1429	0.1222
0.1022	0.0828	0.0642	0.0464	0.0295	0.0135	-0.0016	-0.0157	-0.0289
-0.0410	-0.0520	-0.0619	-0.0708	-0.0785	-0.0850	-0.0904	-0.0946	-0.0976
-0.0994	-0.1000	-0.0994	-0.0976	-0.0946	-0.0904	-0.0850	-0.0785	-0.0708
-0.0619	-0.0520	-0.0410	-0.0289	-0.0157	-0.0016	0.0135	0.0295	0.0464

```
 0.0642   0.0828   0.1022   0.1222   0.1429   0.1643   0.1862   0.2087   0.2316
 0.2549   0.2785   0.3025   0.3266   0.3510   0.3755   0.4000   0.4245   0.4490
 0.4734   0.4975   0.5215   0.5451   0.5684   0.5913   0.6138   0.6357   0.6571
 0.6778   0.6978   0.7172   0.7358   0.7536   0.7705   0.7865   0.8016   0.8157
 0.8289   0.8410   0.8520   0.8619   0.8708   0.8785   0.8850   0.8904   0.8946
 0.8976   0.8994   0.9000   0.8994   0.8976   0.8946   0.8904   0.8850   0.8785
 0.8708   0.8619   0.8520   0.8410   0.8289   0.8157   0.8016   0.7865   0.7705
 0.7536   0.7358   0.7172   0.6978   0.6778   0.6571   0.6357   0.6138   0.5913
 0.5684   0.5451   0.5215   0.4975   0.4734   0.4490   0.4245   0.4000   0.3755
 0.3510   0.3266   0.3025   0.2785   0.2549   0.2316   0.2087   0.1862   0.1643
 0.1429   0.1222   0.1022   0.0828   0.0642   0.0464   0.0295   0.0135  -0.0016
-0.0157  -0.0289  -0.0410  -0.0520  -0.0619  -0.0708  -0.0785  -0.0850  -0.0904

-0.0946  -0.0976  -0.0994  -0.1000  -0.0994  -0.0976  -0.0946  -0.0904  -0.0850
-0.0785  -0.0708  -0.0619  -0.0520  -0.0410  -0.0289  -0.0157  -0.0016   0.0135
 0.0295   0.0464   0.0642   0.0828   0.1022   0.1222   0.1429   0.1643   0.1862
 0.2087   0.2316   0.2549   0.2785   0.3025   0.3266   0.3510   0.3755   0.4000
 0.4245   0.4490   0.4734   0.4975   0.5215   0.5451   0.5684   0.5913   0.6138
 0.6357   0.6571   0.6778   0.6978   0.7172   0.7358   0.7536   0.7705   0.7865
 0.8016   0.8157   0.8289   0.8410   0.8520   0.8619   0.8708   0.8785   0.8850
 0.8904   0.8946   0.8976   0.8994
```

Obtained Coefficients

```
 0.0000   0.0000   0.0000   0.0000   0.0000   0.0000   0.0000   0.0000   0.0000
 0.0000   0.0000   0.0000   0.0000   0.0000   0.0000   0.0000   0.0000   0.0000
 0.0000   0.0000   0.0000   0.0000   0.0000   0.0000   0.0000   0.0000   0.0000
 0.0000   0.0000   0.0000   0.0000   0.0000        0   0.0000   0.0000   0.0000
 0.0000   0.0000   0.0000   0.0000   0.0000   0.0000   0.0000   0.0000   0.0000
 0.0000   0.0000   0.0000   0.0000   0.0000   0.0000   0.0000   0.0000   0.0000
 0.0000   0.0000   0.0000   0.0000   0.0000   0.0000   0.0000   0.0000   0.0000
 0.0000        0   0.0000   0.0000   0.0000   0.0000   0.0000   0.0000   0.0000
 0.0000   0.0000   0.0000   0.0000   0.0000   0.0000   0.0000   0.0000   0.0000
 0.0000   0.0000   0.0000   0.0000   0.0000   0.0000   0.0000   0.0000   0.0000
 0.0000   0.0000   0.0000   0.0000   0.0000   0.0000        0   0.0000   0.0000
 0.0000   0.0000   0.0000   0.0000   0.0000   0.0000   0.0000   0.0000   0.0000
 0.0000   0.0000   0.0000   0.0000   0.0000   0.0000   0.0000   0.0000   0.0000
 0.5000   0.0000   0.8000   0.0000   0.5000   0.0000   0.0000   0.0000   0.0000
 0.0000   0.0000   0.0000   0.0000   0.0000   0.0000   0.0000   0.0000   0.0000
 0.0000   0.0000   0.0000   0.0000   0.0000   0.0000   0.0000   0.0000   0.0000
 0.0000   0.0000   0.0000   0.0000   0.0000   0.0000   0.0000        0   0.0000
 0.0000   0.0000   0.0000   0.0000   0.0000   0.0000   0.0000   0.0000   0.0000
 0.0000   0.0000   0.0000   0.0000   0.0000   0.0000   0.0000   0.0000   0.0000
 0.0000   0.0000   0.0000   0.0000   0.0000   0.0000   0.0000   0.0000   0.0000
 0.0000   0.0000   0.0000        0   0.0000   0.0000   0.0000   0.0000   0.0000
```

0.0000	0.0000	0.0000	0.0000	0.0000	0.0000	0.0000	0.0000	0.0000
0.0000	0.0000	0.0000	0.0000	0.0000	0.0000	0.0000	0.0000	0.0000
0.0000	0.0000	0.0000	0.0000	0.0000	0.0000	0.0000	0.0000	0
0.0000	0.0000	0.0000	0.0000	0.0000	0.0000	0.0000	0.0000	0.0000
0.0000	0.0000	0.0000	0.0000	0.0000	0.0000	0.0000	0.0000	0.0000
0.0000	0.0000	0.0000	0.0000	0.0000	0.0000	0.0000	0.0000	0.0000
0.0000	0.0000	0.0000	0.0000					

50Hz Square Wave
Signal Samples

-1	-1	-1	-1	-1	-1	-1	-1	-1	-1	-1	-1	-1	-1	-1
-1	-1	-1	-1	-1	-1	-1	-1	-1	-1	-1	-1	-1	-1	-1
-1	-1	-1	-1	-1	-1	-1	-1	-1	-1	-1	-1	-1	-1	-1
-1	-1	-1	-1	-1	-1	-1	-1	-1	-1	-1	-1	-1	-1	-1
-1	-1	-1	-1	-1	-1	-1	-1	-1	-1	-1	-1	-1	-1	-1
-1	-1	-1	-1	-1	-1	-1	-1	-1	-1	-1	-1	-1	-1	-1
-1	-1	-1	-1	-1	-1	-1	-1	-1	-1	-1	-1	-1	-1	-1
-1	-1	-1	-1	-1	-1	-1	-1	-1	-1	-1	-1	-1	-1	-1
-1	-1	-1	-1	-1	-1	-1	1	1	1	1	1	1	1	1
1	1	1	1	1	1	1	1	1	1	1	1	1	1	1
1	1	1	1	1	1	1	1	1	1	1	1	1	1	1
1	1	1	1	1	1	1	1	1	1	1	1	1	1	1
1	1	1	1	1	1	1	1	1	1	1	1	1	1	1
1	1	1	1	1	1	1	1	1	1	1	1	1	1	1
1	1	1	1	1	1	1	1	1	1	1	1	1	1	1
1	1	1	1	1	1	1	1	1	1	1	1	1	1	1
1	1	1	1	1	1	1	1	1	1	1	1	1	1	1
1														

Obtained Coefficients

0.0156	0.0002	0.0156	0.0006	0.0156	0.0010	0.0156	0.0013	0.0156
0.0017	0.0156	0.0021	0.0156	0.0025	0.0156	0.0029	0.0156	0.0033
0.0156	0.0037	0.0156	0.0041	0.0156	0.0045	0.0156	0.0049	0.0156
0.0054	0.0156	0.0058	0.0156	0.0062	0.0156	0.0067	0.0156	0.0072
0.0156	0.0076	0.0156	0.0081	0.0156	0.0086	0.0156	0.0091	0.0156
0.0096	0.0156	0.0102	0.0156	0.0107	0.0156	0.0113	0.0156	0.0119
0.0156	0.0125	0.0156	0.0131	0.0156	0.0138	0.0156	0.0145	0.0156
0.0152	0.0156	0.0160	0.0156	0.0168	0.0156	0.0177	0.0156	0.0186
0.0156	0.0195	0.0156	0.0205	0.0156	0.0216	0.0156	0.0228	0.0156
0.0240	0.0156	0.0254	0.0156	0.0268	0.0156	0.0284	0.0156	0.0301
0.0156	0.0320	0.0156	0.0341	0.0156	0.0365	0.0156	0.0391	0.0156
0.0420	0.0156	0.0454	0.0156	0.0493	0.0156	0.0539	0.0156	0.0593

```
0.0156    0.0658    0.0156    0.0738    0.0156    0.0839    0.0156    0.0971    0.0156
0.1150    0.0156    0.1409    0.0156    0.1814    0.0156    0.2543    0.0156    0.4242
0.0156    1.2732    0.0156    1.2732    0.0156    0.4242    0.0156    0.2543    0.0156
0.1814    0.0156    0.1409    0.0156    0.1150    0.0156    0.0971    0.0156    0.0839
0.0156    0.0738    0.0156    0.0658    0.0156    0.0593    0.0156    0.0539    0.0156
0.0493    0.0156    0.0454    0.0156    0.0420    0.0156    0.0391    0.0156    0.0365
0.0156    0.0341    0.0156    0.0320    0.0156    0.0301    0.0156    0.0284    0.0156
0.0268    0.0156    0.0254    0.0156    0.0240    0.0156    0.0228    0.0156    0.0216
0.0156    0.0205    0.0156    0.0195    0.0156    0.0186    0.0156    0.0177    0.0156
0.0168    0.0156    0.0160    0.0156    0.0152    0.0156    0.0145    0.0156    0.0138
0.0156    0.0131    0.0156    0.0125    0.0156    0.0119    0.0156    0.0113    0.0156
0.0107    0.0156    0.0102    0.0156    0.0096    0.0156    0.0091    0.0156    0.0086
0.0156    0.0081    0.0156    0.0076    0.0156    0.0072    0.0156    0.0067    0.0156
0.0062    0.0156    0.0058    0.0156    0.0054    0.0156    0.0049    0.0156    0.0045
0.0156    0.0041    0.0156    0.0037    0.0156    0.0033    0.0156    0.0029    0.0156
0.0025    0.0156    0.0021    0.0156    0.0017    0.0156    0.0013    0.0156    0.0010
0.0156    0.0006    0.0156    0.0002
```

50Hz Triangular Wave
Signal Samples

```
0.0000    0.0156    0.0313    0.0469    0.0625    0.0781    0.0938    0.1094    0.1250
0.1406    0.1563    0.1719    0.1875    0.2031    0.2188    0.2344    0.2500    0.2656
0.2813    0.2969    0.3125    0.3281    0.3438    0.3594    0.3750    0.3906    0.4063
0.4219    0.4375    0.4531    0.4688    0.4844    0.5000    0.5156    0.5313    0.5469
0.5625    0.5781    0.5938    0.6094    0.6250    0.6406    0.6563    0.6719    0.6875
0.7031    0.7188    0.7344    0.7500    0.7656    0.7813    0.7969    0.8125    0.8281
0.8438    0.8594    0.8750    0.8906    0.9063    0.9219    0.9375    0.9531    0.9688
0.9844    1.0000    0.9844    0.9688    0.9531    0.9375    0.9219    0.9063    0.8906
0.8750    0.8594    0.8438    0.8281    0.8125    0.7969    0.7813    0.7656    0.7500
0.7344    0.7188    0.7031    0.6875    0.6719    0.6563    0.6406    0.6250    0.6094
0.5938    0.5781    0.5625    0.5469    0.5313    0.5156    0.5000    0.4844    0.4688
0.4531    0.4375    0.4219    0.4063    0.3906    0.3750    0.3594    0.3438    0.3281
0.3125    0.2969    0.2813    0.2656    0.2500    0.2344    0.2188    0.2031    0.1875
0.1719    0.1563    0.1406    0.1250    0.1094    0.0938    0.0781    0.0625    0.0469
0.0313    0.0156         0   -0.0156   -0.0313   -0.0469   -0.0625   -0.0781   -0.0938
-0.1094   -0.1250   -0.1406   -0.1563   -0.1719   -0.1875   -0.2031   -0.2188   -0.2344
-0.2500   -0.2656   -0.2813   -0.2969   -0.3125   -0.3281   -0.3438   -0.3594   -0.3750
-0.3906   -0.4063   -0.4219   -0.4375   -0.4531   -0.4688   -0.4844   -0.5000   -0.5156
-0.5313   -0.5469   -0.5625   -0.5781   -0.5938   -0.6094   -0.6250   -0.6406   -0.6563
-0.6719   -0.6875   -0.7031   -0.7188   -0.7344   -0.7500   -0.7656   -0.7813   -0.7969
-0.8125   -0.8281   -0.8438   -0.8594   -0.8750   -0.8906   -0.9063   -0.9219   -0.9375
-0.9531   -0.9688   -0.9844   -1.0000   -0.9844   -0.9688   -0.9531   -0.9375   -0.9219
-0.9063   -0.8906   -0.8750   -0.8594   -0.8438   -0.8281   -0.8125   -0.7969   -0.7813
-0.7656   -0.7500   -0.7344   -0.7188   -0.7031   -0.6875   -0.6719   -0.6563   -0.6406
-0.6250   -0.6094   -0.5938   -0.5781   -0.5625   -0.5469   -0.5313   -0.5156   -0.5000
-0.4844   -0.4688   -0.4531   -0.4375   -0.4219   -0.4063   -0.3906   -0.3750   -0.3594
```

```
-0.3438   -0.3281   -0.3125   -0.2969   -0.2813   -0.2656   -0.2500   -0.2344   -0.2188
-0.2031   -0.1875   -0.1719   -0.1563   -0.1406   -0.1250   -0.1094   -0.0938   -0.0781
-0.0625   -0.0469   -0.0313   -0.0156
```

Obtained Coefficients

```
     0    0.0001         0    0.0001         0    0.0001         0    0.0001         0
0.0001         0    0.0001         0    0.0001         0    0.0001         0    0.0001

     0    0.0001         0    0.0001         0    0.0001         0    0.0001         0
0.0001         0    0.0001         0    0.0001         0    0.0001         0    0.0001
     0    0.0002         0    0.0002         0    0.0002         0    0.0002         0
0.0002         0    0.0002         0    0.0002         0    0.0002         0    0.0002
     0    0.0002         0    0.0002         0    0.0002         0    0.0002         0
0.0002         0    0.0003         0    0.0003         0    0.0003         0    0.0003
     0    0.0003         0    0.0003         0    0.0004         0    0.0004         0
0.0004         0    0.0004         0    0.0005         0    0.0005         0    0.0006
     0    0.0006         0    0.0007         0    0.0008         0    0.0009         0
0.0010         0    0.0012         0    0.0013         0    0.0016         0    0.0019
     0    0.0023         0    0.0028         0    0.0036         0    0.0048         0
0.0067         0    0.0100         0    0.0166         0    0.0325         0    0.0901
     0    0.8106         0    0.8106         0    0.0901         0    0.0325         0
0.0166         0    0.0100         0    0.0067         0    0.0048         0    0.0036
     0    0.0028         0    0.0023         0    0.0019         0    0.0016         0
0.0013         0    0.0012         0    0.0010         0    0.0009         0    0.0008
     0    0.0007         0    0.0006         0    0.0006         0    0.0005         0
0.0005         0    0.0004         0    0.0004         0    0.0004         0    0.0004
     0    0.0003         0    0.0003         0    0.0003         0    0.0003         0
0.0003         0    0.0003         0    0.0002         0    0.0002         0    0.0002
     0    0.0002         0    0.0002         0    0.0002         0    0.0002         0
0.0002         0    0.0002         0    0.0002         0    0.0002         0    0.0002
     0    0.0002         0    0.0002         0    0.0001         0    0.0001         0
0.0001         0    0.0001         0    0.0001         0    0.0001         0    0.0001
     0    0.0001         0    0.0001         0    0.0001         0    0.0001         0
0.0001         0    0.0001         0    0.0001         0    0.0001         0    0.0001
     0    0.0001         0    0.0001
```